Angiotensin II Type 1 Receptor Activation in the Subfornical Organ Mediates Sodium-Induced Pressor Responses in Wistar Rats

Missale Tiruneh

This thesis is submitted to the Faculty of Graduate and Postdoctoral Studies as a partial fulfillment of the requirements for the M.Sc degree in Cellular and Molecular Medicine.

2012.04.05

Department of Cellular and Molecular Medicine
Faculty of Medicine, University of Ottawa

Abstract

Na^+ sensitive hypertension in Dahl salt sensitive rats (Dahl S) or spontaneously hypertensive rats (SHR) is linked to intrinsic changes in the brain that favour increased Na^+ entry into the cerebrospinal fluid (CSF) followed by increases in sympathetic hyperactivity and hypertension (Huang et al 2004). Similar responses are observed in salt resistant and Wistar rats that receive an intracerebroventricular (icv) infusion of Na^+ rich artificial cerebrospinal fluid (aCSF) (Huang et al 2001, 2006). Downstream to increased CSF[Na^+], a pathway has been described involving mineralocorticoid receptors (MRs), benzamil sensitive Na^+ channels, "ouabain", and angiotensin II type 1 receptors (AT_1-R) (Huang et al 1998, Zhao et al 2001, Wang and Leenen 2003, Huang et al 2008). Blood pressure (BP) responses to increased CSF[Na^+] may involve activation of AT_1-R in the subfornical organ (SFO) as the BP response to injection of NaCl into a lateral ventricle can be blocked by AT_1-R blockade in the SFO (Rohmeiss et al 1995a). The role of aldosterone and AT_1-R in the SFO was investigated in mediating the BP and heart rate (HR) response to increases in CSF[Na^+] and local [Na^+]. Results show that infusion of 0.45M and 0.6M Na^+ rich aCSF into the SFO increases BP but not HR. The BP is unchanged by infusion of a mannitol solution osmotically equivalent to 0.6M Na^+ rich aCSF indicating that the SFO is Na^+ sensitive. The BP response to a lower concentration of Na^+ (0.45M) is enhanced by prior infusion of aldosterone while BP response to 0.6M is not further enhanced suggesting that the SFO may have maximal responsiveness to acute increases in [Na^+] at 0.6M. The BP responses to Na^+ rich aCSF in the SFO and the enhancement of those responses by aldosterone can be blocked by infusion of the AT_1-R blocker Candesartan in the SFO. This response appears therefore to be mediated in the SFO through AT_1-R activation, likely through Ang II release

in the SFO. ICV infusion of Na^+ rich aCSF increases BP but not HR and this response is partially blocked by infusion of the AT_1-R blocker Candesartan in the SFO. This indicates that nearly half the BP responses to icv infusion of Na^+ rich aCSF is mediated through AT_1-R activation in the SFO. Lastly, contrary to icv, PVN and MnPO studies (Huang and Leenen 1996, Budzikowski and Leenen 2001, Gabor and Leenen 2009) ouabain in the SFO does not increase BP or HR.

In conclusion, these results show that the SFO is Na^+ sensitive and mediates half the BP responses to changes in CSF[Na^+] through a mechanism that involves AT_1-R activation. The SFO is further sensitized to Na^+ by aldosterone presumably through its genomic effects. Lastly, ouabain in the SFO does not increase BP or HR suggesting that endogenous ouabain in the SFO is not involved in modulating BP or HR responses.

Table of Contents

List of Tables

List of Figures

List of Abbreviations

11βHSD2: 11beta-hydroxysteroid dehydrogenase type 2

3V: third ventricle

3βHSD: 3β-hydroxysteroid dehydrogenase

ACE: angiotensin converting enzyme

aCSF: artificial cerebrospinal fluid

AGN: angiotensinogen

AMPA-R: 2-amino-3-(5-methyl-3-oxo-1,2- oxazol-4-yl)propanoic acid receptor

Ang II: angiotensin II

AP: area postrema

AT_1-R: angiotensin II receptor type 1

AT_2-R: angiotensin II receptor type 2

AV3V: anteroventral third ventricle

AVP: arginine vasopressin

BBB: blood brain barrier

BNST: bed nucleus of the stria terminalis

BP: blood pressure

cc: corpus callosum

CNS: central nervous system

CSF[Na^+]: cerebrospinal fluid sodium concentration

cSFO: ventromedial core of the SFO

CVLM: caudal ventrolateral medulla

CVO: circumventricular organ

CYP11A1: side chain cleavage enzyme

CYP11β1: 11β-hydroxylase

CYP11β2: aldosterone synthase

CYP21: 21-hydroxylase

Dahl R: Dahl salt resistant

Dahl S: Dahl salt sensitive

DOC: 11-deoxycorticosterone

DOCA: 11-deoxycorticosterone acetate

ECF: extracellular fluid

ENaC: epithelial sodium channel

FAD 286: an aldosterone synthase inhibitor

Fos-IR : Fos immunoreactivity

Fra: Fos related antigen

GABA: gamma-aminobutyric acid

GAD: glutamic acid decarboxylase

GR: glucocorticoid receptor

HR: heart rate

ICV: intracerebroventricular

IML: intermediolateral cell column

IV: intravenous

LPBN: lateral parabrachial nucleus

MAP: mean arterial pressure

mGluR: metabotropic glutamate receptor

MnPO: median preoptic nucleus

mPVN : magnocellular region of the PVN

MR: mineralocorticoid receptor

MRI: magnetic resonance imaging

Na^+/K^+ ATPase: sodium potassium adenosine triphosphatase

NE: norepinephrine

NMDA-R: N-methyl-D-aspartate

NTS: nucleus tractus solitarius

OLC: ouabain like compound

OVLT: organum vasculosum of lamina terminalis

PHA-L : phaseolus vulgaris leucoagglutinin

Pit: pituitary

pPVN: parvocellular region of the PVN

pSFO: periphery or outer shell of the SFO

PVN: paraventricular nucleus

RAS: renin angiotensin system

RSNA: renal sympathetic nerve activity

RT-PCR: reverse transcription polymerase chain reaction

RVLM: rostral ventrolateral medulla

SFO: subfornical organ

SHR: spontaneously hypertensive rats

SNS: sympathatic nervous system

SON: supraoptic nucleus

StAR: steroidogenic acute regulatory protein

TCA: tricarboxylic acid

vAV3V: ventral AV3V

vGlut2: type 2 vesicular glutamate transporter

vhc: ventral hippocampal commissure

Acknowledgements

Firstly, I would like to express my gratitude to my supervisor, **Dr. Frans Leenen**, who gave me the chance to learn and grow in his lab. I admire and respect the amount of knowledge, insight and dedication you bring to the work you do and likewise expect from your students. I will never forget being asked whether I had crocodile skin during the interview to start my MSc. I was not sure then, but I can assure you I have certainly developed it since.

To the members of my advisory committee, **Dr. Jim Van Huysse and Dr. Leo Renaud**, thank you for the guidance and support throughout my studies. My thanks to **Dr. Bing Huang** and **Dr. Monir Ahmad**, both of whom guided me through the many little aspects of surgical techniques. I am greateful for all the alterations to your shedules to accommodate my experiments. Dr. Ahmad missed many lunches to finish his surgeries and make sure I had time to do mine. **Dr. Hong-wei Wang**, although I did not have a chance to work with you on experiments, I will always cherish your kind words and support. To **Roselyn White** and **Danielle Oja**, many thanks for the guidance and support in the lab. I will miss the Christmas Parties and Afternoon Lunches you both kindly organized.

To my fellow students, many many thanks first to **Alex Gabor**. I have learned nearly everything during my MSc. from you and am greateful for the patience and kindness throughout. I wish you all the best in your future and am excited that we may graduate together. **Naimeh Rafatian**, full of sweetness and kindness, you will always remain a good friend. I know you will do great things in the future and hope we will keep in touch. To **Sara Ahmadi**, I will certainly miss your friendship. I know you will have many more wonderful milestones still to come. If ever in town, call me and we will visit Thyme Again, again! To the very knowledgeable **Dr. Anastasia Drobysheva**, I will miss your beauty tips and tricks. I hope you continue with your studies and have all your ambitions realized. To **Katherine Westcott**, I wish you happiness and all the best in your future.

Dedication

This thesis paper is dedicated to **my family**, with special recognition to my wonderful mother. I am the product of you kindness, dedication and sacrifice and I would not have made it this far without you. Thank you!

1 Overview

During episodes of increased Na^+ intake in both humans and rats, there is a transient increase in plasma [Na^+] (Fang et al 2000, Suckling et al 2011). This increase will be sensed by central osmoreceptors located in the subfornical organ (SFO) and organum vasculosum lamina terminalis (OVLT), sensory circumventricular organs (CVO's), which detect small changes in plasma osmolarity and signal the release of vasopressin via efferents to the magnocellular neurons of the paraventricular nucleus (PVN) and supraoptic nucleus (SON). This results in the increased absorption of water by the kidneys and an overall increase in the extracellular fluid (ECF). Hindbrain regions like the nucleus of the solitary tract (NTS), lateral parabrachial nucleus (LPBN) and area postrema (AP) will receive input from peripheral baroreceptors and osmosensors to integrate the inputs within the brain (Franchini and Vivas 1999). Other efferent neuronal connections from the SFO and OVLT to forebrain regions involved in the generation of thirst may also be involved in the behavioral response of increased drinking to balance the increased plasma [Na^+] (McKinley et al 1999). At the same time increased Na^+ intake will result in reduced levels of renin and Ang II production effectively reducing the sympathoexcitatory actions of circulating Ang II in the periphery and in the central nervous system (CNS) (Brooks et al 2001, Harrison-Bernard 2009). Decreased plasma Ang II levels also result in decreased aldosterone release resulting in decreased Na^+ absorption by the kidneys (Harrison-Bernard 2009). Although high Na^+ intake has minimal impact on the plasma Na^+ levels in both normal and hypertensive animals (Huang et al 2004), during high Na^+ consumption, sympathetic hyperactivity and hypertension develop in salt-sensitive models (Huang et al 2009).

Na^+ sensitive hypertension in Dahl salt sensitive rats (Dahl S) or spontaneously hypertensive rats (SHR) is linked to intrinsic changes in the brain that favour increased Na^+ entry into the cerebrospinal fluid (CSF) followed by increases in sympathetic hyperactivity and hypertension (Huang et al 2004). Similar responses are observed in salt resistant and Wistar rats that receive an intracerebroventricular (icv) infusion of Na^+ rich aCSF (Huang et al 2001, 2006). Downstream to increased CSF[Na^+], a pathway has been described involving mineralocorticoid receptors (MRs), benzamil sensitive Na^+ channels, "ouabain", and angiotensin II type 1 receptors (AT_1-R) (Huang et al 1998, Zhao et al 2001, Wang and Leenen 2003, Huang et al 2008). Blood pressure (BP) responses to increased CSF[Na^+] may involve activation of AT_1-R in the SFO as the BP response to injection of NaCl into a lateral ventricle can be blocked by AT_1-R blockade in the SFO (Rohmeiss et al 1995a). Recent studies demonstrated the co-expression of MRs and epithelial Na^+ channels (ENaC) in the SFO consistent with a role for the SFO in mediating responses to CSF[Na^+] and neuronal excitation through this pathway (Amin et al 2005). Although these components are present in the SFO, whether they are involved in the pathway leading to sympathetic hyperactivity and hypertension to an increase in CSF[Na^+] and local SFO [Na^+] has not yet been determined.

The following thesis paper investigates the role of aldosterone, MRs, and AT_1-R in the SFO in mediating the BP and heart rate (HR) response to increases in CSF[Na^+] and local [Na^+]. To accomplish this, Na^+ rich aCSF was infused into the SFO or lateral cerebroventricle of Wistar rats and the resulting effect on BP and HR determined. Various agonists and antagonists of the receptors and molecules thought to be involved in this BP and HR

response were injected or infused into the SFO to determine the effect on BP and HR to changes in CSF and SFO [Na^+].

1.1 Dietary Salt and Na^+ Homeostasis

1.1.1 Central Cardiovascular Regulation

A balance between excitatory and inhibitory signaling regulates sympathetic tone and arterial pressure and these excitatory and inhibitory signals are in turn modulated by various peripheral and central mechanisms. The central component of cardiovascular regulation relies heavily on regions of the brain comprising the nuclei of the lamina terminalis (LT). Among these, the SFO and OVLT lack a blood brain barrier (BBB) and are responsible for the detection of various central and peripheral stimuli. The SFO and OVLT have significant efferent projections to cardiovascular regulatory regions such as the PVN and SON (Figure 1) and relay information to these regions to modulate sympathetic nerve activity (SNA) (McKinley et al 2001).

The PVN has direct efferent connections to the rostral ventrolateral medulla (RVLM) and also has direct sympathetic efferents to sympathetic vasomotor neurons in the intermediolateral cell column (IML) (Figure 1) contributing to tonic cardiovascular regulation (Pyner and Coote 2000). The PVN along with the SON is also involved in the production and release of key hormones such as arginine vasopressin (AVP).

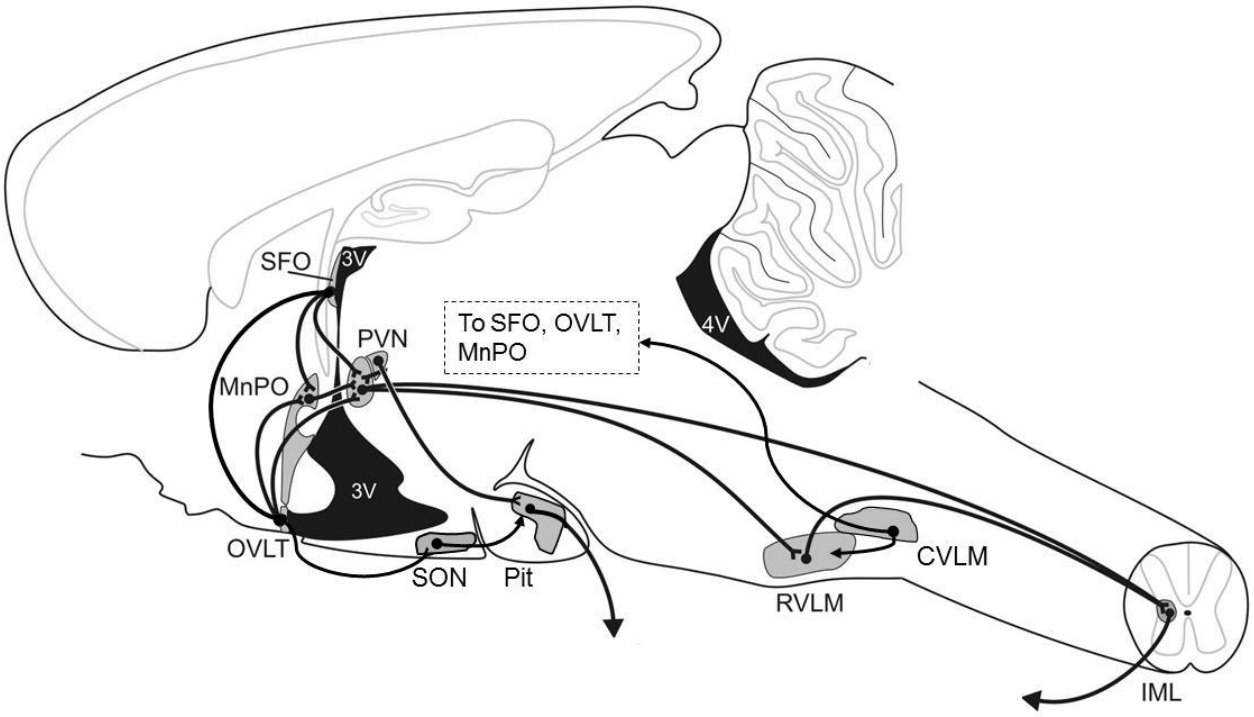

Figure T1. Central components in cardiovascular regulation. SFO: subfornical organ, OVLT: organum vasculosum lamina terminalis, MnPO: median preoptic nucleus, PVN: paraventricular nucleus, SON: supraoptic nucleus; RVLM: rostral ventrolateral medulla, CVLM: caudal ventrolateral medulla; IML: intermediolateral cell column, Pit: pituitary.

Image modified from Abrams and Osborne 2008

1.2 Circumventricular Organs of the Lamina Terminalis (LT)

The CVO's of the LT, SFO and OVLT, are two groups of neurons that are critical in the maintenance of cardiovascular and body fluid homeostasis. Several distinctions separate the SFO and OVLT from other regions in the brain. First, the SFO and OVLT along with other CVO's lack the normal BBB that shields the rest of the brain from circulating factors. Through the presence of specialized capillaries that contain fenestrations in their

endothelial cells, circulating factors can 'circumvent' the BBB and access these two regions. A second distinction involves the sensory aspect of these two nuclei. The SFO and OVLT have few afferent connections while containing a great number of neuronal efferents, and are termed sensory CVO's as they are able to sense and transmit information to appropriate brain centers. The median preoptic nucleus (MnPO) is the third structure comprising the LT. Although it lacks the characteristics of the other two nuclei in the LT, the MnPO contains numerous reciprocal connections to both the SFO and OVLT.

1.3 Structure and neuroanatomical connections of the SFO, OVLT and MnPO

1.3.1 SFO

The SFO is located on the midline anterior wall of the third ventricle and bulges into the third ventricle. Scanning electron microscopy studies show that the structures of the ependymal cells across the surface of the SFO itself are different. These include distinctions in structure and immunostaining pattern dividing the ependymal cells on the surface of the SFO into the rostral, central and caudal segments indicating a possible difference in function (Dellman and Simpson 1976 and 1979). The central region of the SFO has neurons that lie entirely on the surface of the ventricle (Dellman and Simpson 1976). In addition there are ependymal tanycytes, specialized ependymal cells that have elongated processes, on the surface of the ventricular space that project their processes deep into the SFO to contact neurons, dendrites, axons, capillaries and glial cells providing a route for the SFO to contact the CSF as well as creating a point of contact between the plasma and CSF (Dellman 1985, 1998).

Unlike the majority of the brain that is shielded from circulating substances by a tight BBB, the SFO contains a network of type III capillaries classified so by the fenestrations in their endothelial cells that allows entry to circulating substances. These capillaries, found densest in the center or ventromedial core of the SFO where most neurons are located, are often surrounded by an unusually large perivascular connective tissue space which branch into surrounding tissue (Bouchard et al 1989, Dellman 1998). Blood flow to the SFO is nearly double as compared to other regions while plasma transit time was 3-4 times greater (Gross 1991). This suggests that the SFO has increased perfusion while at the same time a slow velocity in blood flow allowing for greater exposure of circulating substances to receptors in the SFO

The SFO has two functional subdivisions, ventromedial core and periphery or outer shell (Figure 2), which show distinctions in their capillary densities, receptor binding, c-fos expression and immunostaining pattern. Neuroanatomical tracings have shown that a large majority of the axons that terminate in hypothalamic regions like the PVN and SON arise from the periphery or outer shell of the SFO (pSFO) (Sunn et al 2003). On the other hand efferents from the ventromedial core (cSFO), where a large majority of fenestrated capillaries appear to be confined, have traditionally been documented to project to the rostral bed nucleus of the stria terminalis (BNST) (Swanson et al 1986, Sunn et al 2003). Recently, Kawano and Masuko (2010) demonstrated that neuronal projections from both the periphery and core of the SFO terminate in the PVN. Using anterograde and retrograde tracing techniques, neurons from the pSFO were found terminating in the magnocellular region (mPVN) of the PVN while neurons from the cSFO were found terminating in the

parvocellular region (pPVN) of the PVN indicating that the cSFO may be involved in regulating changes in sympathetic activity.

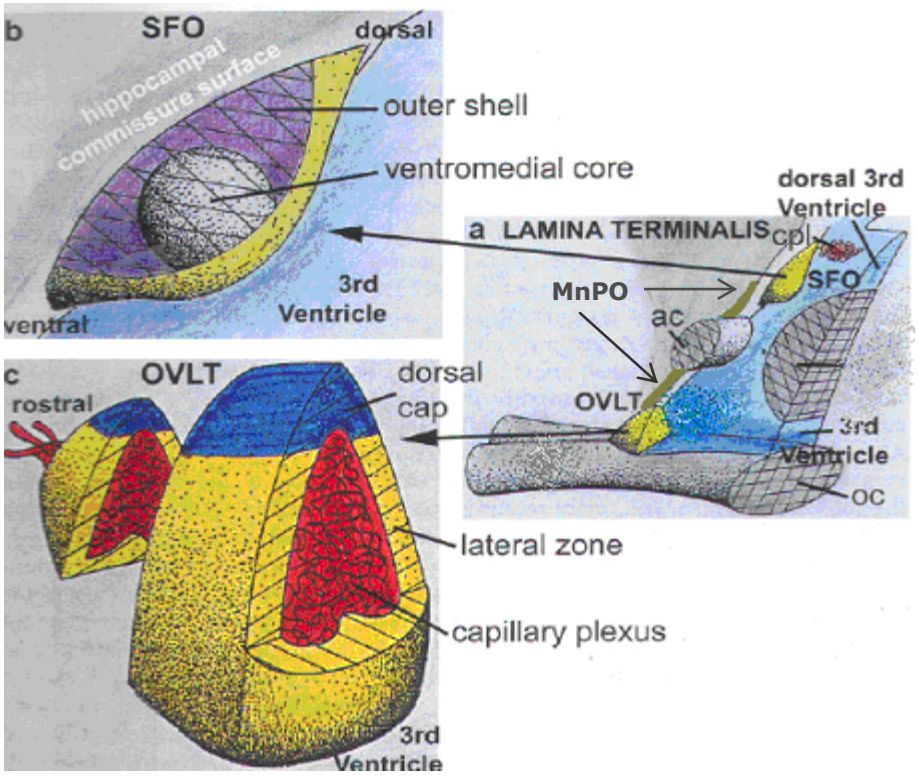

Figure T2. The nuclei of the lamina terminalis (a). Functional subdivisions of the subfornical organ (b) and organum vasculosum lamina terminalis (c). SFO: subfornical organ, OVLT: organum vasculosum lamina terminalis, MnPO: median preoptic nucleus, ac: anterior commisure, oc: optic chiasm, cp: choroid plexus. Mckinley et al 2003

Within the lamina terminalis the SFO has reciprocal projections to both the OVLT and MnPO indicating that these nuclei potentially function as a unit (Camacho and Phillips 1981, Lind et al 1982). Studies using double retrograde tracer analysis have shown that the SFO has axons from the same neuron ending in the MnPO and PVN (Duan et al 2008). Nuclei like the CVLM may function to modulate the activity of the SFO, OVLT and MnPO.

Direct projections from the CVLM to the SFO, OVLT and MnPO were identified through ionotrophic uptake of Phaseolus vulgaris leucoagglutinin (PHA-L), a plant lectin that is anterogradely transported (Babic et al 2004). Stimulation of CVLM neurons that had anterograde transport into the SFO, OVLT and MnPO with L-glutamate resulted in a significant BP decrease (-21 +/- 3.2 mmHg) confirming that the CVLM modulates BP (Babic et al 2004).

1.3.2 OVLT

The OVLT is situated along the ventral end of the midline anterior wall of the third ventricle. Together with the ventral MnPO, it is termed the ventral anteroventral third ventricle region (vAV3V). This elongated structure contacts the MnPO at its dorsal border where the characteristic absent BBB in the OVLT serves as the anatomical distinction among the two regions (Mckinley et al 2003). A population of fenestrated capillaries arise in the adjacent pia matter and perfuse the OVLT, thus allowing for the sensing of blood borne substances (Yamaguchi et al 1993). The OVLT is distinguishable from surrounding tissue via the distinct non-ciliated surface of its bulbous base that slightly bulges into the third ventricle (Yamaguchi et al 1993, Mckinley et al 2003).

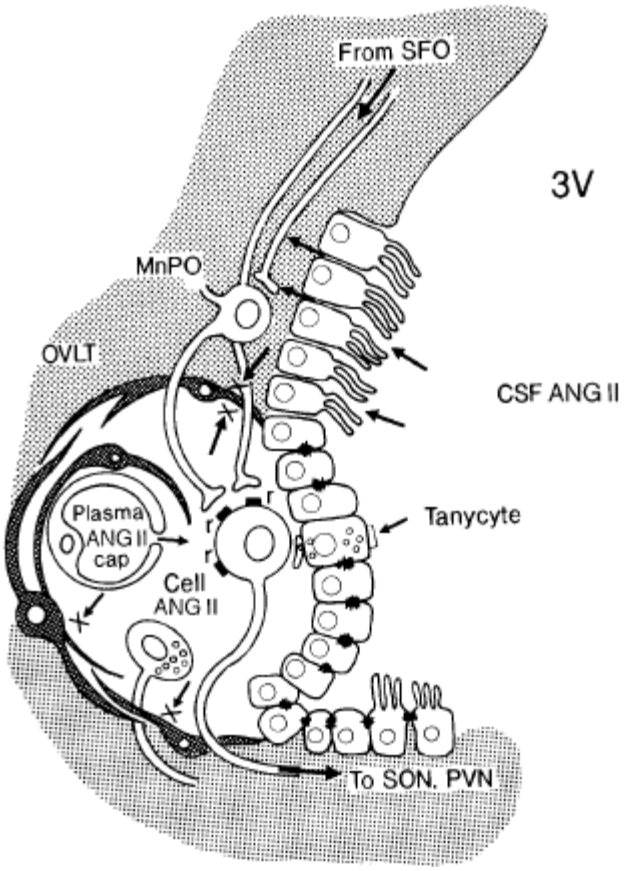

Figure T3. The OVLT and its inner structure. Glial cells form a separation between OVLT and remainder of brain while fenestrated capillaries allow for the entry of blood born substances into the OVLT.

The surface of the OVLT contains non-ciliated ependymal cells that form tight junctions while nearby regions exposed to CSF are ciliated

The presence of ependymal tanycytes (specialized ependymal cells that have processes going deep into the OVLT) also allow for contact between CSF and the inner structures of the OVLT. (Fitzsimons 1998)

Similar to the functional subdivisions of the SFO, the OVLT has distinctions in its vascular architecture, neural connectivity, receptor density and immediate early gene expression to stimuli which divide it into three regions. The first is in the rostromedial vascular region, characterized by its dense capillary plexus (McKinley et al 2003). A second subdivision involves the region of the dorsal cap (Figure 2) which is the site from where neuronal projections terminating in the SON and mPVN arise (McKinley et al 2003, Shi et al 2008). The last subdivision consists of the lateral and posterior periventricular tissues and neuronal projections terminating in the BNST, lateral hypothalamus and pPVN arise from this region of the OVLT (Mckinley et al 2003, Shi et al 2008,). Retrograde tracer analysis has

shown that the OVLT has connections with the SFO, MnPO, SON and PVN (Camacho and Phillips 1980, Shi et al 2008)

1.3.3 MnPO

The tissue lying in the midline anterior wall of the third ventricle between the SFO and OVLT is termed the median preoptic nucleus (MnPO). This region extends from the ventral end of the SFO to the dorsal end of the OVLT, interrupted half way by the anterior commissure (Figure 2). Although the MnPO is behind the BBB it is extensively connected to both the SFO and OVLT. Neuroanatomical studies indicate the presence of direct projections from the MnPO to the PVN and SON (Figure 1), in particular to the vasopressin and oxytocin secreting neurons in these sites (Sawchenko and Swanson 1983, Yasuda et al 2000).

1.4 Ion channels and receptor distribution

1.4.1 Renin-Angiotensin System

The presence of the pro-renin receptor, a receptor that binds the inactive pro-renin and activates it through a non-proteolytic mechanism, has been measured through RT-PCR and immunohistochemistry in both human and rat hypothalamus (Shan et al 2009, Takahashi et al 2010). This receptor was found localized in the magnocellular neurons of the PVN and SON of humans and dissociated hypothalamic and brainstem cell cultures of Wistar rats. Renin mRNA has been detected in rat and mouse whole brain extracts through Northern

blot analysis and RT-PCR from the brainstem of wistar rats (Dzau et al 1986, Iwai and Inagami 1992, Jo et al 1996, Nishimura et al 1997). Assays conducted on brain punches with the addition of inhibitors for angiotensinase and in a pH where cathepsin D would be inactive have indicated the presence of renin-like activity in the PVN, SFO and OVLT of rats (Naruse et al 1980, Schelling et al 1982, Naruse et al 1985). Within the lamina terminalis renin immunoreactive cells have been detected using a renin antibody (Inagami et al 1980). Immunohistochemistry studies in human, rat and mouse brain sections have shown the presence of renin staining in neurons of hypothalamic nuclei such as the PVN and SON (Slater et al 1980, Fuxe et al 1980). In the rat, staining was found specifically in the neurosecretory oxytocin and vasopressin containing nerve cell bodies (Fuxe et al 1980, Inagami et al 1980). The substrate for renin, angiotensinogen (AGN), is also present throughout the brain and specifically in the SFO, OVLT and MnPO (Bunnemann et al 1992, Lippoldt et al 1993, Riftina et al 1995, Son et al 2003, O'Callaghan et al 2011). AGN mRNA has also been detected in the PVN and SON through in situ hybridization (Bunnemann et al 1992). Using in-situ hybridization combined with immunocytochemistry for glial fibrillary protein, angiotensinogen mRNA within these regions was found localized in astroglial cells and not neurons (Bunnemann et al 1992, Lippoldt et al 1993). More recent studies have shown through RT-PCR on cultured rat brain cells that neurons as well as astroglia express similar levels of AGN (Ferrari et al 2007).

ACE mRNA and binding densities have been demonstrated in neurons and astroglia and specifically in the SFO, OVLT and MnPO through RT-PCR and autoradiography (Cheung et al 2006, Ferrari et al 2007, Lu et al 2009, Bourassa and Speth 2010). Angiotensin II

immunoreactive cells and fibers are also present in the SFO (Lind et al 1984, Strittmatter and Snyder 1987, Chai et al 1987, Bourassa and Speth 2010). Ang II stained cells, likely neurons, were observed in the periphery of the SFO while fibers were seen densely in the core of the SFO. Retrograde transport of Fast Blue in combination with Ang II immunoreactivity showed that Ang II fibers both enter and leave the SFO with fibers entering the SFO possibly arising from the perifornical zone of the lateral hypothalamic area (Lind et al 1984). The same study showed that Ang II is likely within SFO neurons as it appears to undergo axonal transport in the SFO as pretreatment with colchicine, a blocker of axoplasmic transport, increased Ang II staining within cell bodies while decreasing staining in axons. ACE, Ang II and AT_1-R are found within the SON and the magnocellular and parvocellular regions of the PVN while ACE and AT_1-R mRNA and binding densities are also present within the RVLM (Strittmatter et al 1984, Lind et al 1985, Weyhenmeyer and Phillips 1985, Phillips et al 1993, Lenkie et al 1998, Wang et al 2003, Lu et al 2009, Bourassa and Speth 2010, Huang et al 2011). Both ACE and AT_1-R binding densities were greater within the mPVN than the pPVN (Huang et al 2011). Efferent signaling from the SFO and OVLT terminate in both magnocellular and parvocellular regions of the PVN and SON (Mckinley et al 2003, Kawano and Masuko 2010) and some of these efferents may be using Ang II as a neurotransmitter. In support, Jhamandas and group showed that the magnocellular neurons in the SON that receive efferents from the periphery of the SFO are Ang II positive (Jhamandas et al 1989). As well, electrical stimulation or direct application of Ang II in the SFO results in excitation of PVN neurons, responses which can both be blocked by Losartan in the PVN (Li and Ferguson 1993). The study also showed that

electrical stimulation of the SFO activates neurons in the pPVN that have efferents terminating in the IML.

The SFO and OVLT contain receptors for a large number of circulating hormones, neurotransmitters and neuropeptides. Among these, the best studied is the AT_1-R which is present with high concentrations in both the SFO and OVLT (Wang et al 2003, Bourassa and Speth 2010). Distribution of the AT_1-R in the SFO and OVLT varies in the structural subdivisions of these nuclei. In vitro autoradiography using the Ang II peptide analog ^{125}-I[Sar^1, Ile^8]-angiotensin II, showed that the cSFO and the lateral zone of the OVLT have the highest densities of AT_1-R while the pSFO and dorsal cap of the OVLT contain smaller densities (McKinley et al 1998). The cSFO also has greater concentrations of AT_1-R mRNA indicating that the AT_1-R has a heterogeneous distribution within the SFO and OVLT. Studies on AT_2-R in the SFO show conflicting results. Lenkie et al (1997) failed to detect AT_2-R mRNA in the SFO or OVLT by in situ hybridization but recent studies by Lu et al (2009) described the presence of AT_2-R in the SFO and OVLT through RT-PCR. AT_2-R mRNA has also been identified in the SON and PVN (Lu et al 2009). AT_2-R positive immunoreactivity was found predominantly in the mPVN while the SON expressed greater densities of the receptor that had a cytoplasmic localization (Reagan et al 1994).

1.4.2 Aldosterone, MR and Benzamil sensitive Na^+ channels

All components required for the biosynthesis of aldosterone have been detected in the human and rat brain indicating that aldosterone may be synthesized within the brain. The

ancilliary protein steroidogenic acute regulatory protein (StAR), required for transport of cholesterol into the inner membrane of mitochondria to begin the first step of aldosterone synthesis has been found in the hypothalamus (Furukawa et al 1998). Messenger RNA for adrenodoxin, involved in electron transfer to CYP11A1 for the side chain removal of cholesterol has been detected in whole brain extracts localized to glial cells (Mellon and Deschepper 1993) and more specifically in the hypothalamus and brainstem (Strömstedt and Waterman 1995, MacKenzie et al 2000). Messenger RNA levels have been detected for the side chain cleavage enzyme (CYP11A) in the hypothalamus and brain stem (Strömstedt and Waterman 1995, MacKenzie et al 2000) while mRNA and protein levels for the 3β-hydroxysteroid dehydrogenase (3βHSD) have been detected in the hypothalamus (Guennoun et al 1995). 21-hydroxylase (CYP21) was detected in the brainstem (Strömstedt and Waterman 1995) and assessment of dissociated rat brain cells revealed that CYP21 is found localised in astrocytes (Lovelace et al 2003). Through the use of RT-PCR mRNA levels have been detected for the 11β-hydroxylase (CYP11β1) and aldosterone synthase (CYP11β2) in the hypothalamus and brain stem (Strömstedt and Waterman 1995, MacKenzie et al 2000, Ye et al 2008, Gomez-Sanchez et al 2010). Messenger RNA for CYP11β1 and CYP11β2 was found in the SFO, OVLT, PVN, SON, RVLM and CVLM (Kumar et al 2006, Wang et al 2010), but protein levels have only been detected in the cortex of rats, particulairly in purkinje cells (MacKenzie et al 2000). Aldosterone has been measured in the brain stem, hypothalamus, hippocampus and cerebellum (Huang et al 2008, Huang et al 2009, Gomez-Sanchez et al 2010) with corticosterone having a much greater concentration than aldosterone (Huang et al 2008). In adrenal intact rats, a low salt diet increases plasma and brain aldosterone levels while a high salt diet suppresses levels in both plasma and

brain (Gomez-Sanchez et al 2005, Huang et al 2009). In adrenalectomized rats, plasma levels of aldosterone and corticosterone are undetectable (Gomez-Sanchez et al 2005). In these rats brain aldosterone levels were still detected but not corticosterone. This confirms that the aldosterone biosynthesis components measured in the brain can be active and can synthesize low levels of this hormone locally.

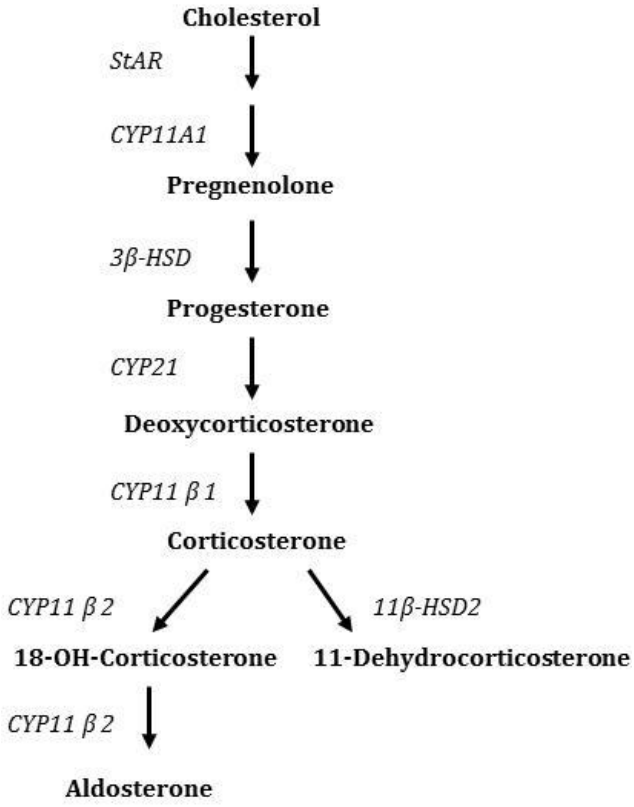

Figure T4. Aldosterone biosynthesis pathway. StAR: steroidogenic acute regulatory protein; CYP11A1: side chain cleavage enzyme; 3βHSD: 3β-hydroxysteroid dehydrogenase; CYP21: 21-hydroxylase; CYP11β1: 11β-hydroxylase; CYP11β2: aldosterone synthase; 11βHSD2: 11beta-hydroxysteroid dehydrogenase type 2.

In the kidneys, preference for aldosterone binding to MR is conferred with the presence of 11beta-hydroxysteroid dehydrogenase type 2 (11βHSD2), an enzyme that inactivates corticosterone (Gomez-Sanchez et al 2005). RT-PCR showed that 11βHSD2 is expressed in the brain stem, hypothalamus (Gomez-Sanchez et al 2010) and cortex (Zhang et al 2006) of rats. More specifically 11βHSD2 was found in the NTS and PVN of rats with levels in the

PVN being 2.6-fold higher than that in the cortex of rats (Geerling et al 2006, Zhang et al 2006). Expression of 11βHSD2 mRNA and protein was also detected in the NTS, subcommisural organ and ventromedial hypothalamus (Roland et al 1995, Geerling et al 2006). Importantly, expression of 11βHSD2 mRNA has also been detected in the SFO of rats (Leenen et al unpublished observations). Thus, 11βHSD2 may function similarly in the hypothalamus and brainstem, as seen in the kidneys, by enhancing aldosterone binding to MR.

The mineralocorticoid receptor (MR) is a ligand activated transcription factor belonging to the nuclear hormone receptor family. Upon binding to it receptor, the Aldosterone-MR translocates into the nucleus and increases the expression of genes such as those of ENaC in the distal nephron of the kidneys, a genomic effect that requires at least 30min-1hr (Booth et al 2002). A faster non-genomic effect also occurs within minutes resulting in the modulation of intracellular ion concentrations (Booth et al 2002, Lösel et al 2003). In rats, following implantation of DOCA salt into the amygdala, sodium appetite was increased within 15min of DOCA implanting and absent the following day (Saki et al 2000). This indicates that in the brain, non-genomic effects of aldosterone are present and may function to modulate behavior such as sodium appetite.

Within the SFO and other nuclei of the LT, mRNA and immunohistochemistry analysis demonstrated MR is co-expressed with the voltage-insensitive, amiloride-blockable channel ENaC (Amin et al. 2005). Messenger RNA for the α-ENaC, β-ENaC and γ-ENaC subunits along with MR was found in neurons of the lamina terminalis, strongly suggesting

a functional relationship where perhaps MR, through aldosterone binding, may modulate ENaC channel activity (Booth et al 2002, Amin et al. 2005). Although mRNA levels were high, protein for the γ-ENaC was not detectable in the SFO and OVLT (Amin et al. 2005). These results indicate that there may either be transcriptional regulation on the γ-ENaC protein or a quick turnover rate of this protein making it undetectable. Although all three ENaC subunits are required for an optimally active channel, the expression of α and β-ENaC is sufficient for the presence of an active channel. Protein and mRNA for the three ENaC subunits were also found co-expressed with MR in the SON and PVN, with high concentrations in the mPVN and little in the pPVN (Amin et al. 2005).

1.4.3 Na^+/K^+ ATPase and Ouabain

The Na^+/K^+ ATPase is an integral membrane protein found in all cells and important for the maintenance of electrochemical gradients of Na^+ and K^+ across cell membranes. This ATPase is composed of two subunits (α and β) with the α1β1 isozyme being largely conserved in all cells and functioning to maintain basal ionic gradients (Lingrel and Kuntzweiler 1994). The catalytic α-subunit of this enzyme contains a binding site for cardiac glycosides such as Ouabain (Price et al 1989). Although all three isoforms of the α-subunit are found in the CNS, the α3 isoform is found almost exclusively in neurons (Brines and Robbins 1993, Van Huysse 2007). This isoform has a high affinity for ouabain and helps to restore resting membrane potentials during repeated firing and depolarization of neurons (Brines and Robbins 1993). In situ hybridization using adult mouse SFO sections showed that mRNAs encoding the α1 and α2 isoforms of Na^+/K^+ ATPase were expressed in astrocytes and ependymal cells of the SFO, but signals for the α3 isoform were not detected

(Shimizu et al 2007). Whether this pattern of distribution is similar in the SFO of rats has not yet been studied.

A ouabain like compound (OLC) has been isolated from bovine hypothalamus (Li et al 1998, Kawamura et al 1999). In rat and macaque brain slices ouabain immunoreactivity has been detected in the magnocellular neurons of the PVN and SON (Yamada et al 1992b). Fibers were seen running through the lateral hypothalamic area to the infundibulum. "Ouabain"IR-positive fibres were also identified in the SFO while the origin of these fibres is not clearly known (Yamada et al 1992a). ICV injection of ouabain or the OLC from hypothalamic and pituitary extracts increases BP, HR and RSNA (Huang et al 1992). This response is blocked by an icv injection of Fab-fragments, which bind ouabain with high affinity (Huang et al 1992) indicating that ouabain in the brain acts to increase sympathetic activity and BP. Direct injection of ouabain into the MnPO and the PVN results in increases of BP indicating that these regions are sensitive to ouabain (Budzikowski and Leenen 2001, Gabor and Leenen 2009). In wistar rats, BP, HR and RSNA responses to acute (10min) infusions of 0.3M Na^+ rich aCSF can be blocked by icv infusion of Fab-fragments (Wang et al 2003). Chronic icv infusion of Na^+ rich aCSF causes a 50% increase in brain OLC content of mice and rats and increases BP, HR and RSNA (Huang et al 2006, Van Huysse et al 2011). The BP, HR and RSNA increase to chronic icv infusion of Na^+ rich aCSF can be blocked by icv Fab-fragments in rats indicating that a locally produced OLC is involved in these responses to Na^+ (Huang et al 1998). In mice, the α2 subunit of the Na^+/K^+ ATPase appears to bind the OLC and mediate the downstream responses to increases in CSF[Na^+]. Mutation of the α2 subunit, resulting in a functional Na^+/K^+ ATPase that is resistant to ouabain, fully prevents the BP and HR responses to chronic infusion of Na^+ rich aCSF (Van Huysse et al 2011).

1.4.4 Na_x Channel

Recently, a [Na^+] sensitive Na_x channel involved in sensing Na^+ levels in the brain was found in the SFO, OVLT, median eminence (ME) and the neurohypophysis (Noda 2006). The expression appears to be mainly in the astrocytes and ependymal cells of the CVO's (Wanatabe et al 2006). In mice, the expression of this channel in the SFO is critical for Na^+ sensing. Following a 2 day dehydration period or injection of a hypertonic Na^+ solution (0.5M NaCl) into a cerebral ventricle water intake was induced in mice and an aversion to saline while in Na_x knockout mice this reaction was fully blocked and restored only with re-introduction of Na_x into the SFO (Hiyama et al 2004). Sodium sensitivity assays done on dissociated SFO cells, by bathing cells in a Na^+ solution and measuring entry of sodium into cells, showed that these Na_x channel expressing astrocytes were sensitive to Na^+ concentration just above physiological (0.170M) levels (Wanatabe et al 2006). Althougn no documented link has been made between the Na_x-channel and the aldosterone-MR-ouabain pathway involved in mediating responses to increases in CSF[Na+], the activity of these Na_x-channels is dependent on Na^+/K^+ATPase as Na_x expressing cells are no longer able to take up Na^+ in the presence of 1M ouabain (Shimizu et al 2007). This shows that ouabain is able to bind Na^+/K^+ATPase in the SFO but whether this is associated with changes in BP is not known. Ouabain is likely binding the α2 subunit in the SFO as the Na_x channel, associated with the Na^+/K^+ATPase, is found in glia while α3 is found only in neurons (Wanatabe et al 2006). Thus ependymal cells facing the cerebral ventricles and Na_x channel containing astrocytes located around blood vessels may contribute to sensing sodium levels in the CSF and blood. Gamma-aminobutyric acid (GABA) producing neurons,

identified through the presence of the enzyme glutamic acid decarboxylase (GAD) which catalyzes the conversion of glutamate to GABA, were found surrounded by Na_x channel containing glial cells (Wanatabe et al 2006). Na_x positive glial processes were also seen extending to neurons that did not have GAD positive staining indicating that in the SFO Na_x associates with both GABAergic and non-GABAergic neurons (Wanatabe et al 2006). Whether BP and HR are affected through the Na_x channel still remains to be investigated.

1.4.5 Excitatory and Inhibitory Molecules

Reciprocal signaling between the neurons of the lamina terminalis largely involves the release of glutamate and GABA excitatory and inhibitory molecules that are stored and released from pre and post-synaptic terminals of neurons. Glutamate can be produced in both neurons and astrocytes using glucose as a substrate. Glucose is converted to pyruvate in both neurons and astrocytes through glycolysis. Pyruvate is then fed into the tricarboxylic acid (TCA) cycle for conversion into glutamate (Hertz et al 1999). In astrocytes, pyruvate can aso be converted into lactate or alanine and transported to neurons in what is known as the lactate-alanine shuttle. In neurons, glutamate is released upon depolarization but is quickly taken up by astrocytes via the glutamate transporters GLAST (L-glutamate/L-aspartate transporter) (Bauer et al 2012) and GLT-1 (L-glutamate transporter) (Pines et al 1992). In a process known as the glutamate-glutamine cycle, this glutamate is converted to glutamine in astrocytes through glutamine synthase (Norenberg and Martinez-Hernandez 1979) and released back into the synaptic cleft where it is taken up by neurons (McKenna et al 1996). Once glutamine enters neurons, is is converted back to glutamate through the enzyme phosphate-activated glutaminase (PAG) (Hertz et al

1999). The glutamate-glutamine cycle and lactate-alanine shuttle thus supply glutamine and pyruvate to neurons and maintain synthesis of glutamate (Hertz et al 1999, Waagepetersen et al 2003). The type 2 vesicular glutamate transporter (vGlut2), a positive marker for glutamatergic neurons, is responsible for vesicular glutamate uptake at the nerve terminal following glutamate release and is found localized on axon terminals (Lin et al 2003). This transporter has been detected in SFO, OVLT, MnPO, PVN (magnocellular and parvocellular) and SON neurons (Grob et al 2003, Lin et al 2003). Receptors for glutamate are found throughout the brain in a nonuniform pattern (Halpain et al 1984) and are classified into metabotrophic receptors (mGluR) that utilize an intracellular second messenger to cause the opening of ion channels and ionotrophic receptors [N-methyl-D-aspartate (NMDA-R) and 2-amino-3-(5-methyl-3-oxo-1,2- oxazol-4-yl)propanoic acid (AMPA-R)]. During depolarization Na^+ enters the neurons through the opening of ion channels (Carter and Bean 2009). The ionotrophic NMDA-R and AMPA-R have been detected in the SFO, OVLT and MnPO (Guilhaume and Corrêa 2001). In this study NMDA, an NMDA-R agonist, was used to cause excitotoxic lesions in the SFO, OVLT and MnPO through the selective over stimulation and destruction of neurons. This resulted in 65% and 48% reduction of AT_1-R binding densities in the SFO and MnPO respectively but not in the OVLT indicating that a large majority of AT_1-R in the SFO and MnPO are colocalized with glutamatergic neurons. Electrophysiological studies have also shown that following electrical activation of SFO neurons that project to the MnPO, the application of AMPA-R and NMDA-R (glutamate receptor) antagonists in the MnPO results in inhibitory responses in MnPO neurons (Kolaj et al 2004) illustrating that SFO efferents terminating in the MnPO use glutamatergic signalling. The OVLT sends excitatory signaling to the SFO as electrical

activation of OVLT neurons resulted in both excitatory and inhibitory responses in SFO neurons (Osaka et al 1992). The molecules involved in the excitatory responses were suggested to be glutamate as between 50-75% SFO neurons tested were excited by application of this neurotransmitter.

Messenger RNA and protein levels for the two isoforms of glutamic acid decarboxylase GAD65 and GAD67, responsible for the synthesis of GABA, have been measured in neurons of the SFO, OVLT and MnPO (Esclapez et al 1994, Grob et al 2003). GAD65 was found clustered predominantely in nerve terminals while GAD67 is found primarily in the neuronal cell body (Esclapez et al 1994). Receptors for GABA are classified into $GABA_A$-R, ionotrophic receptors which utilize the opening and closing of ion channels, and $GABA_B$-R, metabotrophic receptors which are G-protein coupled receptors that utilize a metabolic process. Binding of GABA to $GABA_A$ results in the opening of ion channels that allow entry of Cl^- (ionotrophic receptors) resulting in the hyperpolarization of the neurons, effectively inhibiting the firing of these neurons. Both receptor subtypes are found throughout the brain (Young and Chu 1990). Osaka et al (1992) showed that the SFO has interneurons that are involved in mediating inhibitory signals. Electrical activation of SFO interneurons coming from the dorsal and ventral SFO regions resulted in excitatory responses in SFO neurons, responses that were not sensitive to kynurenic acid, a glutamate receptor (NMDA-R) antagonist showing that the electrical activation and resulting excitatory response was not a result of glutamate release. However, application of the $GABA_A$-R antagonist bicuculline resulted in excitation of SFO neurons (Osaka et al 1992). Thus, the excitatory responses seen to electrical activation of the SFO interneurons is likely via the inhibition of

tonically active inhibitory GABAergic signaling coming from these interneurons. This is in agreement with experiments by Honda et al (2001) that showed populations of spontaneously active GABAergic interneurons within the SFO whose activity was completely abolished by bicuculline. Electrophysiological studies showed that electrical activation of SFO neurons that project to the MnPO, the application of $GABA_A$-R antagonist in the MnPO results in excitatory responses in MnPO neurons (Kolaj et al 2004) illustrating that SFO efferents terminating in the MnPO use GABAergic signalling to modulate responses. In the OVLT, application of the GABA receptor antagonists bicuculline ($GABA_A$-R antagonist) or phaclofen ($GABA_B$-R antagonist) result in NA release in the MnPO indicating that the efferents from the OVLT to the MnPO involve tonic GABA mediated inhibitory signaling that prevent basal NA release in the MnPO (Ushigome et al 2003). The OVLT also sends inhibitory signaling to the SFO as electrical activation of OVLT neurons resulted in both excitatory and inhibitory responses in SFO neurons (Osaka et al 1992). The molecules involved in the inhibitory response was suggested to be GABA as between 50-75% SFO neurons tested were inhibited by application of this neurotransmitter. During blockade or activation of GABA receptors in the NTS, NA release in the SFO was dose dependently increased or decreased (Tanaka et al 2002). This may be one mechanism through which the SFO is able to respond to peripheral changes in BP where changes relayed through baroreceptors terminating in the NTS may modulate tonic GABAergic inhibition in the SFO.

1.5 Function of the Lamina Terminalis

The lamina terminalis is implicated in the regulation of fluid and electrolyte balance, specifically the generation of thirst, vasopressin release, Na^+ appetite, SNA and BP are all influenced by this region. The following section will focus mainly on mechanisms involved in the control of SNA and BP by Ang II and Na^+.

1.5.1 CNS Actions of Circulating Ang II

Pioneering work by Simpson and colleagues showed that application of Ang II in the SFO resulted in a dose dependent increase in BP as well as the stimulation of thirst (Mangiapane and Simpson 1980). It soon became clear that the SFO is also a central site of action of blood born Ang II. Both intravenous (iv) and subcutaneous (sc) infusion of Ang II in rats (Mckinley et al 1992, Roland et al 1994a) and in rabbits (Potts et al 1999) result in neuronal activation of the SFO, OVLT, MnPO, PVN and SON and increased BP. In the SFO, OVLT, MnPO, PVN (parvocellular and magnocellular regions) and SON, the Fos related antigen (Fra), an immediate early gene marker for neuronal activation with a longer half-life that Fos, is detected during sc infusion of Ang II (Huang et al 2010). During sc infusion of Ang II, 150ng or 500ng/kg/min, rats become hypertensive with neuronal activity visible first in the SFO by day 1 and day 4 and diminishing by day 14 of treatment (Huang et al 2010). AT_1-R mRNA in the SFO during sc Ang II infusion was significantly decreased levels by 14 days of treatment at 150ng/kg/min suggesting that there is desensitization of the SFO to chronic sc Ang II infusion (Nunes and Braga 2011). Measurement of Fra levels in the MnPO indicates that activation in the MnPO follows that of the SFO where only mild

neuronal activity is detected early on in the MnPO with levels increasing gradually and diminishing by 14 days (Huang et al 2010). Unlike the SFO, other regions like the PVN and SON have gradual increases in neuronal activation that last throughout the 14 days indicating the presence of an alternative mechanism that sustains neuronal activation and BP responses to chronically increased circulating Ang II levels (Huang et al 2010).

In rats the BP responses to chronic (14 days) sc Ang II (150ng/kg/min) infusion is attenuated but not fully blocked by SFO or OVLT lesioning (Osborn et al 2012, Vieria et al 2010). During sc infusion of Ang II (10ng/kg/min) BP increased by 11 ± 3.0 and 16 ± 4mmHg over a 7 or 10 day infusion period respectively (Hendle and Collister 2005, Vieria et al 2010). In SFO lesioned rats BP increases were reduced to 3.7 ± 1.4 mmHg (Hendle and Collister 2005) and 4 ± 1mmHg in OVLT lesioned rats (Vieria et al 2010). Lesioning the vAV3V (OVLT and vMnPO) blocks the BP responses to chronic sc infusion of Ang II. In control rats, chronic infusion of Ang II (490ng/kg/min for 14 days) increased BP by ~40mmHg on day 7 and 14 (Marvar et al 2010). In vAV3V lesioned rats BP was unchanged on day 7 and increased by 7 mmHg on day 14. Studies that ablated both the dorsal and ventral regions of the MnPO showed attenuation of BP responses to chronic iv Ang II (10ng/Kg min) (Ployngam and Collister 2007). In this study BP was increased by ~22mmHg in sham rats and 15mmHg in MnPO lesioned rats by day 2 of infusion and nearly 38mmHg in sham and 18mmHg in MnPO lesioned rats. On the other hand, acute BP responses to circulating Ang II don't appear to require signaling via the MnPO. In experiments where the MnPO was ablated (Gutman et al 1989) or it connections to the SFO electrolytically cut (Lind and Johnson 1982), the BP responses to iv Ang II were not

affected. These results indicate that lesioning one region of the lamina terminalis results only in a significant attenuation of BP responses to circulating Ang II likely because there is a significant amount of reciprocial signaling between the SFO, OVLT and MnPO. However, to fully block the responses ablation of the entire LT appears to be required.

1.5.2 CNS Actions of Central Ang II

After icv injection of Ang II, Fos-IR is detected strongly in the SFO, OVLT, MnPO, PVN and SON (Herbert et al 1992, Roland et al 1994b, Mckinley et al 1995,). Icv injections of low amounts of Ang II (90-100ng) result in Fos-IR activation predominantly in the pSFO and the mPVN (Rowland et al 1994b, Mckinley et al 1995). Moellenhoff and group (2001) showed that Fos-IR after icv injection of Ang II (100ng) is predominantly expressed in the mPVN and SON and colocalized with AT1-R. Higher amounts of icv Ang II (250ng) cause Fos-IR in the entire SFO as well as both parvocellular and magnocellular regions of the PVN (Herbert et al 1992, Xu and Herbert 1995). This indicates that small increases in ventricular Ang II levels may only activate regions that mediate AVP release while greater increases also result in activation of cardiovascular control regions through the activation of the pPVN. Blockade of AT_1-R in the MnPO prevents the excitability of vasopressin secreting PVN neurons during activation of the SFO via circulating Ang II or direct Ang II application in the SFO (Tanaka 1989) indicating that neural inputs from the MnPO to the SON and PVN appear to terminate in vasopressin and oxytocin secreting neurons in these sites. BP was not measured in this study. Activation of the PVN and SON following a slow icv injection of Ang II (250pg/2ul over 120sec) can be blocked by lesioning the MnPO (Xu

and Herbert 1995). The electrolytic lesioning method used may have interrupted SFO fibers in the MnPO bound for downstream targets like the PVN and SON as excitotoxic lesions of the MnPO, that destroy the MnPO neuronal cell bodies while leaving fibres intact, block drinking responses but do not affect BP increases (15-20mmHg) to icv injection of Ang II (50ng) (Jones 1988). Ventral AV3V lesions do not affect Fos-IR levels in the SFO following icv Ang II while levels in the SON are blocked and mPVN and pPVN show reduced Fos-IR activity (Xu and Herbert 1996). Lesioning this region comprised of the OVLT and vMnPO does not affect the BP responses to icv injections of Ang II (10ng or 30ng) (Veerasingham and Leenen 1997). These results indicate that the OVLT and MnPO may not have a role in mediating BP responses to icv Ang II and may instead have a greater role in regulating thirst and vasopressin release. BP responses to icv Ang II appear to be mediated predominantely through the SFO.

Chronic icv infusion of Ang II in rats increases BP by ~66 mmHg (1ug/hr for 10 days) (Porter et al 2003) and 28mmHg (0.5ug/hr for 5 days) (Porter and Potratz 2003). In rabbits chronic icv infusion of Ang II increases BP by 19 mmHg (3ug/hr for 5 days) (Fink et al 1983) and ~10mmHg in dogs (6ug/hr for 3 days) (Ma et al 1999). Responses appear to be mediated through the AV3V as lesioning that region blocks the BP responses to chronic icv infusion of Ang II (3ug/hr for 5 days) in rabbits (Fink et al 1983). In the periphery, the BP response to chronic central increase in Ang II is mediated fully through an increase in sympathetic activity (Bruner and Fink 1986) as acute ganglionic blockade and combined α and β adrenergic receptor antagonists to block sympathetic activity, fully block the BP responses to chronic icv infusion of Ang II (Bruner and Fink 1986).

1.6 Central Sites in Na^+ Homeostasis

In Dahl S and SHR, high Na^+ intake results in activation of the sympathetic nervous system (SNS) and hypertension. This activation is preceded by increases in CSF[Na^+], which does not occur in Dahl R or Wistar rats on a high Na^+ diet indicating that there is increased transport of Na^+ into the CSF of Na^+ sensitive animals (Huang et al 2004). The increases in BP and HR can be mimicked by an icv infusion of Na^+ rich aCSF in Wistar rats (Huang et al 1998). The magnitude of increase in BP and HR resulting from an equivalent increase in CSF[Na^+] in the Dahl S and SHR is significantly enhanced as compared to the Wistar rats suggesting an increase in the sensitivity of those hypertensive animals to Na^+ (Huang et al 2001).

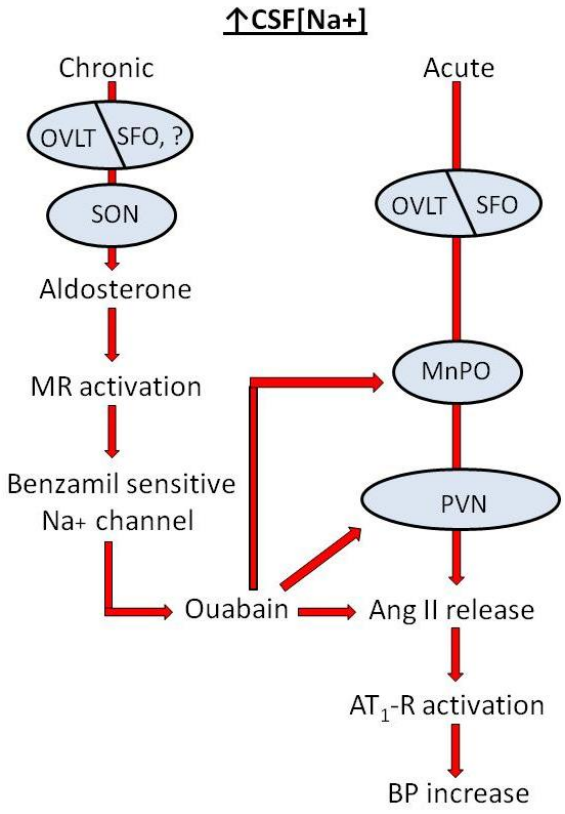

Figure T5. Activation pathway during acute and chronic increases in CSF[Na^+]. Acute increases in CSF[Na^+] may lead to increased Ang II release and AT_1-R activation in the SFO, OVLT, MnPO and PVN leading to BP increases. Ouabain release in the MnPO is also involved in this activation pathway. During chronic increases in CSF[Na^+] an increase in hypothalamic aldosterone may lead to MR activation and the expression of a benzamil sensitive Na^+ channel (possibly ENaC). Increased "ouabain" and Ang II release result in enhanced AT_1-R activation in brain nuclei, possibly the PVN, leading to BP increases.

1.6.1 Acute Increase in CSF [Na^+]

Acute icv infusion of Na^+ rich aCSF increases BP, HR and RSNA (Huang and Leenen 1996, Wang et al al 2003, Moriata et al 2004, Kato et al 2004, Chu et al 2005,). These responses are mediated through brain pathways responding specifically to changes in CSF[Na^+] and not a change in the CSF osmolarity. In rats, icv infusion of 0.7M mannitol, 0.6M sucrose or 0.6M urea (Osborn et al 1989) and icv infusion of sorbitol at 0.9M in sheep did not change BP, HR or RSNA (May and McAllen 1997). Similarly in the PVN, BP responses to acute increases in [Na^+] are a result of changes in [Na^+] per se as an osmotically equivalent solution of Mannitol caused no BP responses (Gabor and Leenen 2009).

Responses to acute icv infusion of Na^+ rich aCSF do not involve an MR dependent pathway as infusion of the MR blocker eplerenone prior to infusion of 0.3M Na^+ rich aCSF does not affect the resulting increases in BP (Leenen et al unpublished data). Benzamil sensitive Na^+ channels are however involved. In acute studies 0.26M/10ul benzamil injected icv before icv infusion of 1.5M NaCl, blocked the BP, HR and abdominal SNA responses to NaCl (Nishimura et al 1998). Benzamil sensitive Na^+ channels like ENaC are present in the ventricular ependyma and on neurons (Wang et al 2010). Whether responses to acute infusion of Na^+ rich aCSF are mediated through the activation of these ventricular channels or benzamil sensitive Na^+ channels located on neurons is not clear. Ouabain also plays a role in the acute responses to increased CSF[Na^+], as icv injection of fab-fragments fully blocks the BP, HR and RSNA responses to an acute icv infusion of 0.3M NaCl (Huang et al 1992, Huang and Leenen 1996). It is not clear if this BP response involves release of newly

synthesized “ouabain” or if tonic levels of “ouabain” already present in the brain are mediating the responses during acute icv infusion of Na^+ rich aCSF. In sheep, responses to acute increases in CSF[Na^+] can be blocked by icv infusion of the AT_1-R blocker Losartan (May and McAllen 1997). Similarly in rats, BP and HR increases by acute icv infusion of Na^+ rich aCSF and icv injection of ouabain can be blocked by icv infusion of Fab fragments or the AT_1-R blocker Losartan. The responses to icv Ang II can only be blocked by icv Losartan and not Fab fragments (Huang and Leenen 1996) indicating that AT_1-R activation, presumably by Ang II release, is downstream to ouabain release.

The responses to Na^+ rich aCSF can be enhanced by a prior infusion of aldosterone (Wang et al 2003). Icv infusion of a non-pressor dose of Na^+ (aCSF with 0.16M Na^+) increases BP and HR when infused following icv aldosterone (Wang et al 2003). The aldosterone mediated enhancement of responses to Na^+ can be blocked by benzamil and fab-fragments, indicating that benzamil sensitive Na^+ channels (possibly ENaC) and “ouabain” release are involved in mediating these aldosterone enhanced responses (Wang et al 2003).

In the PVN, acute increases in [Na^+] increase BP which can be enhanced by a prior infusion of aldosterone (Gabor and Leenen 2009). Only the aldosterone mediated enhancement of responses to Na^+ in the PVN can be blocked by MR blockade, benzamil and fab-fragments. This indicates that benzamil sensitive Na^+ influx (possibly via ENaC) and “ouabain” release are involved downstream to MR activation in mediating these BP and HR responses (Gabor and Leenen 2009). These responses to Na^+ alone and the aldosterone mediated enhancement of responses can both be blocked by AT_1-R blockade in the PVN indicating that Ang II release and AT_1-R activation in the PVN contributes to of these responses.

1.6.2 Chronic Increases in CSF[Na^+]

In Wistar rats, chronic increases in CSF[Na^+] of 4-5mM increase BP, HR and RSNA (Huang et al 2006). These chronic increases in CSF[Na^+] increase hypothalamic aldosterone levels and MR binding as administration of the MR blocker spironolactone prevents the associated BP and HR responses (Huang et al 2006). FAD 286, an aldosterone synthase inhibitor, does not affect the acute increase in BP but fully blocks the increases in hypothalamic aldosterone levels and the BP, HR and RSNA responses observed to chronic increases in CSF[Na^+] (Huang et al 2008). Thus during chronic increases in CSF[Na^+] enhanced MR activation is achieved through increased brain synthesis of aldosterone. Infusion of benzamil, which blocks benzamil sensitive Na^+ channels, fully blocks responses to chronic infusion of aldosterone in 0.15M Na^+ rich aCSF and prevents the increase in hypothalamic "ouabain". This indicates that downstream to increased hypothalamic aldosterone, there is enhanced activation of benzamil sensitive Na^+ channels (possibly ENaC) causing increases in brain "ouabain". The increase in the synthesis of brain "ouabain" is part of the pathway that mediates responses to chronic increases in CSF[Na^+] as Fab-fragments, which bind ouabain and prevent its binding to the Na^+/K^+ ATPase, block responses to chronic central infusion of NaCl (Huang et al 1998). Responses to chronic increases in CSF[Na^+] also involve AT_1-R activation. Icv infusion of an AT_1-R blocker in rats (Huang et al 1998) and sheep (Mathai et al 1998) fully blocks the BP and HR responses to chronic increases in CSF[Na^+] indicating that these responses use an angiotensinergic pathway. During chronic increases in CSF[Na^+] ACE and AT_1-R densities are increased in cardiovascular control regions like the PVN and the nuclei of the lamina terminalis (SFO, OVLT and MnPO) (Huang et al 2006). Icv Fab-fragments prevent these increases in ACE and

AT_1-R densities. Increases in BP, ACE and AT_1-R densities in the mPVN, pPVN and SON are also observed in wistar rats chronically infused with aldosterone, increases which are blocked by concomitant infusion of benzamil and fab fragments (Huang et al 2011). Thus, increases in ACE and AT_1-R densities are downstream to increases in aldosterone levels, activation of benzamil sensitive Na^+ channels and increase in "ouabain" release.

In Dahl S and SHR rats, a high sodium diet increases CSF[Na^+], BP, HR and RSNA (Huang and Leenen 1996, 1998, Huang et al 2009a). The BP and HR responses to chronic high sodium diet in Dahl S rats are mediated via increased hypothalamic aldosterone (Huang et al 2009a). Hypothalamic aldosterone levels increase in Dahl S rats chronically fed with a high sodium diet. Infusion of FAD286 blocks both the increase in hypothalamic aldosterone levels and the Na^+ induced BP and HR responses (Huang et al 2009a) indicating that increases in hypothalamic aldosterone levels are involved in the BP and HR responses. Chronic icv infusion of aldosterone in aCSF causes similar increases in BP, HR, RSNA (Huang et al 2005) supporting the observation that aldosterone in the brain of Dahl S rats mediates the BP and HR responses to a high sodium diet. Downstream to hypothalamic aldosterone, BP, HR and RSNA responses to chronic high sodium diet in Dahl S rats are mediated through activation of a benzamil sensitive sodium channel as infusion of benzamil blocks these responses (Wang et al 2001). Chronic high sodium diet or chronic infusion of aldosterone in Dahl S rats also increases brain ouabain (Huang and Leenen 1996, 1998, Huang et al 2005) which can be blocked by benzamil (Wang et al 2001). This indicates that the activation of benzamil sensitive sodium channels is upstream to increases in brain "ouabain". Blockade of AT_1-receptors with icv losartan blocks the BP, HR

and RSNA responses to chronic high sodium intake in Dahl S rats (Huang et al 1998) indicating that responses to chronic high sodium diet in Dahl S rats also involve AT_1-R activation.

1.7 Brain Regions Involved in Mediating Responses to Increases in CSF[Na^+]

Although this activation pathway has been described in the response to chronic increases in CSF[Na^+] (Figure 5), the brain regions that are responsible for initiating responses to increases in CSF[Na^+] still remain unclear. Studies assessing the sequence of events during changes in CSF[Na^+] indicate that the SFO and OVLT are likely the first to be activated. Through the use of magnetic resonance imaging to follow the time course of magnesium entry into neurons during neuronal activation, icv injection of NaCl (10ul of 1.5M) results in the near immediate activation of the SFO and OVLT followed by the PVN and SON with a time delay of 0-5.8min (Moriata et al 2004). It is possible that the Na_X channel may be activated in the SFO and OVLT during injection of 10ul of 1.5M NaCl as the channel is sensitive to [Na^+] just above physiological concentrations (0.170M). It is however not clear whether the activation of the Na_X channel in the SFO and OVLT is involved in mediating the BP responses following central injection of NaCl. Lesioning the OVLT and vMnPO (Veerasingham and Leenen 1997) attenuates the BP responses to acute icv infusions of Na^+ rich aCSF by ~30%, wheras responses are fully blocked by lesioning the entire LT suggesting that downstream signaling to cardiovascular regions is dependent on an intact SFO, MnPO and/or OVLT (May et al 2000). One region where this pathway may be activated is likely the SFO as BP response to icv injection of NaCl can be blocked fully by AT_1-R blockade in the SFO (Rhomeiss et al 1995).

Ouabain release in the MnPO may have a role in mediating responses to acute increases in CSF[Na^+] as Fab-fragments in the MnPO block the responses to icv Na^+ (Budzikowski and Leenen 1997). The AT_1-R blocker losartan in the MnPO also attenuates BP and HR responses to icv Na^+ (Budzikowski and Leenen 2001). These results indicate that BP and HR responses to increases in CSF[Na^+] involve ouabain release in the MnPO that may be partially mediated through AT_1-R activation. AT_1-R activation in the PVN is also involved in the BP and HR responses to acute increase in CSF[Na^+] as the responses can be blocked by telmisartan, an AT_1-R blocker in the PVN (Gabor and Leenen 2009). BP responses to acute increases in CSF[Na^+] of Wistar rats appear therefore to require the region of the lamina terminalis (Fig T5), and require AT_1-R activation at least in the SFO and MnPO. Downstream signalling from the SFO, OVLT and MnPO involves AT_1-R activation in the PVN.

In SHR, BP and HR gradually increase with age on a regular Na^+ diet and further increase when rats are placed on a high Na^+ diet (Budzikowski and Leenen 1997). These enhanced BP and HR responses are fully blocked by infusion of endogenous ouabain binding Fab-fragments in the MnPO (Budzikowski and Leenen 1997).

In Dahl S rats, chronic high Na^+ diet increases BP and HR (Huang et al 2004). Lesioning the vAV3V (OVLT and vMnPO) blocks 50% of the the sodium induced increases in BP (Goto et al 1982) indicating that in the Dahl S rat this region of the lamina terminalis is involved in mediating these responses. Electrolytic lesions of the PVN block nearly 50% of the BP responses to chronic high sodium diet in Dahl S rats (Goto et al 1981). The hypertension from high Na^+ diet in Dahl S rats can be fully reversed by infusion of an AT_1-R blocker

(candesartan) together with a glutamate receptor blocker (kynurenate) in the PVN (Gabor and Leenen 2012), indicating that increased AT_1-R activation and glutamate release in the PVN contribute to the maintenance of the hypertension from high Na^+ diet in Dahl S rats. Increases in BP and HR are also fully reversed by bilateral injection of an AT_1-R blocker in the RVLM of Dahl S rats on a chronic high Na^+ diet (Ito et al 2003), indicating that the BP and HR increases are sustained through AT_1-R signaling to the RVLM likely from the PVN. Increases in CSF[Na^+] in Dahl S rats by high salt appear therefore to activate a pathway involving AT_1-R activation in the LT, followed by AT_1-R activation in downstream nuclei such as the PVN and RVLM, and hypertension.

1.8 Rational of Study

The accessibility of SFO neurons to the ventricular spaces and its anatomical properties make it a suitable candidate involved in sensing osmotic, ionic or hormonal changes that occur in the plasma or CSF. Injection of 0.2M/1ul NaCl into the SFO caused thirst but no changes in BP or HR (Camargo et al 1984). The effects of higher [Na^+] infusions in the SFO were not studied. Activation of AT_1-receptors in this region appears to be important in mediating responses to increased CSF[Na^+], as AT_1-R blockade using losartan (5ug/200nl) in the SFO prevented BP responses (8 +/-2mmHg) to an icv injection of NaCl (0.3M/5ul) (Rhomeiss et al 1995). However, whether the SFO appears to be detecting increases in CSF[Na^+] or increase in osmolality was not determined. The presence of MR's and ENaC has been confirmed in the SFO but whether they have a role in enhancing Na^+ transport locally has not yet been studied.

For the following project **we hypothesized** first that an acute increase in CSF[Na^+] or in local SFO [Na^+] increases BP via Ang II release in the SFO. Secondly, the BP increases can be enhanced by prior infusion of aldosterone.

1.9 Objectives of Studies in Wistar Rats

1. To assess the responsiveness of the SFO to local increases in [Na^+] and the effect of aldosterone on BP and HR responses to increases in SFO[Na^+].
2. To assess the involvement of AT_1-R in the SFO in mediating responses to increases in CSF and SFO[Na^+].

1.10 Experimental Protocols

SFO Studies

1. Na^+ rich aCSF in the SFO, dose response study
2. Aldosterone and 0.45M Na^+ rich aCSF in the SFO
3. Aldosterone and 0.6M Na^+ rich aCSF in the SFO
4. Candesartan and 0.45M Na^+ rich aCSF in the SFO (Cand DRC)
5. Aldosterone, Candesartan and 0.45M Na^+ rich aCSF in the SFO
6. Aldosterone, Candesartan and 0.6M Na^+ rich aCSF in the SFO
7. Ouabain dose response study in the SFO
8. Osmolality studies in the SFO

Combined ICV and SFO Studies

1. ICV Ang II and Na^+ rich aCSF and Candesartan in the SFO- Infusions
2. ICV Na^+ rich aCSF injection (dose response study)
3. ICV Na^+ rich aCSF and Candesartan in the SFO- Injection

2 Materials and Methods

Animals

Male Wistar rats (200–250 g) were obtained from Charles River Breeding Laboratories (Montreal, QC, Canada). Rats were exposed to a 12h light-dark cycle and fed ad libitum with regular rat chow and tap water. All experiments were carried out according to the guidelines of the Canadian Council on Animal Care, which conforms to National Institutes of Health guidelines, and the study was approved by the University of Ottawa Animal Care and Use Committee. Experiments were conducted after animals had been acclimatized for 1 wk.

Surgical Procedures

For all surgeries, rats were anesthetized with 2% isoflurane in oxygen. Animals were placed in a stereotaxic head frame, and the skull was leveled between the bregma and lambda. For experiments involving infusion of Na^+-rich aCSF in the SFO, a hole was drilled into the skull, and a guide cannula (23 gauge) was positioned 1.3 mm posterior to bregma and 4.5-4.6 mm ventral to the surface of the skull according to the coordinates of the rat brain atlas of Paxinos and Watson (1998). The injection cannula will reach 4.8 mm into the brain, extending another 0.5 mm past the guide cannula. For combined intracerebroventricular and SFO experiments, guide cannulas were positioned in the SFO as mentioned and a second guide cannula placed in a lateral ventricle 0.5 mm posterior and 1.4 mm lateral to bregma. The guide cannula was placed 3.5 mm ventral to the surface of the skull while the injection cannula extend nearly 4 mm into the brain to enter the LV

(Paxino and Watson 1998). Guide cannulas were secured to the skull with two jeweler's screws and acrylic cement. After 1 wk of recovery, the left femoral artery was cannulated with polyethylene-50/10 tubing filled with heparin (1,000 U/ml in 0.9% NaCl).

Experimental Procedures

The morning after the placement of the arterial line, rats were placed in a small cage and given at least 1 hour to acclimatize. The intra-arterial catheters were connected to a pressure transducer interfaced with a PC using AcqKnowledge III software for hemodynamic measurements. The pressure in the Data Acquisition system was standardized to 0 and 200 mmHg. MAP and HR were determined using the AcqKnowledge software which extrapolated these parameters from the raw BP measurements.

For all experiments animals were allowed to settle and baseline levels were recorded for 10 min of stabilization. An "L"-shaped injection cannula (30 gauge) was lowered into the lateral ventricle or SFO through the fixed guide cannula and extended 0.5 mm past the guide. For SFO and icv infusions, cannulas were connected to a 10 or 500 ul Hamilton microsyringe through polyethylene (PE) tubing and mounted on a Harvard infusion pump (model 2400-003). The PE-10 tubing was loaded with alcohol and the corresponding drug to be injected or infused with an air bubble separating the two solutions. A few minutes before the administration of the drug, the injection cannula was inserted into the brain. Once the infusion was started, 10 min was determined from the time the bubble in the PE-tubing started to move indicating movement of drug from the cannula into the brain. Microinjections of 100 nl were conducted by hand over 30 seconds using a 10-ul Hamilton microsyringe. The bubble separating the drug from the alcohol was used to keep track of

the injection as it moved down the PE-10 tubing. Following different pretreatments at least 30 min reset was given before infusion of Na^+-rich aCSF and 45 min rest following Aldosterone treatment. At the end of the experiment, rats were euthanized with carbon dioxide. In some rats 100nl Evans blue dye was injected or infused using the same injections cannulas used for the experiments. Rats were decapitated and brains were collected for histology.

Candesartan is part of a class of drugs known as Angiotensin type 1 receptor blockers. These bind to the AT_1-R to prevent the binding of Ang II. Candesartan was used in our experiments mainly because of its greater affinity for binding the AT_1-R. Competetive binding studies have shown that Candesartan and Losartan bind AT_1-R however Candesartan has an affinity 80X that of Losartan for the receptor (Noda et al 1993, Fabiani et al 2000). Neither compound was seen to bind the AT_2-R (Noda et al 1993). Studies have shown that the Candesartan is able to interact with multiple sites on the AT_1-R while Losartan has a lower number potentially accounting for Candesartan's greater affinity for the receptor (Bhuiyan et al 2009).

Experimental Protocols Using Vehicles

Vehicle: aCSF [which contained (in mmol/l) 115 NaCl, 2.5 KCl, 2.14 $MgCl_2$, 0.65 NaH_2PO_4, 27 $NaHCO_3$, 4.54 Na_2HPO_4, 1 Na_2SO_4, 1 $CaCl_2$ and 5 glucose mmol/L, pH 7.4]

Aldosterone Vehicle: (2% ethanol, 98% aCSF), candesartan (6% DMSO, 94% aCSF at 0.15M Na^+)

Candesartan was generously donated by AstraZeneca. All other injected and infused compounds were purchased from Sigma or Steraloids.

Experimental protocols in the SFO

Na^+-rich aCSF in the SFO. To evaluate the responses to Na^+-rich aCSF in the SFO, Na^+-rich aCSF at 0.45 and 0.6 M Na was infused into the SFO for 10 min at 100 nl/min. Na^+-rich aCSF was prepared by adjusting the [Na^+] of aCSF with additional NaCl.

Aldosterone and Na^+-rich aCSF in the SFO. To evaluate whether aldosterone enhances responses to Na^+-rich aCSF in the SFO, aldosterone was infused into the SFO at 50 and 150ng per 100 nl/min for 10 min. A 45-min recovery period was given to allow for the activation of the early genomic effects of aldosterone (Booth et al 2002) and then infusion of Na^+-rich aCSF (0.45M and 0.6 M Na^+) was carried out. Doses of aldosterone were adjusted from experiments in the PVN that showed enhancement of responses to Na^+ rich aCSF in the PVN by 300 ng per 300 nl/min for 10 min (Gabor and Leenen 2009). Neither dose of aldosterone enhanced the responses to 0.6M Na^+-rich aCSF, thus we determined the possible effect of the higher dose of aldosterone 1500 ng) on the lower [Na^+] of 0.45M. Infusion of Aldosterone (150 ng per 100 nl/min for 10 min) was followed by a 45-min recovery period and infusion of 0.45M Na^+ rich aCSF (100 nl/min for 10 min).

Aldosterone, Candesartan and Na^+ rich aCSF in the SFO. Ang II dose response study was first done to determine a dose that causes a BP response higher than responses observed with infusion of Na^+ rich aCSF. Vehicle, 10ng, 20ng, 40ng and 80ng Ang II were injected slowly into the SFO. All injections were in 500nl/30 sec except for the 80ng Ang II given in 100nl/30 sec. 80ng Ang II was chosen for further experiments. An appropriate dose of Candesartan was then determined by a dose response study. Vehicle (100 nl/min for 10

min), 5 (0.5 ug/100nl/min for 10 min) or 10ug (0.5 ug/100 nl/min for 20 min) Candesartan were infused into the SFO, a 30 min resting period was given and followed by a slow injection of 80 ng/100nl Ang II given over 30 sec. 5 ug Candesartan partially blocked BP responses while 10 ug Candesartan fully blocked BP responses to 80 ng Ang II in the SFO and was used in further experiments.

To evaluate whether responses to Na^+ rich aCSF in the SFO are mediated via AT_1-R activation, Candesartan was used in the SFO. Candesartan was infused into the SFO, a 30 min rest given and followed by infusion of 0.6M Na^+ rich aCSF. In other groups of rats, 10 ug Candesartan or vehicle was infused into the SFO and followed by infusion of Aldosterone + 0.45M Na^+ rich aCSF.

SFO Osmolarity Studies. To assess for possible osmolar effects, a solution of Mannitol osmotically equivalent to 0.6M Na^+ rich aCSF was infused into the SFO. Mannitol (0.85M: 1136 mOsm/kgH_2O) was infused into the SFO (100 nl/min for 10 min), 30 min later 80 ng Ang II was injected (80 ng/100nl over 30 sec) and the resulting BP response recorded.

Combined Intracerebroventricular and SFO Experimental Protocols

ICV Ang II, Na^+ rich aCSF and Candesartan in the SFO: To assess whether BP responses to icv infusions of Na^+ rich aCSF can be fully blocked by AT_1-R blockade in the SFO, a combined ICV-SFO study was performed. 0.3M Na^+ rich aCSF (3.8 ul/min for 10 min) was infused icv 30 min before and 30 min after infusion of 10ug Candesartan (0.5 ug/100nl/min for 20 min) into the SFO. In the same experiment, Ang II (30 ng/3 ul over 30 sec) was injected into a lateral ventricle 1 hr before and 1 hr after infusion of 10 ug Candesartan (0.5 ug/100 nl/min for 20 min) into the SFO to determine effect on responses by AT_1-R blockade in the

SFO. Dose of Ang II injected icv was taken from Huang et al (1996) who reported an increase in BP of 18 ± 3 mmHg by 30ng Ang II icv.

ICV injection of Na^+ rich aCSF and SFO infusion of Candesartan. To assess if BP responses to an injection rather than infusion of Na^+ rich aCSF into a lateral ventricle would be blocked by Candesartan in the SFO we injected a bolus dose of 0.3M Na^+ rich aCSF (10ul of 0.3M Na^+ rich aCSF over 30 sec) 30 min before and 30 min after infusion of 10ug Candesartan (0.5ug/100nl/min for 20min) in the SFO. All icv injections were separated by 30min. Since it was determined that the BP responses to 10ul of 0.3M Na^+ rich aCSF can be blocked by 10ug Candesartan in the SFO, a 20ul injection of 0.3M Na^+ rich aCSF was given to determine if responses would still be blocked. The volume of 0.3M Na^+ rich aCSF to be injected icv was determined by a volume response study. 5u, 10ul and 15ul of 0.3M Na^+ rich aCSF were injected icv slowly over 30seconds. Although BP responses were similar among the three volumes, 10ul injection was chosen and used throughout the remainder of experiments.

Ouabain dose response studies in the SFO. To assess the responsiveness of the SFO to local administration of Ouabain, various doses of Ouabain were initially infused then injected into the SFO. Vehicle, 80ng, 160ng, 320ng, 480ng, 640ng and 960ng of Ouabain were infused (100nl/min for 5min) into the SFO and the resulting effects on BP and HR monitored. Various groups of rats were used in determining responsiveness of the SFO to increasing doses of Ouabain. Each group received only two doses of Ouabain and had at least a 30min resting period until the second infusion. In another group of rats, Ouabain was infused (100nl/min for 5 min) icv then 30 min later injected (500nl/30sec) to

determine the effect on BP and HR. It was determined that an icv infusion of Ouabain gave no BP responses while the slow injection increased BP. We went on to give a slow injection of 640ng and 960ng Ouabain (500nl/30) into the SFO. Injections were separated by a 30 min resting period.

Histology. At the end of all experiments rats were euthanized in CO_2 and decapitated. In some rats, Evans blue Dye was injected or infused to determine extent of brain area saturated by the infused or injected drugs. To remove the brains, the skull was broken away to expose the brain. The brainstem and cerebellum were discarded and the cortex collected. Brains were then frozen in 2-methylbutane at 20°C and sectioned (20 um) using a Leica cryostat or stored at -80 °C. A 1% Neutral Red stain was used to stain collected brain slices. Brain slices were incubated in the stain for 5 min and washed for 30 sec-1 min in distilled water (dH_2O) twice. Slices were then dehydrated in increasing solution of ethanol/H2O ($EtOH/H_2O$) for 1 min with each dehydration step being repeated (2x 50% EtOH, 2x 75% EtOH, 2x 95% EtOH in H_2O). Slides were then left in 100% Xylene overnight. The next day sections were air dried, dipped in xylene briefly, and cover-slipped with Permount. A light microscope was used to visualize the location of the SFO or icv in relation to the placement of the guide cannula. If the extent of tissue damage from the guide cannula was in close proximity to the SFO or entering a lateral ventricle, the rat was included in the experimental groups.

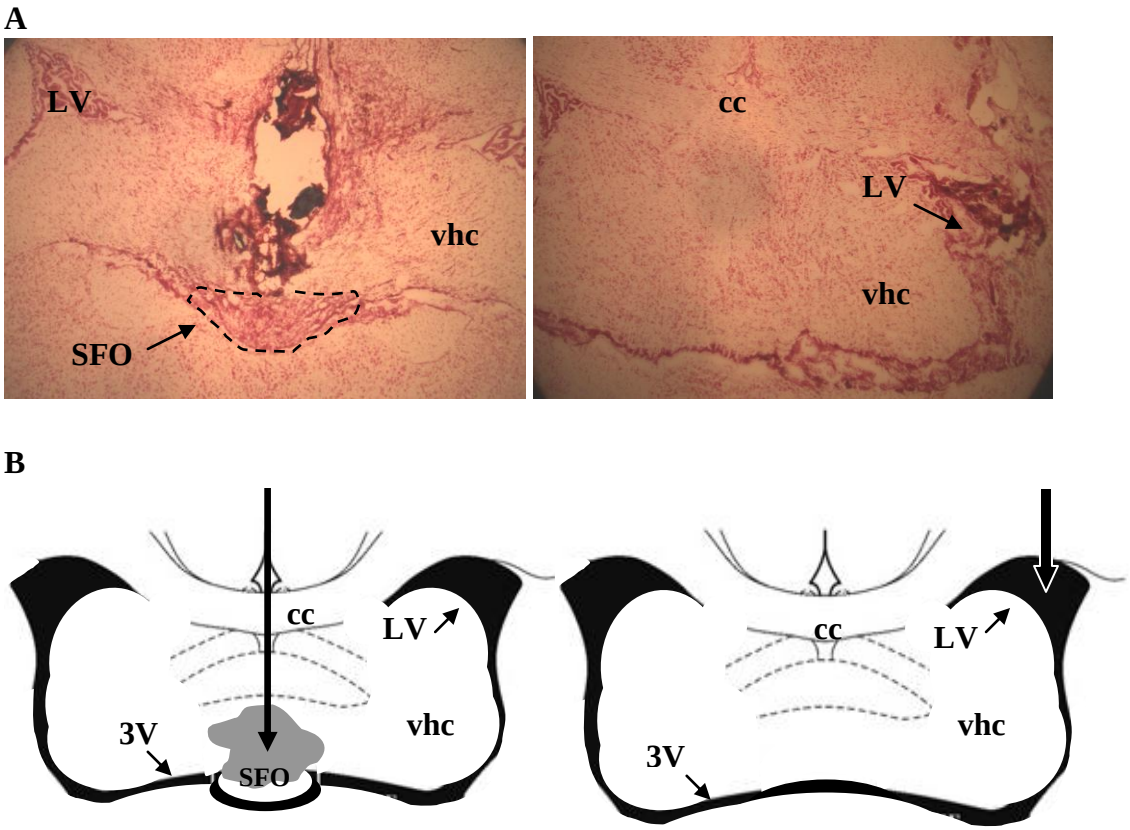

Figure T6. Entry of the guide cannula into the SFO and lateral ventricle. A: actual brain slices depicting the entry of the guide cannula into the SFO and lateral ventricle. Guide cannula can be followed as the regions where the tissue has been destroyed terminating right on the border of the SFO or inside a lateral ventricle. B: Cartoon depicting entry of the guide cannula. LV: lateral ventricle, cc: corpus callosum, 3V: third ventricle, vhc: ventral hippocampal commissure, SFO: subfornical organ.

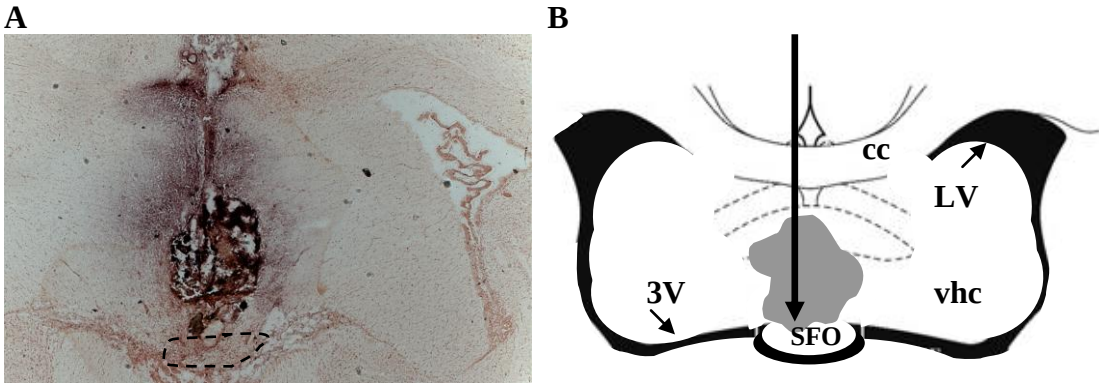

Figure T7. Area of SFO saturated during an infusion. A: Actual brain slices depicting the spread of Evans Blue dye in the region of the SFO during an infusion at 100nl/min for 10 minutes. B: Cartoon depicting spread of dye into region. LV: lateral ventricle, cc: corpus callosum, 3V: third ventricle, vhc: ventral hippocampal commissure, SFO: subfornical organ.

Statistical Analysis. Values are expressed as means ± SE. The following statistical tests were used: 1) for comparisons of peak changes among multiple treatments, one-way ANOVA; 2) for comparison of peak changes among two groups, t-test; and 3) for pairwise comparisons of the area under the curve, t-tests. The level of significance was set at $P < 0.05$.

3 Results

3.1 Na^+ rich aCSF in the SFO

To assess whether infusion of Na^+ in the SFO increases BP and HR, aCSF, 0.45M and 0.6M Na^+ rich aCSF were infused. Each infusion was given over 10 min and followed by a 30 min rest until the next infusion.

Baseline MAP was not different among all three treatment groups (Table R1). Infusion of aCSF alone had no effects on BP while infusions of 0.45M and 0.6M Na^+ rich aCSF into the SFO resulted in dose dependent increases in BP, indicating that SFO neurons may be Na^+ sensitive (Fig R1). Responses reached a plateau at 2-3 min and returned to baseline within 5 min of the end of infusion. BP was raised by 5 ± 1 and 11 ± 2mmHg by 0.45M and 0.6M Na^+ rich aCSF respectively (Fig R2). Peak changes were significantly different from vehicle treated groups as well as between 0.45M and 0.6M respectively (Fig R2). Infusions of the same Na^+ concentrations into regions outside the SFO or into the third ventricle (3V) did not change BP (Fig R3). There was a tendency for HR to go down in some groups but overall HR did not show a statistically significant change from baseline throughout all treatments (Table R2).

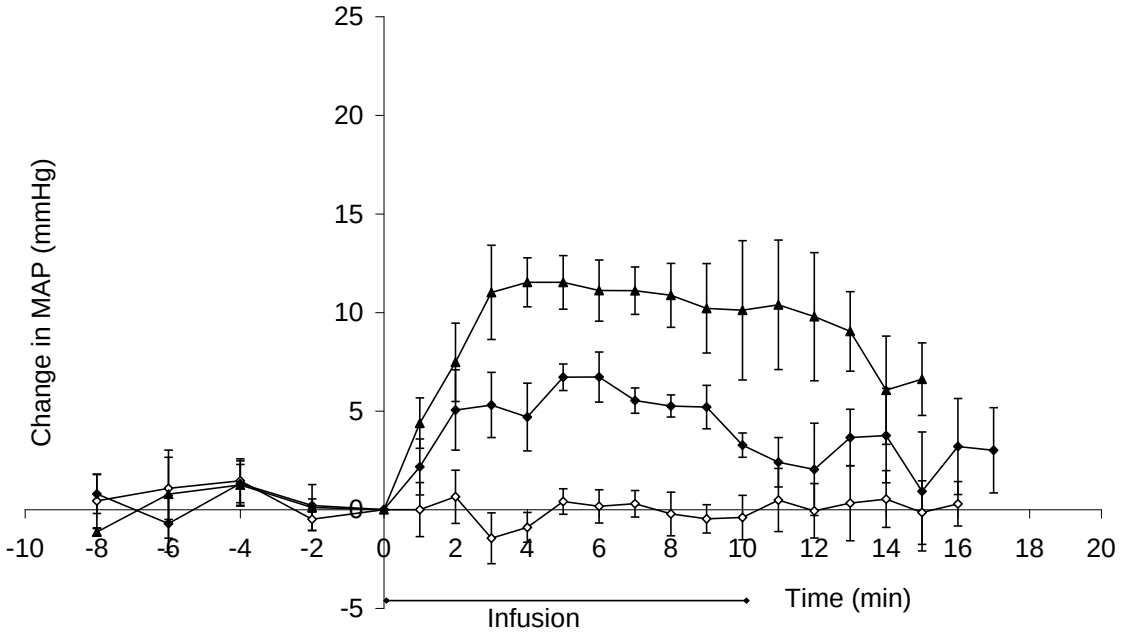

Figure R1. Infusion of Na^+ rich aCSF into the SFO. aCSF (◇), 0.45M (◆) and 0.6M (▲) Na^+ rich aCSF. Points graphed are the mean (every 1 min) with the standard error. One way ANOVA on the area under each curve was used for statistical analysis. $P < 0.05$ for aCSF vs. 0.45M or 0.6M and 0.45M vs. 0.6M. n = 5.

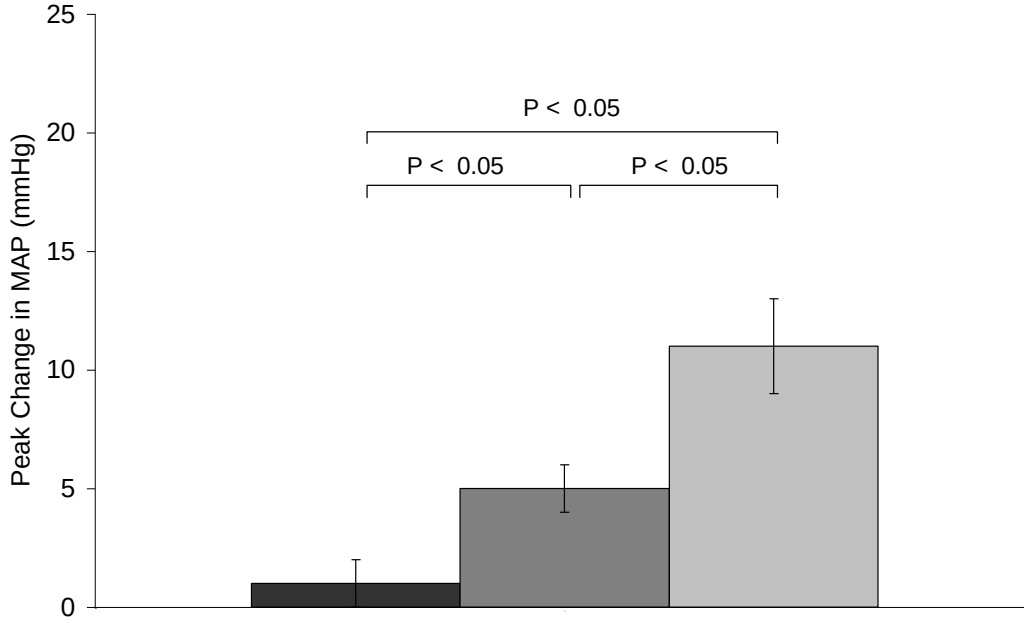

Figure R2.Peak increases in BP to infusion of Na^+ rich aCSF into the SFO. aCSF (■), 0.45M (■) and 0.6M (□) Na^+ rich aCSF. Peak changes were determined between t=4-10 min. One way ANOVA was used for statistical analysis. n =5

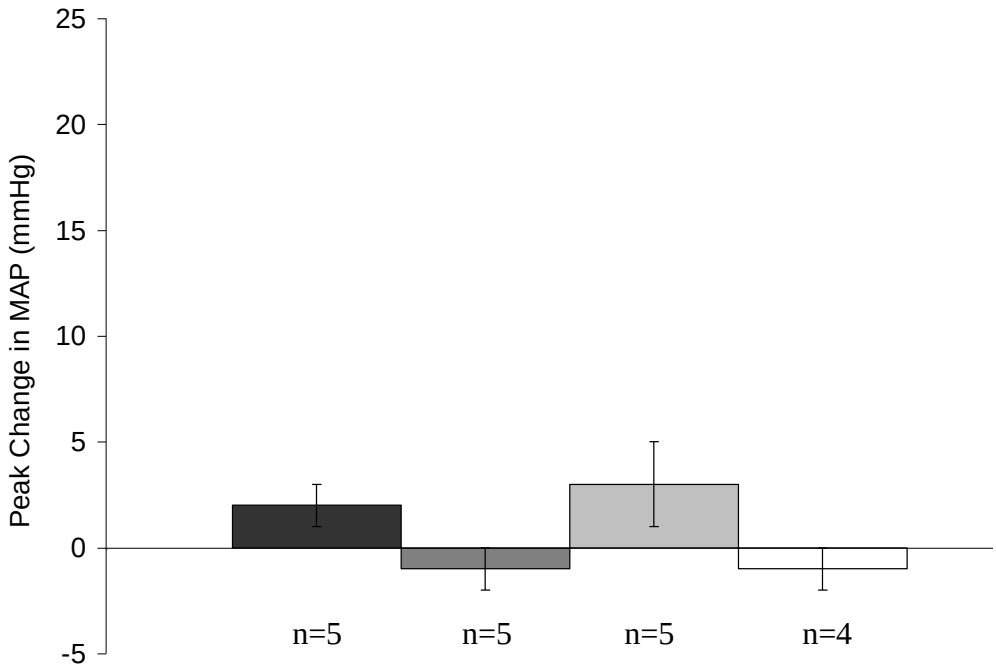

Figure R3. Peak increases in BP to infusion of Na^+ rich aCSF into regions outside the SFO. aCSF (■), 0.45M (■) and 0.6M (□) Na^+ rich aCSF infusion into regions surrounding the SFO and 0.6M (□) Na^+ rich aCSF infusion into the 3V. Peak changes were determined between t=4-10 min. One way ANOVA was used for statistical analysis.

Baseline MAP (mmHg)	Treatment	Baseline MAP (mmHg)	Treatment
Na^+ rich aCSF in the SFO			
124 ± 2	Vehicle	125 ± 4	0.6M
124 ± 3	0.45M		
Angiotensin II in the SFO			
		128 ± 7	80 ng Ang II
136 ± 6	Vehicle	127 ± 8	*Vehicle* + 80 ng Ang II
121 ± 7	5 ug Candesartan	118 ± 5	*5 ug Cand* + 80 ng Ang II
137 ± 5	10ug Candesartan	129 ± 4	*10 ug Cand*+ 80 ng Ang II
Aldosterone and Na^+ rich aCSF in the SFO			
121 ± 5	Vehicle	116 ± 3	*Vehicle* + 0.45M
119 ± 8	1500 ng Aldosterone	116 ± 6	*1500 ng Aldo* + 0.45M
122 ± 3	Vehicle	124 ± 5	*Vehicle* + 0.6M
111 ± 3	500 ng Aldosterone	109 ± 3	*500 ng Aldo* + 0.6M
120 ± 6	1500 ng Aldosterone	116 ± 5	*1500 ng Aldo* + 0.6M
Candesartan and Na^+ rich aCSF in the SFO			
120 ± 4	1500 ng Aldosterone	120 ± 5	*Aldo* + *Veh* + 0.45M
121 ± 5	Vehicle	109 ± 5	*Aldo* + *Cand* + 0.45M
121 ± 3	10 ug Candesartan		
118 ± 5	Vehicle	121 ± 4	*Vehicle* + 0.6M
121 ± 4	10 ug Candesartan	118 ± 3	*Cand* + 0.6M
Mannitol in the SFO			
99 ± 7	Mannitol	98 ± 7	80 ng Ang II
Infusion Study: ICV 0.3M Na^+ rich aCSF infusion + SFO Candesartan			
130 ± 7	0.3M	115 ± 5	*Cand* + 0.3M
122 ± 7	80 ng Ang II	123 ± 7	*Cand* + 80 ng Ang II (2^{nd})
129 ± 7	10 ug Candesartan		
ICV 0.3M Na^+ Injection - Dose Response Study			
123 ± 5	5 ul 0.3M	117 ± 2	15 ul 0.3M
122 ± 1	10 ul 0.3M		
Injection Study: ICV 0.3M Na^+ rich aCSF injection + SFO Candesartan			
98 ± 7	aCSF	94 ± 9	10 ul 0.3M
94 ± 8	10 ug Candesartan	94 ± 7	*Cand* + 10 ul 0.3M
		86 ± 7	*Cand* + 20 ul 0.3M

Table R1. Baseline Mean Arterial Pressure (MAP) for experiments. A baseline of at least 10 min was given before the start of all experiments and baseline MAP was calculated from the last 2 min preceding the treatment. Most rats received multiple injections or infusions of drugs. Those in regular text indicate treatments to which baseline MAPs correspond while those in *italic's* indicate earlier treatments

Na^+ rich aCSF in the SFO		
Treatment	**Δ HR , t = 2-4 min**	**Δ HR , t = 8-10 min**
Vehicle	-5 ± 6	-2 ± 7
0.45M	-28 ± 10	-26 ± 10
0.6M	11 ± 15	-9 ± 8
Angiotensin II in the SFO		
80ng Ang II	-4 ± 3	1 ± 9
Vehicle + 80 ng Ang II	-4 ± 14	-3 ± 21
5 ug Cand + 80 ng Ang II	18 ± 1	24 ± 15
10 ug Cand + 80 ng Ang II	1 ± 2	15 ± 8
Aldosterone and Na^+ rich aCSF in the SFO		
Vehicle + 0.45M	-0.3 ± 6	-12± 9
1500 ng Aldo + 0.45M	-24 ± 9	-22 ± 8
Vehicle + 0.6M	-27 ± 16	-34 ± 10
500 ng Aldo + 0.6M	5 ± 10	1 ± 7
1500 ng Aldo + 0.6M	-9 ± 2	-3 ± 7
Candesartan and Na^+ rich aCSF in the SFO		
Aldo + *Veh* + 0.45M	-11 ± 8	-12 ±10
Aldo + *Cand* + 0.45M	-16 ± 2	-32 ±16
Vehicle + 0.6M	6 ± 12	-14 ± 8
Cand + 0.6M	-3 ± 8	-16 ± 8
Mannitol in the SFO		
Mannitol	1 ± 5	-6 ± 4
80 ng Ang II	-3 ± 5	-6 ± 6
Infusion Study: ICV Ang II or 0.3M Na^+ rich aCSF infusion + SFO Candesartan		
30 ng Ang II	-11 ± 10	-3 ± 16
0.3M	-7 ± 9	-10 ± 5
Cand + Ang II (2^{nd})	13 ± 9	13 ± 6
Cand + 0.3M	10 ± 7	-22 ± 6
ICV 0.3M Na^+ Injection - Dose Response Study		
5 ul 0.3M	3 ± 4	-9 ± 5
10 ul 0.3M	-20 ± 5	-20 ± 15
15 ul 0.3M	-13 ± 5	-14 ± 16
Injection Study: ICV 0.3M Na^+ rich aCSF injection + SFO Candesartan		
10 ul 0.3M	-13 ± 8	-15 ± 9
Cand + 10 ul 0.3M	-18 ± 9	-16 ± 10
Cand + 20 ul 0.3M	-32 ± 11	-22 ± 14

Table R2. Peak changes in HR during infusion or injection of various treatments into the SFO. HR was determined using the averages over the indicated time points (t=2-4 min and t=8-10 min) of the infusion period and following injection for the Ang II studies. Most rats received multiple injections or infusions of drugs. Those in regular text indicate treatments to which Δ HR's correspond while those in *italic's* indicate earlier treatments.

3.2 Aldosterone and 0.45M or 0.6M Na^+ rich aCSF in the SFO

To assess whether Aldosterone in the SFO enhances responses to infusion of Na^+ rich aCSF vehicle, 500 ng or 1500 ng Aldosterone was infused in the SFO. After a 45 min rest 0.6M Na^+ rich aCSF was infused. Pre-treatment with 500 ng and 1500 ng Aldosterone did not enhance responses to infusion of 0.6M Na^+ rich aCSF. To further clarify the potential effect of aldosterone on the responses to infusion of Na^+ rich aCSF, a lower concentration of Na^+ rich aCSF (0.45M Na^+) was infused following pre-treatment with the higher dose of aldosterone (1500ng).

In Wistar rats, infusion of vehicle or aldosterone did not change BP (Table R3). Infusion of 0.45M Na^+ rich aCSF following vehicle increased BP by 8 ± 1 mmHg while aldosterone enhanced these responses to 18 ± 1 mmHg (Fig R4). Responses to vehicle + 0.45M Na^+ rich aCSF peaked by 3min and returned to baseline within 5 min of the end of the infusion. The response to aldosterone + 0.45M Na^+ rich aCSF did not reach a peak response until around 8 min. Peak changes in BP were significantly different from vehicle and between treatment groups during infusion of 0.45M Na^+ rich aCSF (Fig R5). HR did not change from baseline (Table R2).

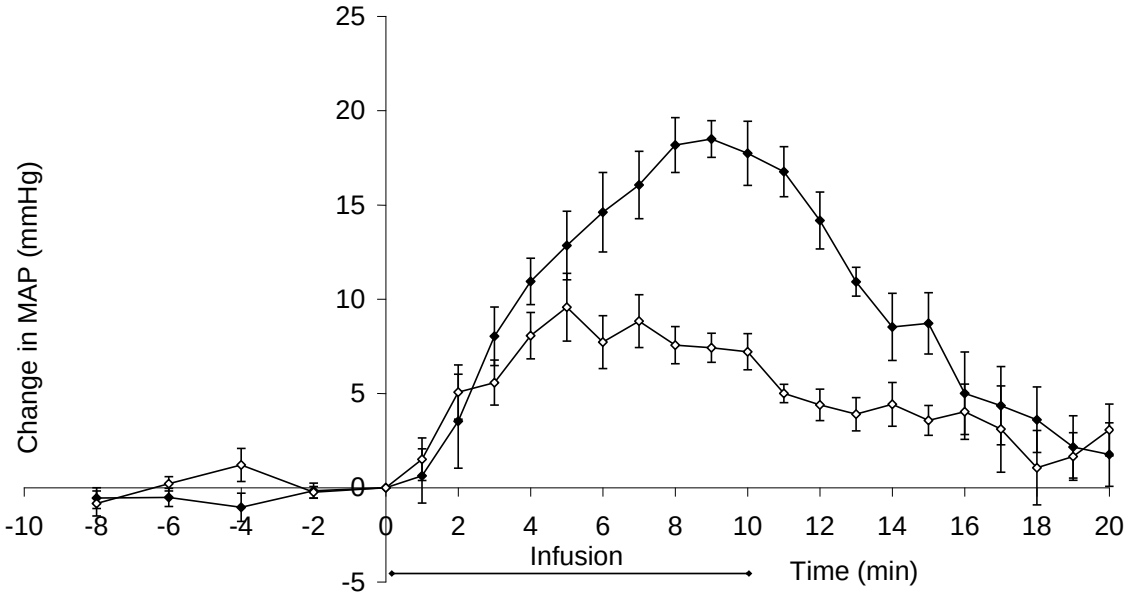

Figure R4. Infusion of 0.45M Na^+ rich aCSF into the SFO of rats pre-treated with vehicle (◇) or 1500 ng Aldosterone (◆). Points graphed are the mean (every 1 min) with the standard error. T-test on the area under the curve for statistical analysis. $p < 0.05$ for Veh/0.45M vs. Aldo/0.45M. All infusions were in the SFO. n = 5

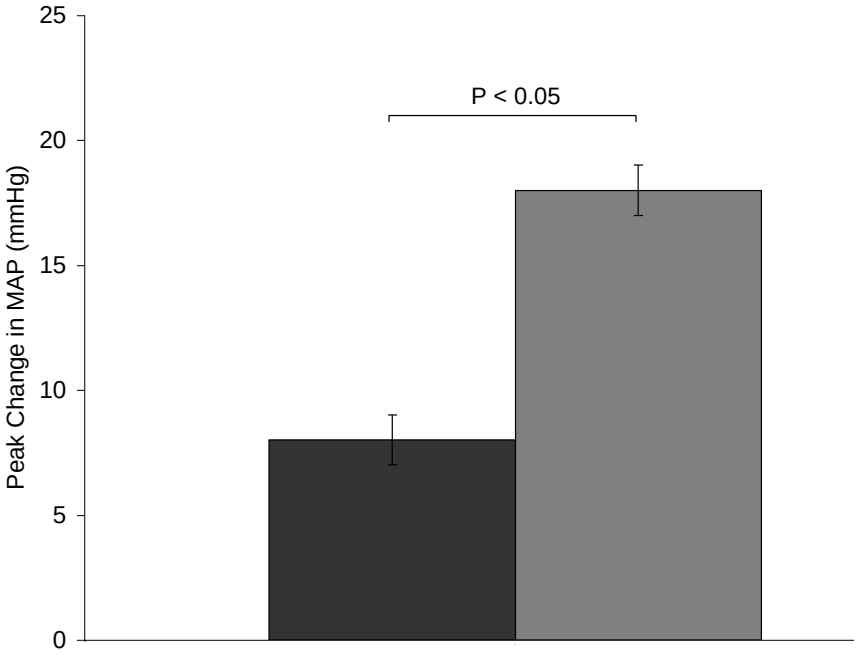

Figure R5. Peak changes in BP to infusion of 0.45M Na^+ rich aCSF into the SFO of rats treated with vehicle (■) or 1500 ng Aldosterone (■). Peak changes were determined between t=4-10 min. A t-test was used for statistical analysis. n =5

SFO Studies			
Treatment	**Δ MAP**		
	At infusion	45 min post infusion	
Aldo + 0.45M Na^+rich aCSF			
Vehicle	0 ± 2	5 ± 3	
1500 ng Aldosterone	-3 ± 1	3 ± 3	
Aldo + 0.6M Na^+rich aCSF			
Vehicle	0 ± 2	5 ± 1	
500 ng Aldosterone	1 ± 2	-4 ± 2	
1500 ng Aldosterone	-1 ± 1	-6 ± 2	
	At infusion	30 min post infusion	
Candesartan Dose Response Study			
Vehicle	-4 ± 2	-8 ± 3	
5 ug Candesartan	1 ± 1	-4 ± 3	
10 ug Candesartan	2 ± 2	-7 ± 3	
Aldo + Veh/Cand + 0.45M Na^+rich aCSF			
	At infusion	30 min post infusion	1 hr post infusion
1500 ng Aldosterone	1 ± 1	-2 ± 1	2 ± 1
Vehicle	-1 ± 2	-2 ± 1	N/A
10 ug Candesartan	1 ± 1	-11 ± 5	N/A
Cand + 0.6M Na^+rich aCSF			
Vehicle	-2 ± 2	3 ± 3	N/A
10 ug Candesartan	-2 ± 2	-3 ± 3	N/A
SFO-ICV combined Studies			
ICV 0.3M Na^+ infusion + SFO Cand			
10 ug Candesartan (SFO)	0 ± 1	-6 ± 2	-10 ± 2
ICV 0.3M Na^+ injection + SFO Cand			
10 ug Candesartan (SFO)	3 ± 4	0 ± 1	-7 ± 2

Table R3. Responses of MAP to infusion of various treatments into the SFO. All infusions were conducted over 10 min except for Candesartan which was given over 20 min. Change in MAP for "At infusion" calculated from t=4-10 min of the infusion period and the "post-infusion" data determined by subtracting initial baseline values from baseline MAP 30 min, 45 min or 1 hr after treatment.

Vehicle, 500 ng or 1500 ng Aldosterone was infused before Na^+ rich aCSF and after a 45 min rest 0.6M Na^+ rich aCSF was infused.

Infusion of vehicle and aldosterone did not have an effect on BP (Table R3). Vehicle + 0.6M Na^+ rich aCSF increased BP by 11 ± 1 mmHg, similar to the responses observed with infusion of 0.6M Na^+ alone (Fig R1 and R6). Infusion of 0.6M Na^+ rich aCSF following 500 ng and 1500 ng aldosterone increased BP by 8 ± 1 and 14 ± 2 mmHg, respectively (Fig R6). All responses peaked by 3 min and returned to baseline within 5 min of the end of the infusion. There were no statistically significant differences in the peak responses between vehicle, 500 ng and 1500 ng aldosterone pre-treated animals (Fig R6, R7). HR remained unchanged in all treatment groups (Table R2).

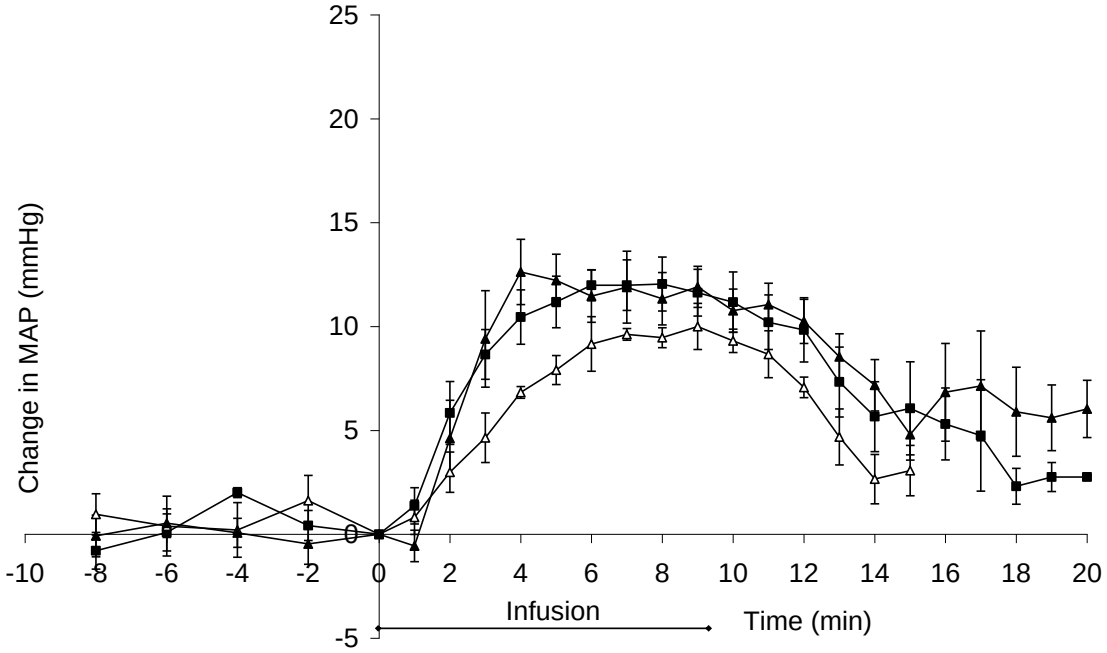

Figure R6. Infusion of 0.6M Na^+ rich aCSF into the SFO following vehicle (■, n=6), 500 ng (△, n=4) and 1500 ng (▲, n=7) aldosterone pre-treatment. Points graphed are the mean (every 1 min) with the standard error. One way ANOVA on the area under the curve used for statistical analysis.

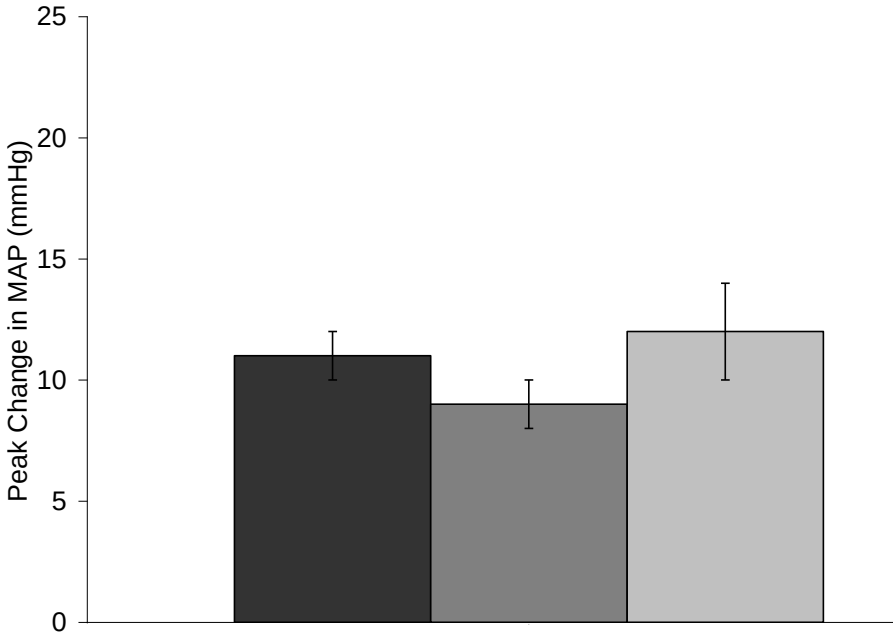

Figure R7. Peak increases in BP to infusion of 0.6 M Na^+ rich aCSF into the SFO following vehicle (■, n=6), 500 ng (■, n=4) or 1500 ng (□, n=7) aldosterone pre-treatment. Peak changes were determined between t=4-10 min.

3.3 Aldosterone, Candesartan and 0.45M Na^+ rich aCSF in the SFO

An Ang II dose response study (vehicle, 10, 20, 40 and 80ng Ang II) showed that a slow injection of Ang II in the SFO causes dose dependent increases in BP but not HR (Table R4). There was no statistically significant difference between 80ng Ang II treated (22 ± 1) and Ang II + vehicle treated rats (21 ± 3) (Fig R8, R9). Responses peaked within the first 2 min. 80ng Ang II was chosen for further experiments.

An effective dose of Candesartan that can fully block responses to infusion of Ang II was determined by a Candesartan dose response study. Response to an injection of 40ng Ang II was fully blocked while responses to 80ng Ang II were partially blocked with 5ug Candesartan (6 ± 1) (Table R4, Fig R8, R9). The higher dose of Candesartan (10 ug) fully blocked the BP responses to 80ng Ang II injection (0 ± 2) (Table R4, Fig R8, R9). No changes in HR were observed in any of these groups (Table R2).

To assess if the BP increases to infusion of 0.45M Na^+ rich aCSF and the observed enhancement of those responses by 1500 ng Aldosterone are mediated via AT_1-R activation, the AT_1 receptor blocker Candesartan was infused into the SFO. Rats first received a 1500 ng Aldosterone infusion, then vehicle or 10 ug Candesartan and finally infusion of 0.45M Na^+ rich aCSF. Infusion of Candesartan and vehicle alone gave no BP responses on their own (Table R3). Following infusion of aldosterone and vehicle, 0.45M Na^+ rich aCSF increased BP by 15 ± 1 mmHg (Fig R10, R11). Responses to Na^+ peaked by 3 min and returned to baseline within 5 min of the end

of the infusion. 10 ug Candesartan fully blocked the BP increases to infusion of 0.45M Na^+ rich aCSF and the aldosterone mediated enhancement of responses (2 ± 1) (Fig R10, R11). No changes in HR were seen in any groups (Table R2)

Treatment in SFO	**MAP**	**HR**	***n***
aCSF	1 ± 1	-7 ± 7	5
10ng Ang II	8 ± 3	3 ± 6	6
20ng Ang II	10 ± 2	-1 ± 2	6
40ng Ang II	15 ± 2	15 ± 34	4
80ng Ang II	21 ± 3	-4 ± 3	4
5ug Cand + 80ng Ang II	6 ± 1	18 ± 1	3
10ug Cand + 80ng Ang II	0 ± 2	2 ± 2	4

Table R 4. Peak changes in MAP and HR to injection of Ang II before and after infusion of Candesartan into the SFO. 10-40ng Ang II treatments were given in 500nl, 80ng Ang II in 100nl. Peak changes were determined between t=2-4 min.

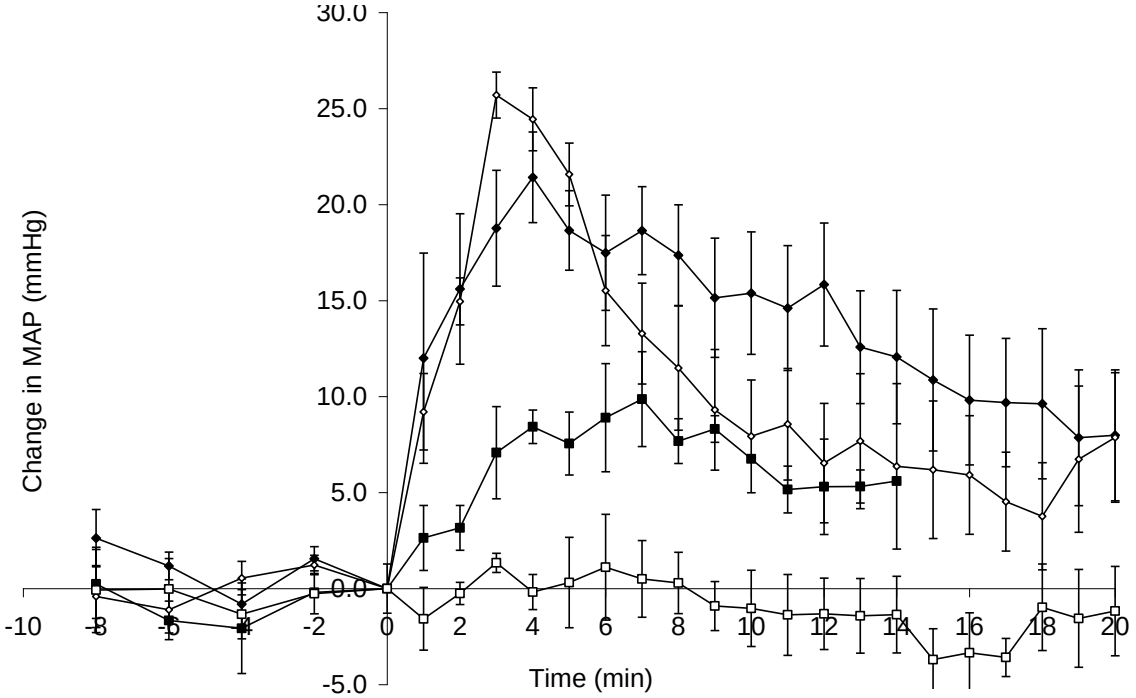

Figure R8. Injection of 80 ng Ang II into the SFO before (◆, n=5) and after (◇, n=4) vehicle infusion and following 5ug (■, n=3) or 10 ug (□, n=4) Candesartan infusion. Ang II was injected slowly in a bolus dose over 30 sec. Injections of Ang II were 1 hr apart. Points graphed are the mean (every 1 min) with the standard error. One Way ANOVA on the area under the curve for statistical analysis. $p < 0.05$ for Ang II or veh/Ang II vs 5 ug Cand/Ang II and Ang II or veh/Ang II vs 10 ug Cand/Ang II.

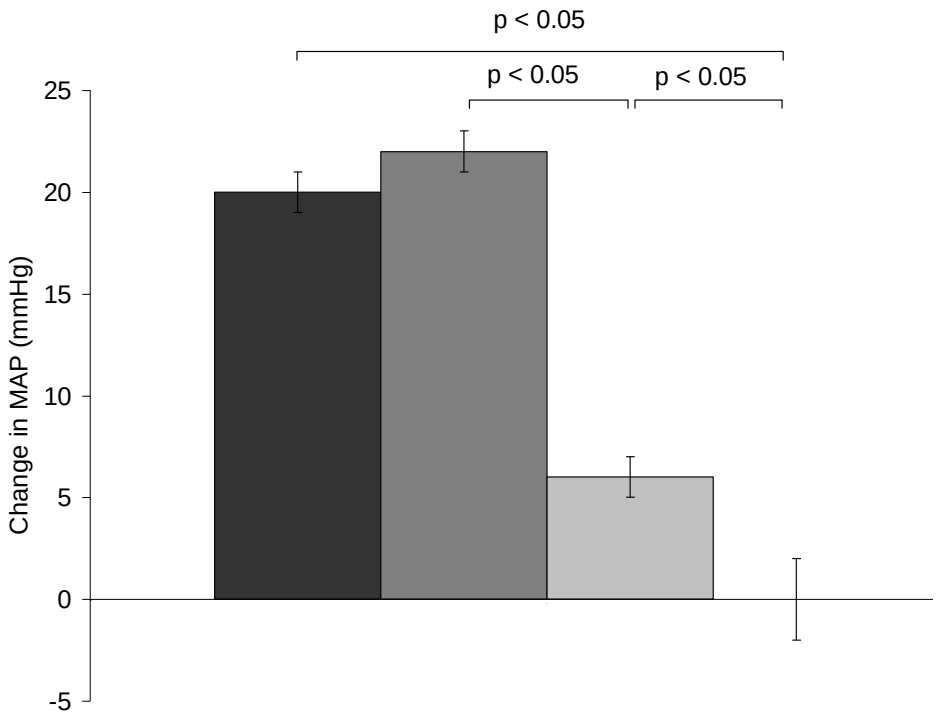

Figure R9. Peak changes in MAP to injection of 80ng Ang II (■, n=5), vehicle + 80 ng Ang II (■, n=4), 5 ug Candesartan + 80 ng Ang II (□, n=3) and 10 ug Candesartan + 80 ng Ang II (□, n=4). All treatments were in the SFO. Peak changes were determined between t=2-4 min. One way ANOVA was used for statistical analysis.

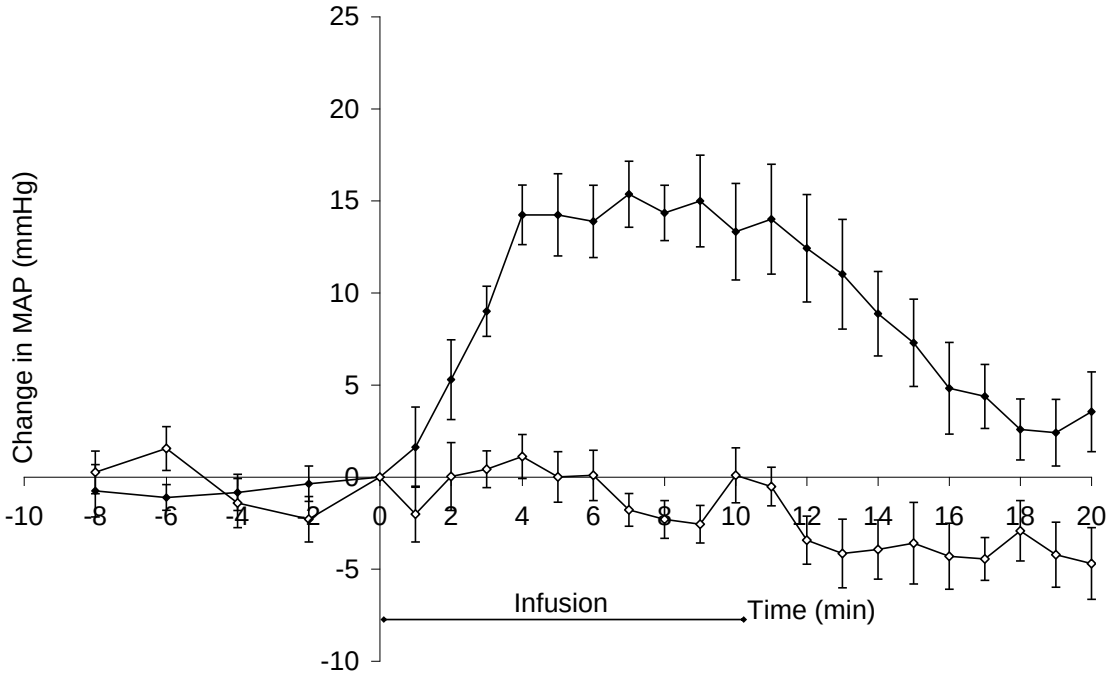

Figure R10. Effect of Candesartan on the BP response to Aldosterone + Na^+ rich aCSF infusion in the SFO. 1500 ng Aldosterone was infused, a 45 min rest given and a 20 min Candesartan (◇) or vehicle (◆) infusion was conducted in the SFO. Following a 30 min rest, 0.45M Na^+ rich aCSF was infused. Points graphed are the mean (every 1 min) with the standard error. T-test on the area under the curve for statistical analysis. $p < 0.05$ Aldo/Veh/Na vs Aldo/Cand/Na. $n = 5$

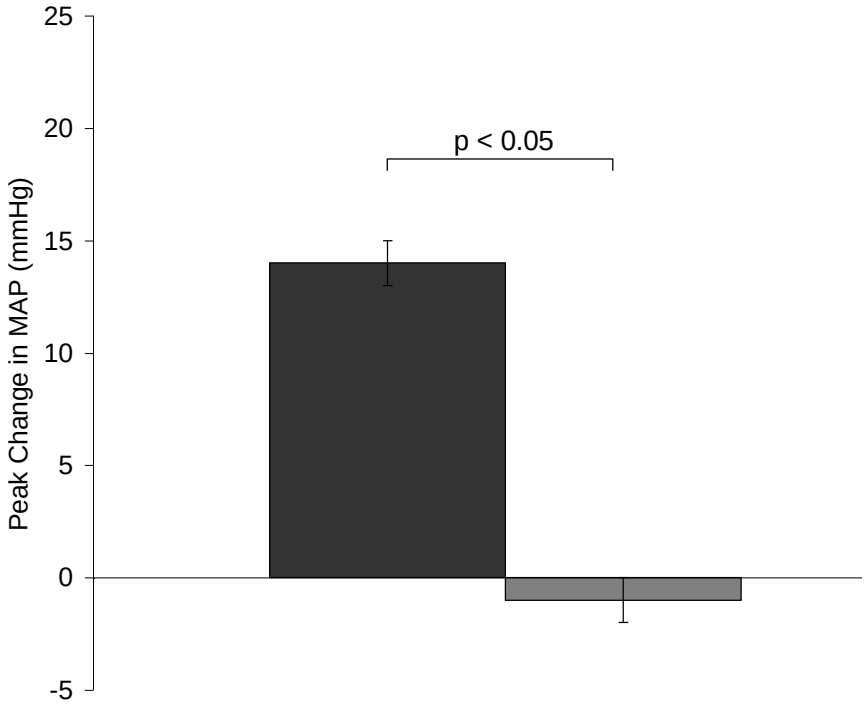

Figure R 11. Effect of Candesartan on the peak changes in MAP from baseline to infusion of Aldosterone and Na^+ rich aCSF in the SFO. Aldosterone – Candesartan (▣) or Vehicle (■) – 0.45M Na^+ rich aCSF. Peak changes were determined during the infusion period between t=4-10 min. A t-test was used for statistical analysis. n = 5

3.4 Candesartan and 0.6M Na^+ rich aCSF in the SFO

To assess if responses to infusion of 0.6M Na^+ rich aCSF in the SFO are mediated by AT_1-R activation, 0.6M Na^+ rich aCSF was infused into the SFO before and after infusion of 10 ug Candesartan or vehicle.

Infusion of vehicle and candesartan alone showed no BP effects (Table R2). Infusion of 0.6M Na^+ alone and vehicle + 0.6M Na^+ rich aCSF both increased BP by 15 ± 1 mmHg (Fig R12, R13). Responses peaked by 2-3 miutes and returned to baseline within 5 min of the end of the infusion. Candesartan fully blocked the BP increases to infusion of 0.6M Na^+ rich aCSF (2 ± 1 mmHg) (Fig R12, R13). No changes in HR were seen in any of these groups (Table R2).

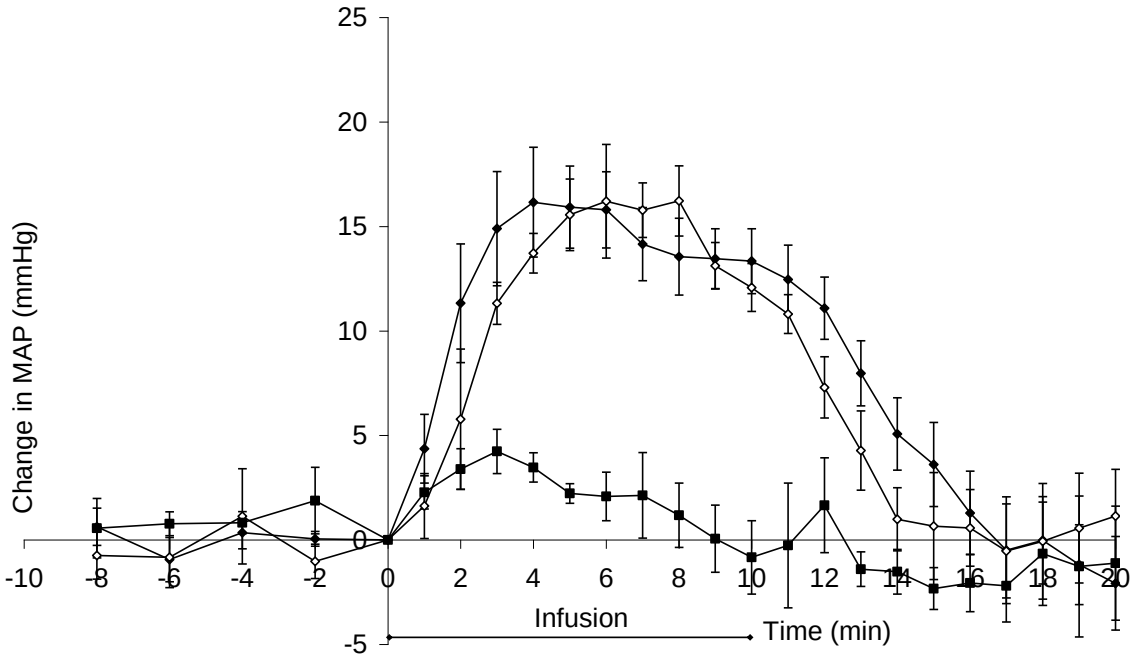

Figure R12. Effect of Candesartan on the BP response to 0.6M Na^+ rich aCSF infusion in the SFO. 0.6M Na^+ rich aCSF (◆, n=7) alone, vehicle + 0.6M (◇, n=4) and 10 ug Candesartan + 0.6M Na^+ rich aCSF (■, n=4). After a first infusion of 0.6M Na^+ rich aCSF, Candesartan or vehicle were infused over 20 min and followed 30 min later by a second infusion of 0.6M Na^+ rich aCSF. Points graphed are the mean (every 1 min) with the standard error. One Way ANOVA on area under the curve used for statistical analysis. $p < 0.05$ 0.6M vs Veh/0.6M and 0.6M vs Cand/0.6M.

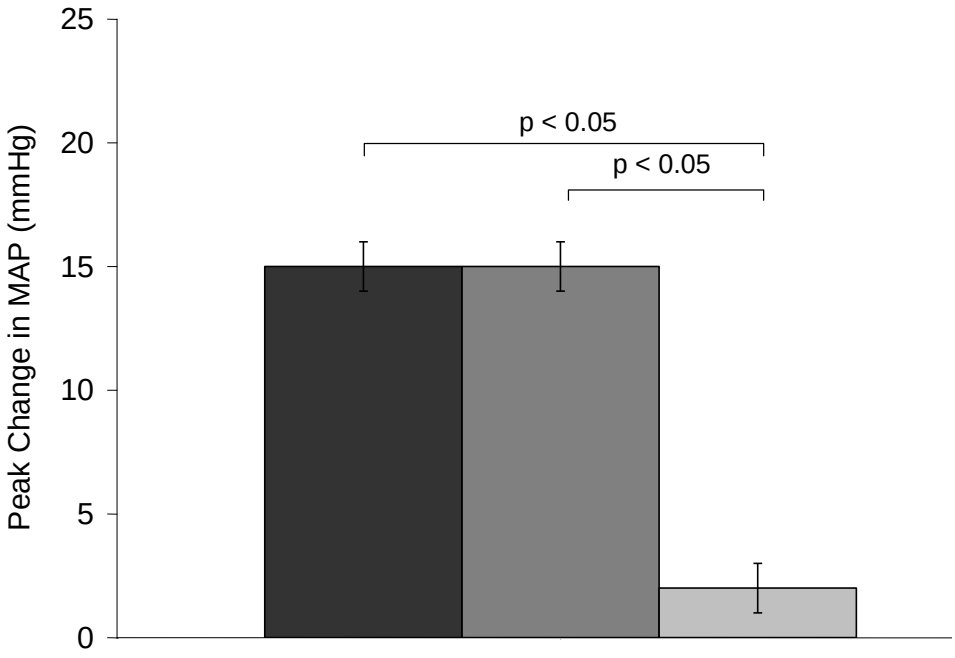

Figure R13. Effect of Candesartan on the peak changes in MAP to infusion of 0.6M Na^+ rich aCSF in the SFO. 0.6M Na^+ rich aCSF was infused before (■, n=7) and after a vehicle (■, n=4) or 10 ug Candesartan (□, n=4) infusion. Peak changes were determined during the infusion period between t=4-10 min. One way ANOVA was used for statistical analysis.

3.5 SFO Osmolarity Studies

To determine whether BP responses to infusion of Na^+ rich aCSF in the SFO are in response to increases in local [Na^+] or changes in osmolarity, a Mannitol solution which is osmotically equivalent to 0.6M Na^+ rich aCSF was infused into the SFO and the resulting changes in BP and HR were measured. A 0.85M Mannitol solution is osmotically equivalent to 0.6M Na^+ rich aCSF and 0.85M Mannitol was infused into the SFO at 100 nl/min for 10 min. As a positive control, 80 ng Ang II was injected in a bolus 100 nl volume in all rats 30 min following the end of the Mannitol infusion.

Infusion of 0.85M Mannitol into the SFO did not change BP or HR (Fig R14, Table R2). Injection of 80 ng Ang II increased BP by 17 ± 3 mmHg (Fig R14).

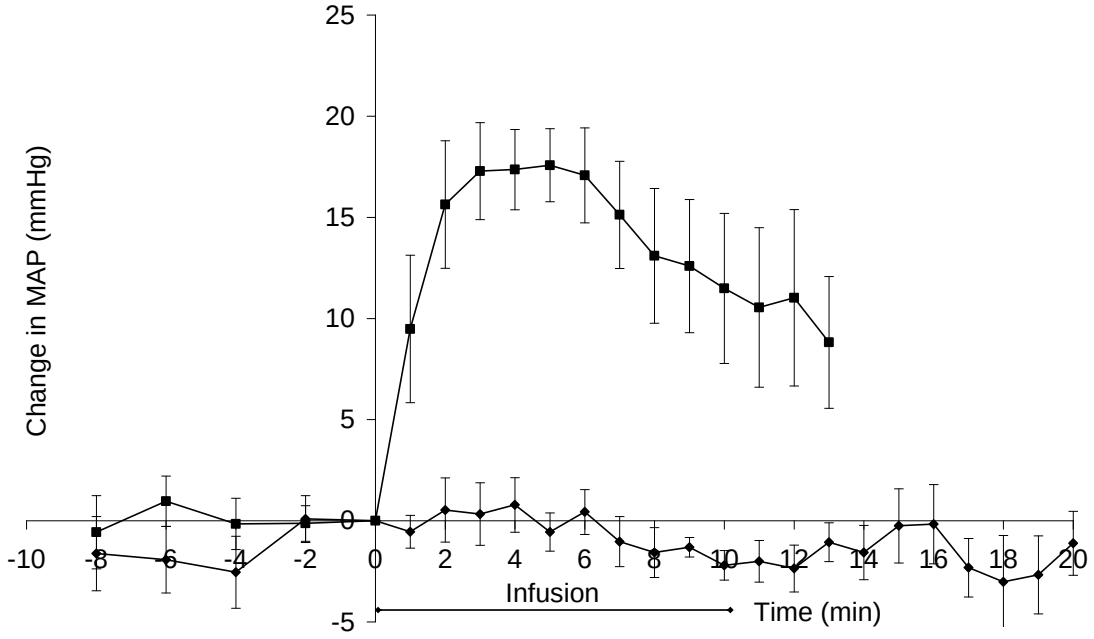

Figure R14. BP responses to increase in local SFO osmolarity. 0.85M Mannitol (◆) was infused into the SFO for 10 min. 30 min following the end of Mannitol infusion, 80 ng AngII (■) was injected in a bolus dose. Points graphed are the mean (every 1 min) with the standard error. n=6

3.6 ICV Ang II, Na^+ rich aCSF and Candesartan in the SFO

To determine whether the SFO mediates responses to icv injection of Ang II and icv infusion of Na^+ rich aCSF, a combined icv/SFO study was done by injecting 30 ng Ang II and infusing 0.3M Na^+ rich aCSF icv before and after infusion of 10 ug Candesartan into the SFO. Bolus icv Ang II injections were given (30 ng/3 ul) after a 30 min rest period followed by a 10 min icv infusion of 0.3M Na^+ rich aCSF (3.8ul/min). Candesartan was infused into the SFO over 20 min as done previously (0.5 ug/100 nl/min). Thirty minutes after the Candesartan infusion, a 10 min infusion of 0.3M Na^+ rich aCSF (3.8ul/min) was given. Thirty minutes after the Na^+ infusion a bolus icv injection of Ang II (30 ng/3 ul) was given. To determine the persistence of Candesartan blockade on possible responses, a third Ang II injection was given icv (30 ng/3 ul) 2-3 hrs following the Candesartan infusion.

In Wistar rats, infusion of 10 ug Candesartan alone did change BP (Table R3) or HR (Table R2). ICV injection of 30 ng Ang II did not change HR (Table R2) and increased BP by 14 ± 1 mmHg which lasted through 20 min and returned to baseline by 30 min (Fig R15, R17). Infusion of 10 ug Candesartan into the SFO fully blocked the BP response (0 ±1 mmHg) to icv injection of 30 ng Ang II (Fig R15, R17). The blockade effect of Candesartan on BP responses to icv Ang II injection appears to persist at least 1 hour following infusion of Candesartan (Fig R15).

ICV infusion of 0.3M Na^+ rich aCSF increased BP by 15 ± 1 mmHg (Fig R16, R17). Peak response was reached within 2-3 min of the start of infusion and returned to

baseline within 5 min of the end of the infusion. Infusion of 10 ug candesartan into the SFO partially blocked the responses to icv infusion of 0.3M Na^+ rich aCSF (Fig R16, R17). Responses were 8 ± 1 mmHg following Candesartan infusion in the SFO, a decrease of nearly half from the original response to 0.3M Na^+ alone. HR remained unchanged in all groups throughout these treatments (Table R2).

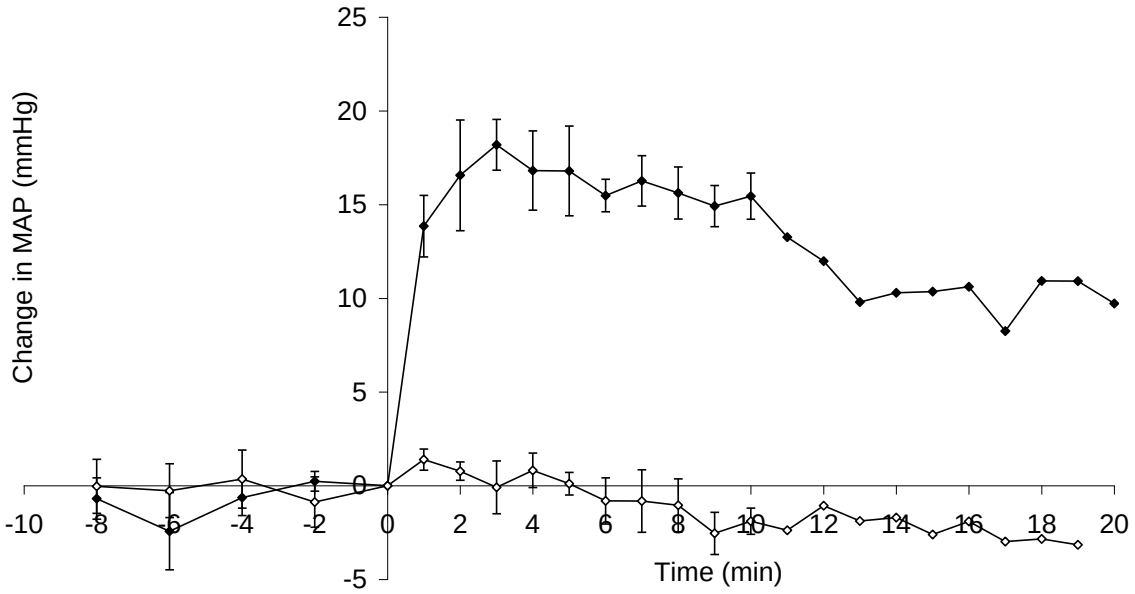

Figure R15. Effect of Candesartan in the SFO on the BP responses to icv injection of Ang II. 30 ng Ang II (◆) was given in a bolus icv injection, 1 hr later 10 ug Candesartan was infused in the SFO and followed by a second 30 ng Ang II injection (◇) 1 hr following Candesartan infusion. Points graphed are the mean (every 1 min) with the standard error. T-test on the area under the curve for statistical analysis. $p < 0.05$ Ang II vs Cand/Ang II. n=4

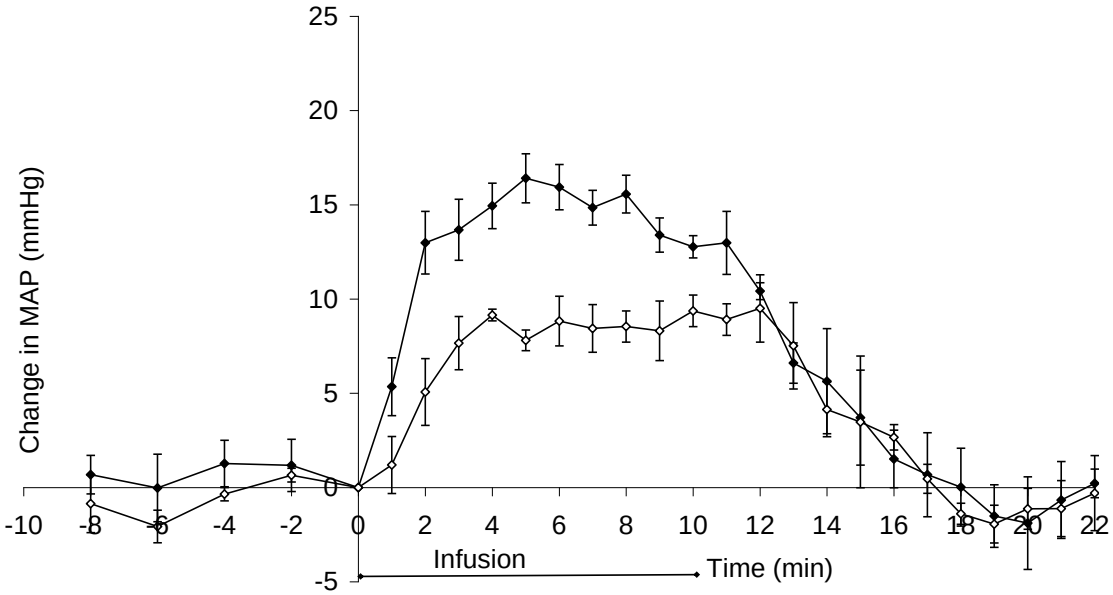

Figure R16. Effect of Candesartan in the SFO on the BP responses to icv infusion of Na^+ rich aCSF. 0.3M Na^+ rich aCSF (◆) was infused icv over 10 min, 30 min later 10 ug Candesartan was infused in the SFO and followed by a second infusion of 0.3 M Na^+ rich aCSF(◇). Points graphed are the mean (every 1 min) with the standard error. T-test on the area under the curve for statistical analysis. $p < 0.05$ 0.3M vs. Cand/0.3M. n=4

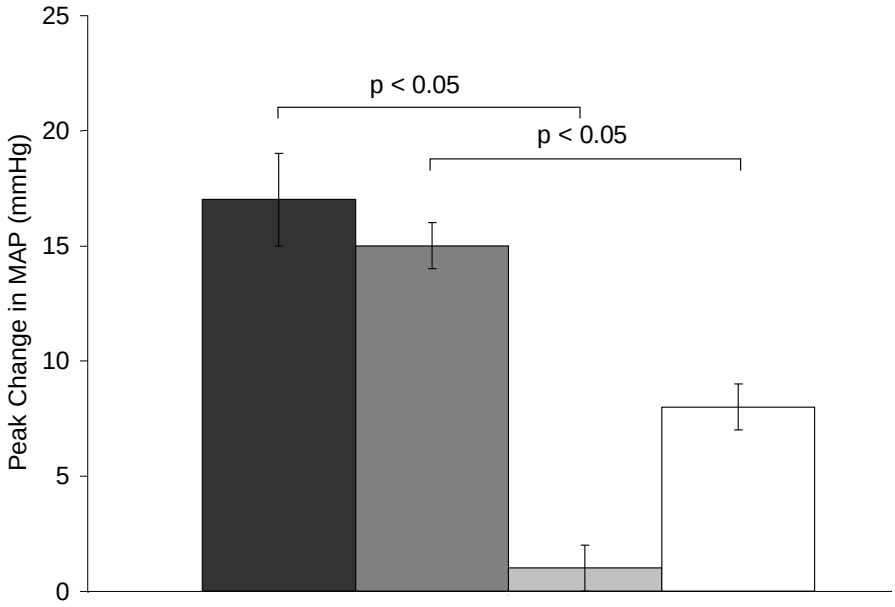

Figure R17. Effect of Candesartan infusion in the SFO on the peak responses to icv injection of Ang II and icv infusion of Na^+ rich aCSF. 30ng Ang II was injected icv before (■) and after (□) 10 ug Candesartan infusion in the SFO and 0.3M Na^+ rich aCSF was infused icv before (■) and after (□) 10 ug Candesartan infusion in the SFO. Peak changes for Ang II injection were determined from t=2-4 min following Ang II injection. For the 0.3M Na^+ infusion, peak changes were determined from the infusion period between t=4-10 min. A t-test was used for statistical analysis. n=4

3.7 ICV 0.3M Na^+ rich aCSF (injection) and 10 ug Candesartan (infusion) in the SFO

BP response to icv injections of 0.3M Na^+ rich aCSF can be fully blocked by AT1-R blockade in the SFO (Rohmeiss 1995). To verify this data and make a comparison with our data that showed partial blockade of the responses to icv infusions of 0.3M Na^+ rich aCSF by Candesartan in the SFO, we conducted similar experiments using icv injections of 0.3M Na^+ rich aCSF in combination with infusions of Candesartan in the SFO. 10 ug Candesartan was infused into the SFO before and after a bolus icv injection of 10 ul 0.3M Na^+ rich aCSF. To determine a volume of Na^+ rich aCSF to be injected icv, a volume response study was conducted using icv injections of 0.3M Na^+ rich aCSF in 5, 10 and 15 ul volumes. These volumes were injected icv and the resulting BP and HR responses measured.

ICV injection of 5, 10 and 15 ul of 0.3M Na^+ rich aCSF resulted in similar increases in BP of 10 ± 2, 10 ± 2 and 10 ± 3 mmHg respectively (Fig R18, R19). Responses peaked by 1 min and returned to baseline by 5 min following the injection. No changes in HR were observed (Table R2).

ICV injection of aCSF and infusion of 10 ug Candesartan into the SFO did not change BP (Table R3). Injection of 10 ul 0.3M Na^+ rich aCSF increased BP by 14 ± 4 mmHg (Fig R20, R21). Infusion of 10 ug Candesartan into the SFO fully blocked responses to a 10 ul injection of 0.3M Na^+ rich aCSF but not that of a 20 ul injection (Fig R20,

R21). Responses peaked by 1 min and returned to baseline by 5 min following the injection (Fig R20). No changes in HR were observed (Table R2).

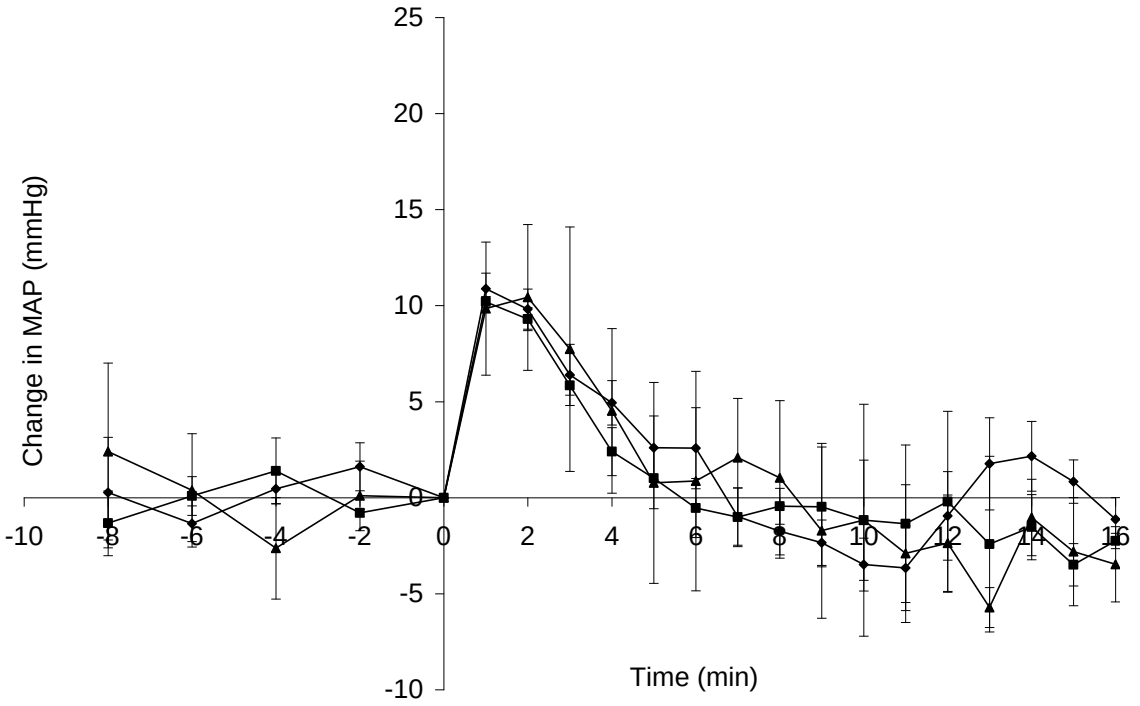

Figure R18. Responses to bolus icv injections of 0.3M Na^+ rich aCSF. Increasing volumes of 0.3M Na^+ rich aCSF, 5 ul (◆), 10 ul (■) and 15 ul (▲), were injected icv and the resulting effects on BP and HR were measured. Injections were separated by 30 min gaps for recovery. Points graphed are the mean (every 1 min)

with the standard error. n=4

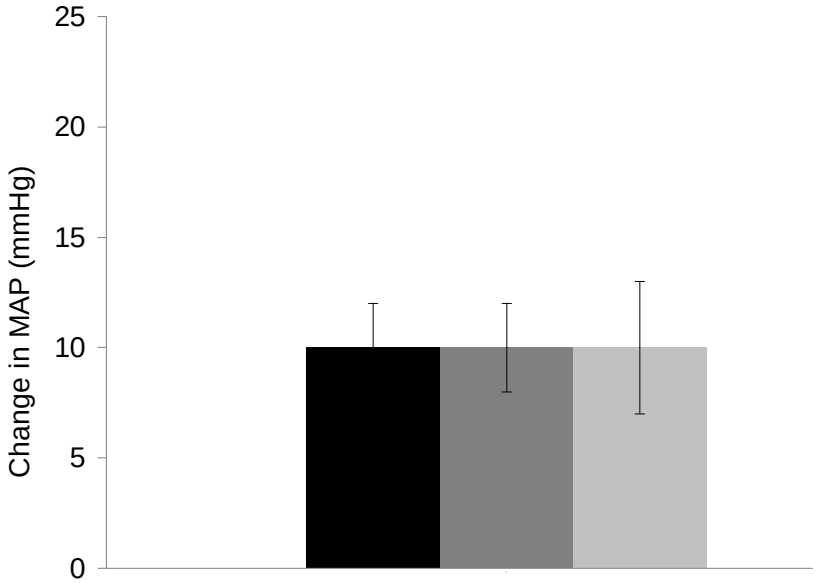

Figure R19. Peak increases in MAP to icv injection of 0.3M Na^+ rich aCSF. Peak increase were determined between t=1-2 min following the bolus icv injection of 5 ul (■), 10 ul (■) and 15 ul (□) 0.3M Na^+ rich aCSF. No significant difference in BP among groups.

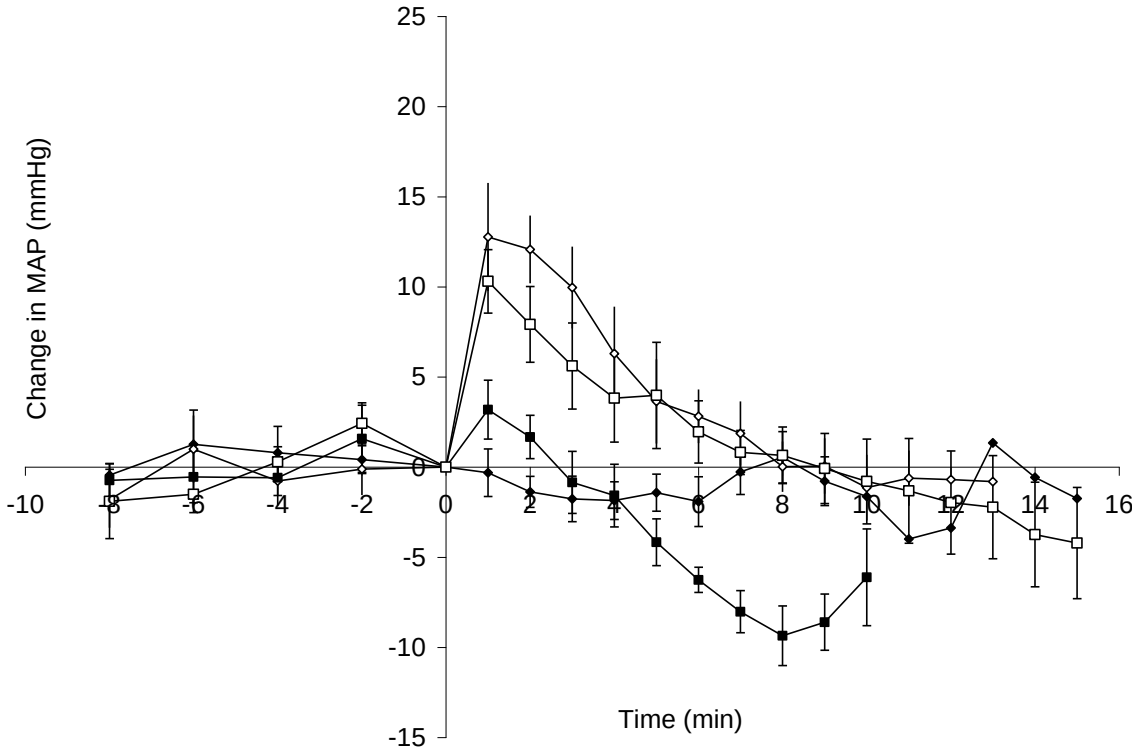

Figure R20. Effect of Candesartan treatment in the SFO on the MAP responses to icv injection of 0.3M Na^+ rich aCSF. Vehicle (◆) and 10 ul (◇) 0.3M Na^+ were injected icv. A second injection of 10 ul (■) and an additional 20 ul (□) injection of 0.3M Na^+ rich aCSF were injected icv following 10 ug Candesartan in the SFO. Points graphed are the mean (every 1 min) with the standard error. One way ANOVA used for statistical analysis. aCSF vs 10 ul 0.3M, aCSF vs 10 ul 0.3M/Cand, 10 ul 0.3M vs 10 ul 0.3M/Cand $p < 0.05$. n=4

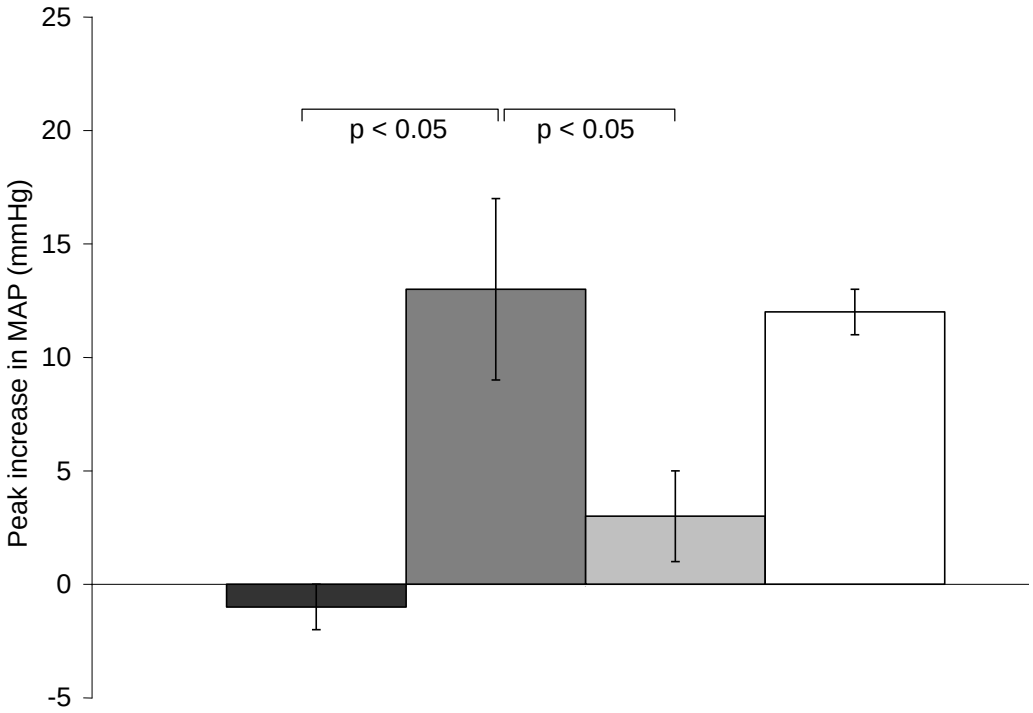

Figure R21. Peak increase in BP during icv injection of 0.3M Na^+ rich aCSF before and after Candesartan infusion in the SFO. ICV injection of vehicle (■) or 10 ul 0.3M Na^+ rich aCSF (■), Cand + 10 ul Na^+ (□) and Cand + 20 ul Na^+ (□). All infusions of Candesartan were in the SFO. A 30min rest was given between each treatment. Peak increase in BP were determined from t=1 min in response to icv injection of 0.3M Na^+ rich aCSF. One way ANOVA on the three 10 ul injections was used for statistical analysis. n=4

3.8 Ouabain dose response studies in the SFO

Responses to infusion and injection of Ouabain into the SFO were evaluated using various doses which cause pressor responses when given icv or in the PVN. Vehicle, 80 ng, 160 ng, 320 ng, 480 ng, 640 ng and 960 ng/500nl were infused (100 nl/min for 5 min) into the SFO. These infused doses did not change BP (Fig R22 and Fig R23) and it was decided to inject the two highest doses and determine possible effects on BP and HR. 640 ng/500nl and 960 ng/500nl were slowly injected 500 nl/30sec and did not affect BP or HR. To make a comparison with icv pressor responses, 640 ng/500nl and 960 ng/500nl doses were either infused (100 nl/min for 5 min) or slowly injected 500 nl/30sec icv.

ICV infusion of 640 ng Ouabain did not change BP and slightely decreased HR. A slow injection of the same dose given over 30 seconds increased BP by 15 ± 2 mmHg (Fig R24) and HR by 27± 5 bpm. Peak increases in BP and HR were reached by 6-8 min following the injection.

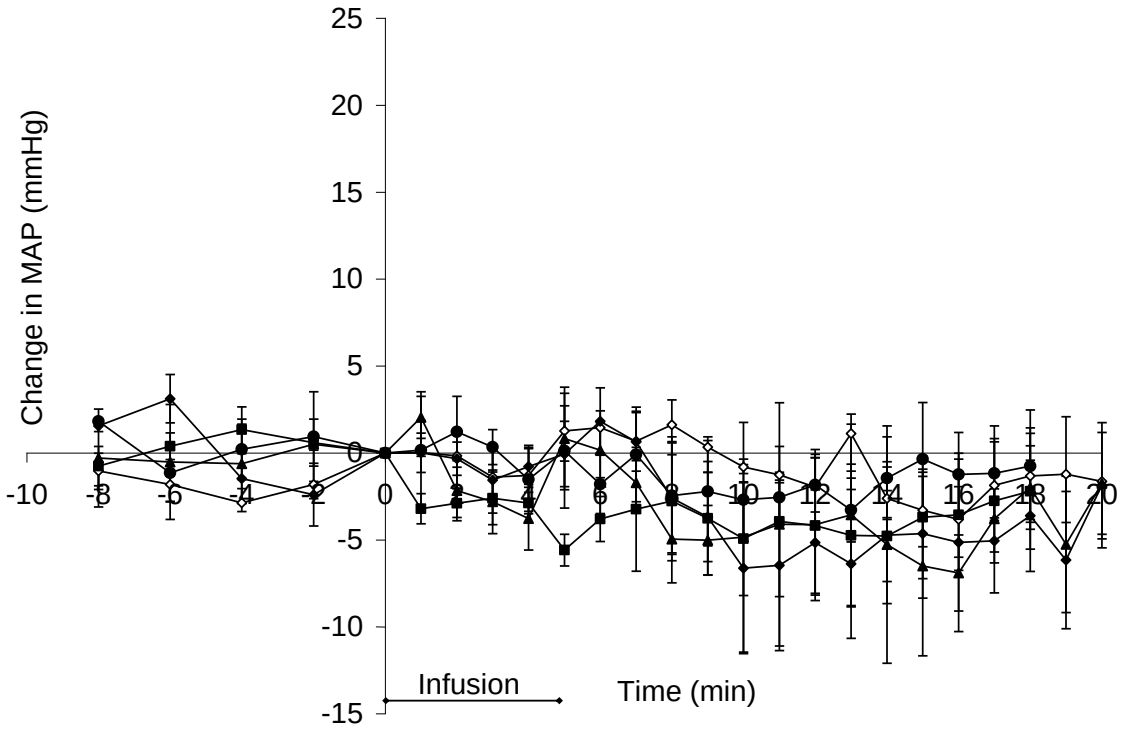

Figure R22. Responses to infusion of Ouabain into the SFO. Doses of Ouabain were infused into the SFO starting with vehicle (◇), 80 ng (◆), 160 ng (▲), 320 ng (■) and 480 ng (●), n=3. All infusions were separated by at least 30 min.

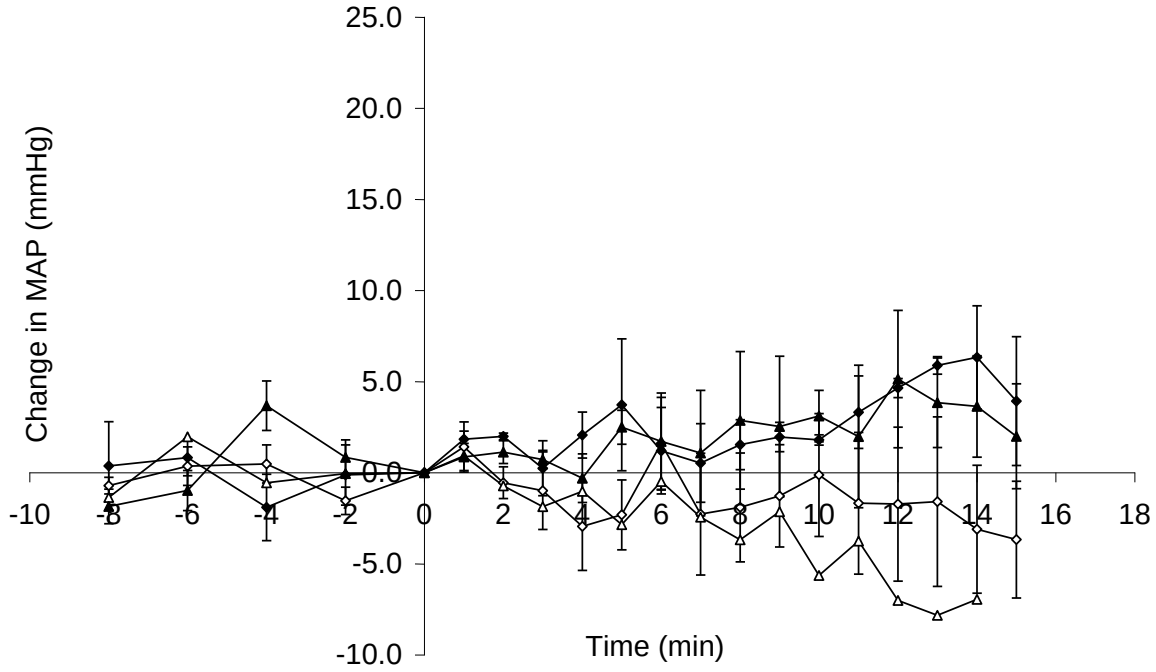

Figure R23. Responses to injection or infusion of Ouabain into the SFO. 640 ng (◇, n=3) and 960 ng (△, n=2) Ouabain were infused followed 30 min later by a slow injection of 640 ng (◆, n=3) and 960 ng (▲, n=3) into the SFO.

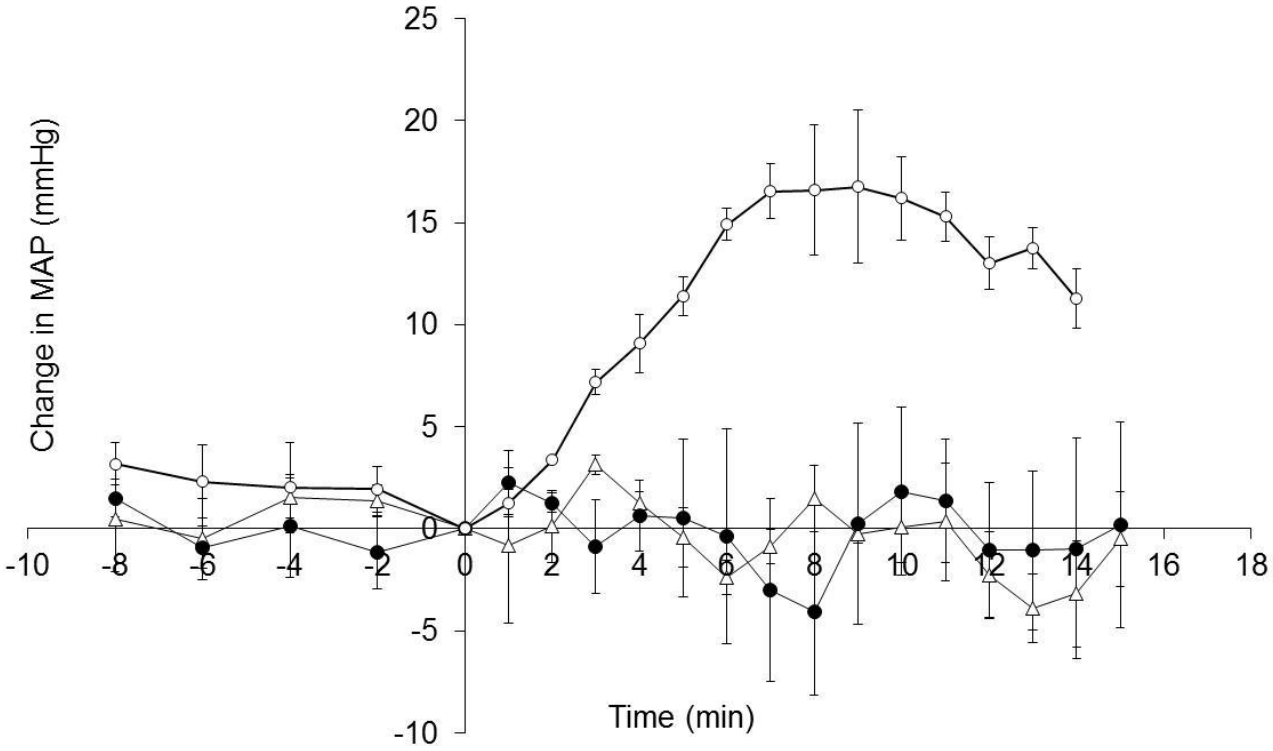

Figure R24. Responses to icv infusion and injection of Ouabain. Vehicle infusion (Δ) and 640 ng of Ouabain infusion (●) or injection (○) into the SFO, n=3.

ICV treatment	***n***	**Baseline**	**ΔHR**
Vehicle	3	449 +/- 29	5 ± 1
640ng Ouabain Infusion	3	463 +/- 32	-20 ± 13
640ng Ouabain Injection	4	411 +/- 16	27 ± 5

Table R 5. Peak increase in HR during icv injection or infusion of Ouabain. Steady state change in HR was calculated from t=6-10min.

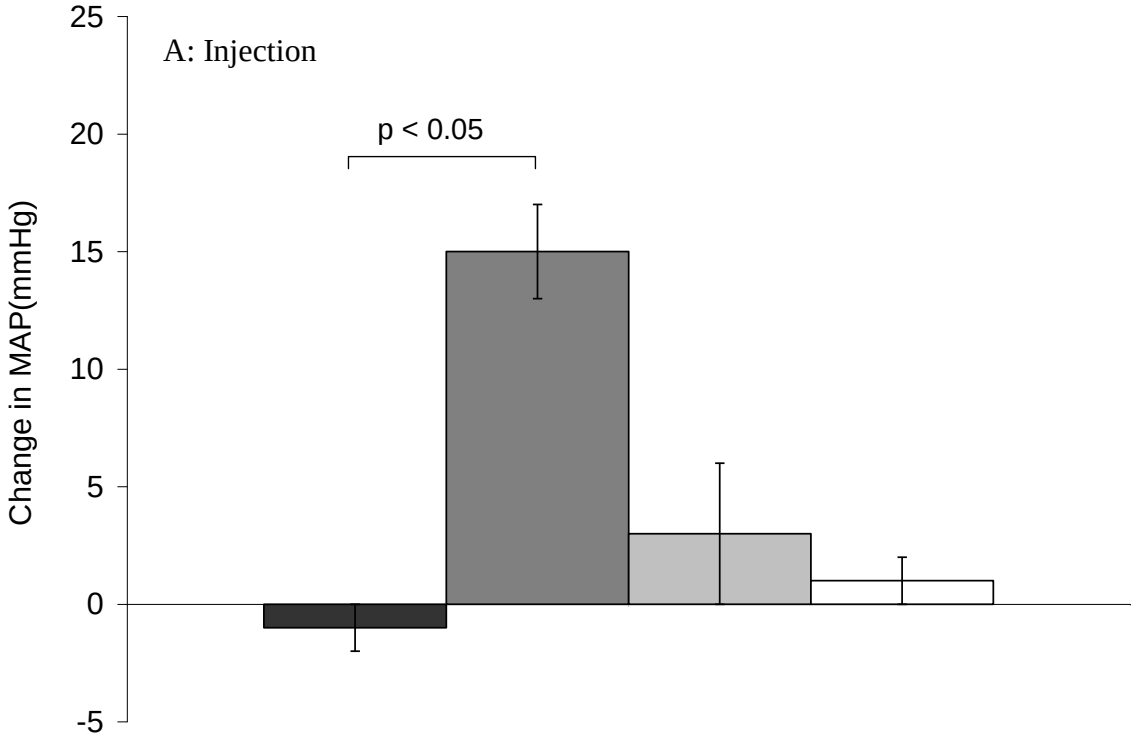

Figure R25. Maximal changes in BP during infused and injected doses of Ouabain. A: Peak changes in BP over t=6-15 min to a slow injection of vehicle (■) and 640 ng (■) Ouabain icv and 640 ng (■) and 960 ng (□) Ouabain into the SFO. T-test used for statistical analysis, n=3.

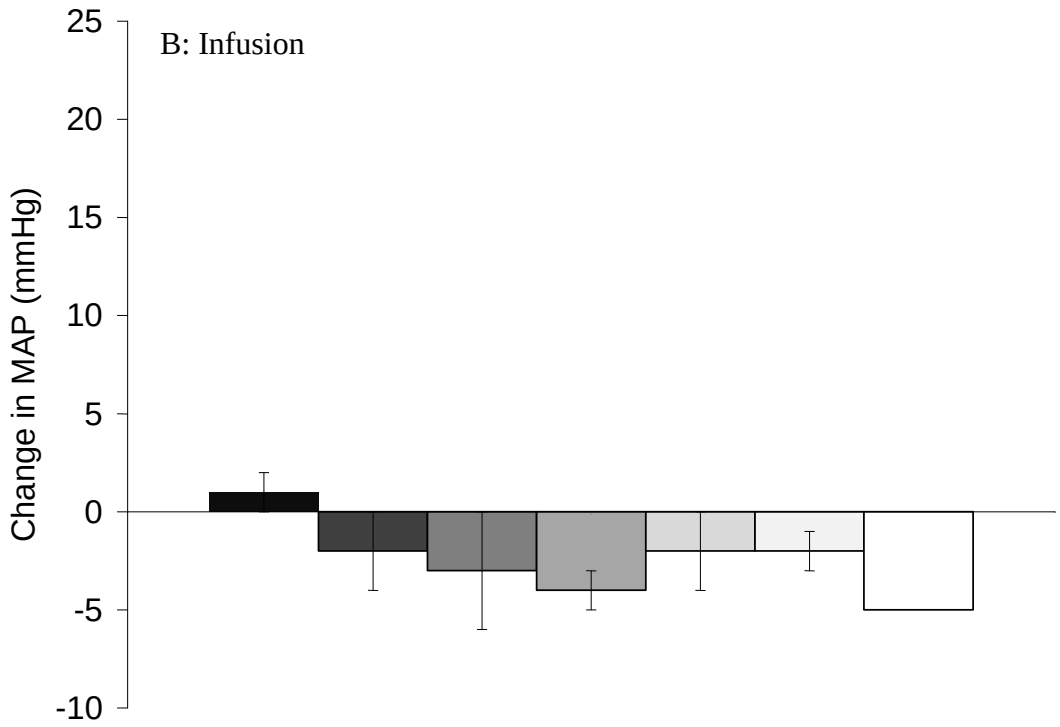

Figure R26. Maximal changes in BP during infused and injected doses of Ouabain. B: Peak changes in BP during infusion of vehicle (■, n=3), 80 ng (■, n=3), 160 ng (■, n=3), 320 ng (■, n=3), 480 ng (□, n=3), 640 ng (□, n=5) and 960 ng (□, n=2) Ouabain.

4 Discussion

4.1 Summary of Main Findings

All studies were performed on male Wistar rats. Acute infusion of Na^+ rich aCSF in the SFO of rats causes dose dependent increases in BP. These BP responses to Na^+ rich aCSF in the SFO are further enhanced by prior infusion of aldosterone in the SFO. The responses to infusion of Na^+ rich aCSF in the SFO and the aldosterone enhanced responses to infusion of Na^+ rich aCSF are mediated via AT_1-R activation in the SFO as blockade of these receptors fully blocks the BP responses. AT_1-R activation in the SFO also mediates the BP responses to bolus icv injections of Ang II as Candesartan infusion in the SFO fully blocks these BP responses. AT_1-R activation in the SFO appears partially responsible for mediating the responses to acute increases to CSF[Na^+] as the BP response observed to icv infusion of Na^+ rich aCSF is attenuated by 50% by AT_1-R blockade in the SFO. A brief infusion of Na^+ rich aCSF in the SFO and a lateral ventricle did not change HR. Lastly, bolus injections and infusions of various doses of Ouabain in the SFO do not change BP or HR suggesting that ouabain in the SFO is not associated with changes in BP and HR.

4.2 BP Responses to Na^+ rich aCSF in the SFO, Role of AT_1-Receptors

A 10min infusion of 0.45M and 0.6M Na^+ rich aCSF (45 and 60 nmol/min of Na^+) into the SFO increased BP that lasted throughout the infusion period and terminated within 5 min of the end of the infusion. To our knowledge no other study has assessed the effects of Na^+ rich aCSF in the SFO on BP. Our findings are comparable to acute studies in the PVN that infused 0.7M Na^+ rich aCSF (210 nmol/min) into the PVN for 15min (Gabor and Leenen

2009). The SFO may have greater sensitivity to Na^+ as compared to the PVN since similar BP increases of 15 ± 1mmHg in the SFO and 13 ± 1mmHg in the PVN were achieved with a significantly higher amount of Na^+ in the PVN (210 nmol/min) as compared to the SFO (60 nmol/min). Taking the volume of the SFO (0.23mm^3, preliminary calculations) and PVN (0.45 ± 0.03 mm^3) (Conn and Freeman 2000) into account, the SFO is nearly half the size of the PVN but requires 1/3 the amount of Na^+ to cause an increase in BP. If [Na^+] increase differs accordingly, SFO neurons show greater sensitivity to sodium than neurons in the PVN. Infusion of a mannitol solution (0.85M) osmotically equivalent to 0.6M Na^+ rich aCSF into the SFO did not change BP or HR indicating that the SFO is responding to local changes in [Na^+] and not to changes in osmolarity. This is in agreement with studies that reported no change in BP or HR to icv infusions of mannitol (0.7M) (Osborne et al 1989), sucrose (0.6M) and urea (0.6M) in rats (Bunag and Miyajima 1984) and icv sorbitol (0.9M) in sheep (May and McAllen 1997). This specific Na^+ responsiveness is also present in the PVN where a solution of mannitol osmotically equivalent to 0.7M Na^+ rich aCSF in the PVN did not result in BP or HR responses (Gabor and Leenen 2009).

The SFO has efferent connections from both the peripheral and core regions that end in the parvocellular and magnocellular nuclei of the PVN and SON (Kawano and Masuko 2010) and the BP responses may have been mediated through SFO efferents projecting to these regions. Infusion into the SFO would activate all Na^+ sensitive neurons in the SFO and it is likely both the periphery and core of the SFO are involved in causing the observed increases in BP. Downstream signaling to the pPVN would result in signaling to RVLM and increased sympathetic activity while signaling to the mPVN and SON would result in release of vasopressin.

The responsiveness of the SFO to direct application of Ang II has been well established with Simpson and group (1980) being one of the first to measure BP increases following Ang II injection in the SFO. 40ng Ang II produced BP responses similar to infusion of 0.6M Na^+ rich aCSF (15 ± 2 mmHg) whereas 80ng Ang II increased BP by 22 ± 1mmHg. The BP responses to 80ng Ang II and 25ng Ang II are fully blocked by prior infusion of the AT_1-R blocker candesartan (10ug) or losartan (9ug) respectively (Saad et al 2008) in the SFO indicating that AT_1-receptors in the SFO mediate responses to Ang II. Electrophysiological studies have shown that nearly 70% of SFO neurons are responsive to Ang II (Okuya et al 1987, Schmid et al 1992). Patch clamp recordings of SFO neurons show that Ang II decreases the current that is thought to be responsible for the after spike hyperpolarization or resting phase of the neuron, allowing the spontaneously active neurons to increase their firing rate (Ferguson and Li 1996). HR remained unchanged following Ang II injections in the SFO, similarly as reported by Ku and group (1999) (Ku et al 1999).

Infusion of Na^+ rich aCSF into the SFO causes an AT_1-R mediated increase of BP as the increase is blocked by prior infusion of the AT_1-R blocker Candesartan. This data is consistent with mechanisms activated during acute icv (Huang and Leenen 1996) and PVN (Gabor and Leenen 2009) infusions of Na^+ rich aCSF which result in an AT_1-R dependent increase in BP. Microdialysis infusion of 0.3M and 0.6M NaCl into the PVN causes a dose dependent release of Ang II in the PVN (Quadri et al 1994). In this study, an osmotically equivalent amount of glucose did not cause release of Ang II in the PVN indicating that the release of Ang II is directly related to local increases in $[Na^+]$. A similar mechanism is likely activated in the SFO where a sudden increase in extracellular Na^+ may result in increased entry of Na^+ into neurons. This may then increase the activity of the Na^+/Ca^{2+} exchanger

and result in increased entry of Ca^{2+} into the cell to reduce the amount of Na^+ (Kosh and Barish 1994). This increase entry of Ca^{2+} into SFO neurons would lead to fusion of synaptic vesicles to the cell membrane and results in exocytosis (Annunziato et al 2004), a likely mechanism that results in Ang II release.

Infusion of Na^+ rich aCSF in the SFO or icv did not have an effect on HR (Table R2). Heart rate tended to decrease in some groups but not statistically significant from baseline. Larger experimental groups may have clarified whether HR decreases or remains the same during these experimental conditions. In acute icv or PVN infusion of Na^+ rich aCSF (Huang and Leenen 1992, Gabor and Leenen 2009) HR decreases initially but then increases within 5-10min. The reduction in HR that follows acute increases in $[Na^+]$ can be prevented by prior iv injection of an AVP-antagonist (Gabor and Leenen 2009). The initial decrease in HR appears therefore due to release of vasopressin into the circulation. This decrease in HR is likely through the activation of V_1 receptors in the area postrema (AP) that signal a reduction in cardiac sympathetic efferent activity and HR (Hasser and Bishop 1990). In our studies vasopressin may have a greater role in causing a reflex inhibition of HR throughout the infusion period, but our studies did not address the role of AVP on BP and HR.

4.3 Aldosterone and Na^+ rich aCSF in the SFO

BP responses to 0.45M Na^+ rich aCSF in the SFO are enhanced by infusion of a high dose aldosterone in the SFO 45min prior to the Na^+ infusion. These BP responses were enhanced to the levels observed with infusion of 0.6M Na^+ rich aCSF. The aldosterone enhanced BP

responses to infusion of 0.45M Na^+ rich aCSF in the SFO were fully blocked with prior infusion of the AT_1-R blocker Candesartan indicating that the response is mediated via AT_1-R activation. The current results are in agreement with studies performed icv and in the PVN where the aldosterone mediated enhancement of responses to acute increases in [Na^+] icv and in the PVN were fully blocked by pretreatment with an AT_1-R blocker (Huang and Leenen 1999, Gabor and Leenen 2009).

In icv (Wang et al 2003) and PVN (Gabor and Leenen 2009) studies, BP and HR responses to infusions of Na^+ rich aCSF are also enhanced by aldosterone. These enhanced responses are mediated through a pathway that requires benzamil sensitive Na^+ channels, possibly ENaC, as prior icv or PVN infusion of benzamil blocks the enhanced responses but not the response to Na^+. In our studies, aldosterone may be having both a genomic and non-genomic effect. The genomic effects may be mediated through the actions of aldosterone acting as a transcription factor and enhancing the expression of target genes like ENaC and/or other genes that result in increased sensitivity of the SFO to local elevations in [Na^+]. The presence of 11βHSD2 (Leenen et al unpublished), MR and all three subunits of ENaC have been determined in SFO neurons (Amin et al 2005, Wang et al 2010). This suggests that the SFO may be able to selectively bind aldosterone and express target genes like ENaC. It is however not clear if aldosterone levels in the SFO are increased during chronic increases in CSF[Na^+]. Assessment of MR and ENaC expression in the SFO following chronic icv infusion of Na^+ rich aCSF showed that MR (mRNA levels) and ENaC (mRNA and protein levels) are not changed (Wang et al 2010) suggesting that aldosterone in the SFO may not be directly involved in the BP and HR responses to chronic increases in CSF[Na^+]. The non-genomic actions of aldosterone may be occurring through residual aldosterone in

the SFO that has not been cleared from the area during the 45 min wait until the Na^+ infusion. This is a likely possibility because we are infusing a high dose aldosterone (1500ng). In kidney cells, aldosterone is able to regulate ENaC activity in the presence of spironolactone (Zhou & Bubien 2001). The non-genomic effects of aldosterone may thus be activating amiloride sensitive epithelial sodium channels through the actions of a postulated plasma membrane steroid receptor (Zhou & Bubien 2001). Similar mechanisms may be present in the brain and could have contributed to the results obtained in our studies. By enhancing entry of Na^+ into neurons through the actions of ENaC, the non-genomic effects of aldosterone may then lead to increased neuronal firing resulting in enhanced Ang II release and increases in BP.

Responses to 0.6M Na^+ rich aCSF were not enhanced by aldosterone. Considering that BP responses to 0.45M Na^+ rich aCSF in the SFO are enhanced with aldosterone to the levels seen with 0.6M Na^+ rich aCSF, it is possible that the 0.6M Na^+ rich aCSF may have activated all possible Na^+ sensitive neurons in the SFO and caused maximum activation. Further studies by infusing Na^+ above 0.6M are needed to determine whether the SFO has a maximal response to [Na^+].

4.4 ICV Ang II and Na^+ rich aCSF and Candesartan in the SFO

The lamina terminalis is crucial for the responses to changes in CSF[Na^+] as lesions restricted to this area; which includes the SFO, OVLT and MnPO; fully block responses to acute icv infusion of 0.6M NaCl (May et al 2000). Our results indicate that AT_1-R activation

in the SFO partially mediates this response as the BP increase observed by icv infusion of 0.3M Na^+ rich aCSF was reduced by nearly half with Candesartan infusion in the SFO. Rohmeiss and group (1995a) showed that AT_1-R activation in the SFO is fully responsible for mediating BP responses to icv injection of NaCl, as the response was fully blocked with Losartan in the SFO. Both studies (ours and Rohmeiss et al 1995a) gave 0.3M Na^+ icv and an AT_1-R blocker in the SFO. The variation in blockade of responses may lie in the method of Na^+ administration as the Rohmeiss study injected a 5ul bolus dose while our study infused a total of 38ul over 10min. It is likely that a 5ul injection of NaCl only momentarily increases [Na^+] in the region close to the injection site, thus all Na^+ sensitive regions are not activated. An injection in the lateral ventricle is close to the SFO potentially resulting in the activation of SFO neurons while other areas like the OVLT, which appears to be Na^+ sensitive (Veerasingham and Leenen 1997), may not be activated. We were able to reproduce these results by giving bolus icv injections (10ul) of 0.3M Na^+ rich aCSF which resulted in an increase in MAP of 14 ± 4mmHg. This response was fully blocked with 10ug of Candesartan in the SFO confirming the data by the Rohmeiss study. In contrast, the BP response to a 20ul volume of the 0.3M Na^+ rich aCSF following 10ug Candesartan in the SFO was not blocked. This indicates that the larger volume is perhaps able to reach other Na^+ sensitive regions beyond those that were blocked by Candesartan in the SFO supporting our conclusion that a bolus injection of NaCl will not activate all Na^+ sensitive areas. The SFO may sense changes in CSF[Na^+] through neurons projecting into the CSF or ependymal tanycytes on the surface of the SFO in contact with the CSF (Dellman and Simpson 1976, Dellman 1985, 1998). During an infusion, a steady state of increased CSF[Na^+] is reached over the 10min of infusion and all Na^+ sensitive areas are able to respond including the

OVLT and even perhaps the PVN as the PVN has neuronal dendrites that project into the ventricles and are in contact with the CSF (Panzica and Viglietti-Panzica 1983). Similar studies have shown that AT_1-R activation in the PVN also mediate responses to acute icv infusions of Na^+ rich aCSF (0.3M at 3.8ul/min, 10min) as telmisartan in the PVN fully blocks BP response to icv 0.3M Na^+ (Gabor and Leenen 2009).

These results indicate that the SFO mediates half the BP responses to acute increases in CSF[Na^+]. The remainder of the response is likely mediated through the OVLT (Veerasingham and Leenen 1997). Both the SFO and OVLT may send angiotensinergic projections to the MnPO as losartan in MnPO fully blocks BP response to icv 0.3M Na^+ (Budzikowski and Leenen 2001). Activation of the MnPO may lead to Ang II release in the PVN and downstream increase in sympathetic activity.

4.5 Ouabain dose response studies in the SFO

In the current study, we confirmed previous results that showed BP and HR increase to icv injection of ouabain (Huang and Leenen 1996). Injection of ouabain resulted in a slow increase of BP that reached a peak 7min following the injection. In our study an icv infusion of ouabain (640ng) did not change in BP. This is likely because the infusion results in dilution of the ouabain while an injection would deliver a large enough dose to increase ouabain levels in the CSF. The MnPO and PVN were found to be ouabain sensitive as local injections of ouabain increased BP and HR (Budzikowski and Leenen 2001, Gabor and Leenen 2009). In the PVN, a dose dependent BP and HR response was observed to acute

injections of 20, 40 and 80ng ouabain. In contrast, in the SFO ouabain appears not involved in modulating BP or HR responses.

Our results suggest that the SFO does not mediate BP responses to changes in CSF[Na^+] through a mechanism that involves "ouabain" release in the SFO. "Ouabain-IR" positive fibres have been identified in the SFO while the origin of the fibres is not clearly known (Yamada et al 1992a). Studies on the distribution of Na^+/K^+ ATPase subunit isoforms in the SFO have revealed species differences. In Sprague-Dawley rats using complimentary ^{35}S-labeled cRNA probes to target the α1, α2 and α3 isoforms of the Na^+/K^+ ATPase, α3 isoform was detected in neurons of the SFO (Watts et al 1991). In adult mice, mRNAs encoding the α1 and α2 isoforms were found expressed in the SFO, but signals for the α3 isoform were not detected (Shimizu et al 2007).

Ouabain has been demonstrated to bind Na^+/K^+ATPase in SFO glial cells that express the Na_x-channel (Shimizu et al 2007). In this case, ouabain is likely binding the α2 subunit in the SFO as the Na_x channel, associated with Na^+/K^+ATPase, is found on glia (Wanatabe et al 2006) while α3, if present, would be found only on neurons. It appears that under our experimental conditions, ouabain binding Na^+/K^+ATPase in SFO glia is not associated with changes in BP or HR and may instead be involved in the regulation of Na^+ appetite (Shimizu et al 2007).

4.6 Conclusion

Our study shows for the first time that the SFO is Na^+ sensitive and shows a dose dependent increase in BP but not HR. Na^+ rich aCSF in the SFO may have maximal responses to acute increases in [Na^+] at 0.6M as the BP response to a lower dose of Na^+ (0.45M) is enhanced

with prior infusion of aldosterone while 0.6M is not further enhanced. Similar to icv and PVN studies (Huang et al 1996, Gabor and Leenen 2009), the mechanism responsible for the enhanced responses is likely through the genomic effects of aldosterone affecting target genes like ENaC and enhancing the sensitivity of the SFO to Na^+. BP responses to infusion of Na^+ rich aCSF and the enhancement of those BP responses by aldosterone are all mediated through AT_1-R activation in the SFO.

Our study shows that AT_1-R activation in the SFO is responsible for nearly 50% of the BP responses to brief increases in CSF[Na^+]. The SFO likely senses changes in CSF[Na^+] through ependymal tanycytes on the surface of the SFO at the CSF side or neurons projecting into the CSF. This increase in CSF[Na^+] results in AT_1-R activation in the SFO likely through Na^+ induced Ang II release.

Lastly, contrary to PVN and MnPO studies (Huang and Leenen 1996, Budzikowski and Leenen 2001, Gabor and Leenen 2009) we show that ouabain in the SFO is not associated with changed in BP or HR. In vitro studies have shown ouabain capable of binding Na^+/K^+ ATPase in the SFO of mice (Shimizu et al 2007) but, under our experimental conditions, ouabain binding Na^+/K^+ ATPase in the SFO appears not to be involved in regulation of BP or HR.

4.7 Limitations and Future Studies

Our studies have certain limitations that need to be considered. Although we determined that the SFO is Na^+ sensitive, we did not measure responsiveness to Na^+ above the 0.6M Na^+ rich aCSF to confirm that there may be maximal activation at that dose. It is not clear how

much SFO[Na^+] increases during infusion of 0.45M or 0.6M Na^+ rich aCSF as compared to increases in SFO [Na^+] during increased CSF[Na^+]. Further studies can determine how much the [Na^+] in the SFO changes through insertion of a microcapillary glass [Na^+] electrode (Kato et al 2004) in the SFO.

Similarly, it is not clear if acute or chronic increases in CSF[Na^+] increase aldosterone's role in the SFO. This can be determined through infusion studies with icv Na^+ rich aCSF and injection of an siRNA in the SFO targeting aldosterone synthase (AS) or MR to reduce expression. Blocking AS and MR would clarify whether de-novo synthesis of aldosterone potentially occurring in the SFO and binding to MR is involved in the responses to icv infusion of Na^+ rich aCSF.

HR changes were not observed and this finding was attributed to the release of AVP resulting in the reflex inhibition of HR responses. This can be confirmed by infusing Na^+ rich aCSF in the SFO with or without iv injection of an AVP antagonist.

In conclusion, these results show that the SFO is Na^+ sensitive and AT_1-R activation in the SFO mediates half the BP responses to increases in CSF[Na^+]. The SFO is further sensitized to Na^+ by aldosterone presumably through its genomic effects. Lastly, ouabain in the SFO does not appear to contribute to BP or HR regulation.

5 References

Abrams JM, Osborn JW. A role for benzamil-sensitive proteins of the central nervous system in the pathogenesis of salt-dependent hypertension. Clin Exp Pharmacol Physiol. 2008, 35:687-94.

Amin MS, Wang HW, Reza E, Whitman SC, Tuana BS, Leenen FH. Distribution of epithelial sodium channels and mineralocorticoid receptors in cardiovascular regulatory centers in rat brain. Am J Physiol Regul Integr Comp Physiol. 2005, 289:R1787-97.

Annunziato L, Pignataro G, Di Renzo GF. Pharmacology of brain $Na^+/Ca2^+$ exchanger: from molecular biology to therapeutic perspectives. Pharmacol Rev. 2004, 56:633-54.

Babic T, Roder S, Ciriello J. Direct projections from caudal ventrolateral medullary depressor sites to the subfornical organ. Brain Res. 2004, 1003:113-21

Bains JS, Ferguson AV. Paraventricular nucleus neurons projecting to the spinal cord receive excitatory input from the subfornical organ. Am J Physiol. 1995, 268:R625-33.

Bauer DE, Jackson JG, Genda EN, Montoya MM, Yudkoff M, Robinson MB. The glutamate transporter, GLAST, participates in a macromolecular complex that supports glutamate metabolism. Neurochem Int. 2012 (In Press)

Booth RE, Johnson JP, Stockand JD. Aldosterone. Adv Physiol Educ. 2002, 26:8-20.

Bourassa EA, Speth RC. Water deprivation increases angiotensin-converting enzyme but not AT(1) receptor expression in brainstem and paraventricular nucleus of the hypothalamus of the rat. Brain Res. 2010, 1319:83-91.

Brines ML, Robbins RJ. Cell-type specific expression of Na^+, $K(^+)$-ATPase catalytic subunits in cultured neurons and glia: evidence for polarized distribution in neurons. Brain Res. 1993, 631:1-11.

Brooks VL, Scrogin KE, McKeogh DF. The interaction of angiotensin II and osmolality in the generation of sympathetic tone during changes in dietary salt intake. An hypothesis. Ann N Y Acad Sci. 2001, 940:380-94.

Bruner CA, Fink GD. Neurohumoral contributions to chronic angiotensin-induced hypertension. Am J Physiol. 1986, 250:H52-61.

Budzikowski AS, Leenen FH. ANG II in median preoptic nucleus and pressor responses to CSF sodium and high sodium intake in SHR. Am J Physiol Heart Circ Physiol. 2001, 281:H1210-6

Budzikowski AS, Leenen FH. Brain 'ouabain' in the median preoptic nucleus mediates sodium-sensitive hypertension in spontaneously hypertensive rats. Hypertension. 1997, 29:599-605.
Budzikowski AS, Vahid-Ansari F, Leenen FH. Chronic activation of brain areas by high-sodium diet in Dahl salt-sensitive rats. Am J Physiol. 1998;274:H2046-52.

Buñag RD, Miyajima E. Sympathetic hyperactivity elevates blood pressure during acute cerebroventricular infusions of hypertonic salt in rats. J Cardiovasc Pharmacol. 1984, 6:844-51.

Bunnemann B, Fuxe K, Metzger R, Bjelke B, Ganten D. The semi-quantitative distribution and cellular localization of angiotensinogen mRNA in the rat brain. J Chem Neuroanat. 1992, 5:245-62.

Camacho A, Phillips MI. Horseradish peroxidase study in rat of the neural connections of the organum vasculosum of the lamina terminalis. Neurosci Lett. 1981;25 :201-4.

Camargo LA, Menani JV, Saad WA, Saad WA. Interaction between areas of the central nervous system in the control of water intake and arterial pressure in rats. J Physiol. 1984, 350:1-8.

Carter BC, Bean BP. Sodium entry during action potentials of mammalian neurons: incomplete inactivation and reduced metabolic efficiency in fast-spiking neurons. Neuron. 2009, 64:898-909.

Cernes R, Mashavi M, Zimlichman R. Differential clinical profile of candesartan compared to other angiotensin receptor blockers. Vasc Health Risk Manag. 2011, 7:749-59.

Cheung WJ, Kent MA, El-Shahat E, Wang H, Tan J, White R, Leenen FH. Central and peripheral renin-angiotensin systems in ouabain-induced hypertension. Am J Physiol Heart Circ Physiol. 2006, 291:H624-30.

Conn PM, Freeman ME. Neuroendocrinology in Physiology and Medicine. Totowa, NJ: Humana, 2000, p. 25.

Cunningham JT, Beltz T, Johnson RF, Johnson AK. The effects of ibotenate lesions of the median preoptic nucleus on experimentally-induced and circadian drinking behavior in rats. Brain Res. 1992, 580:325-30.

Dellmann HD, Simpson JB. Regional Differences in the Morphology of the Rat Subfornical Organ. Brain Research. 1976, 116:389-400

Dellmann HD, Simpson JB. The subfornical organ. Int Rev Cytol. 1979;58:333-421.

Dellmann HD. Fine Structural Subdivision of the Subfornical Organ: A Concise Review. Brain Research Bulletin. 1985, 15: 71-78

Dellmann HD. Structure of the subfornical organ: a review. Microsc Res Tech. 1998, 41:85-97.
Di Nicolantonio R, Mendelsohn FA, Hutchinson JS, Takata Y, Doyle AE. Dissociation of dipsogenic and pressor responses to chronic central angiotensin II in rats. Am J Physiol. 1982, 242:R498-504.

Duan PG, Kawano H, Masuko S. Collateral projections from the subfornical organ to the median preoptic nucleus and paraventricular hypothalamic nucleus in the rat. Brain Res. 2008, 1198:68-72.

Dzau VJ, Ingelfinger J, Pratt RE, Ellison KE. Identification of renin and angiotensinogen messenger RNA sequences in mouse and rat brains. Hypertension. 1986, 8:544-8.

Esclapez M, Tillakaratne NJ, Kaufman DL, Tobin AJ, Houser CR. Comparative localization of two forms of glutamic acid decarboxylase and their mRNAs in rat brain supports the concept of functional differences between the forms. J Neurosci. 1994, 14:1834-55.

Fang Z, Carlson SH, Peng N, Wyss JM. Circadian rhythm of plasma sodium is disrupted in spontaneously hypertensive rats fed a high-NaCl diet. Am J Physiol Regul Integr Comp Physiol. 2000, 278:R1490-5.

Ferguson AV, Bains JS. Actions of angiotensin in the subfornical organ and area postrema: implications for long term control of autonomic output. Clin Exp Pharmacol Physiol. 1997, 24:96-101

Ferguson AV, Li Z. Whole cell patch recordings from forebrain slices demonstrate angiotensin II inhibits potassium currents in subfornical organ neurons. Regul Pept. 1996, 66:55-8.

Ferrari MF, Raizada MK, Fior-Chadi DR. Nicotine modulates the renin-angiotensin system of cultured neurons and glial cells from cardiovascular brain areas of Wistar Kyoto and spontaneously hypertensive rats. J Mol Neurosci. 2007, 33:284-93.

Fink GD, Bryan WJ, Mann ME. Effect of forebrain lesions on response to chronic intraventricular angiotensin II. Am J Physiol. 1983, 244:R45-50.

Franchini LF, Vivas L. Distribution of Fos immunoreactivity in rat brain after sodium consumption induced by peritoneal dialysis. Am J Physiol. 1999, 276:R1180-7.

Furukawa A, Miyatake A, Ohnishi T, Ichikawa Y. Steroidogenic acute regulatory protein (StAR) transcripts constitutively expressed in the adult rat central nervous system: colocalization of StAR, cytochrome P-450SCC (CYP XIA1), and 3beta-hydroxysteroid dehydrogenase in the rat brain. J Neurochem. 1998, 71:2231-8.

Fuxe K, Ganten D, Hökfelt T, Locatelli V, Poulsen K, Stock G, Rix E, Taugner R. Renin-like immunocytochemical activity in the rat and mouse brain. Neurosci Lett. 1980, 18:245-50.

Gabor A, Leenen FH. Mechanisms in the PVN mediating local and central sodium-induced hypertension in Wistar rats. Am J Physiol Regul Integr Comp Physiol. 2009, 296:R618-30.

Gabor A, Leenen FH. Cardiovascular effects of angiotensin II and glutamate in the PVN of Dahl salt-sensitive rats. Brain Res. 2012, 1447:28-37.

Geerling JC, Kawata M, Loewy AD. Aldosterone-sensitive neurons in the rat central nervous system. J Comp Neurol. 2006, 494515-27.

Gomez-Sanchez EP, Ahmad N, Romero DG, Gomez-Sanchez CE. Is aldosterone synthesized within the rat brain? Am J Physiol Endocrinol Metab. 2005, 288 :E342-6.

Gomez-Sanchez EP, Gomez-Sanchez CM, Plonczynski M, Gomez-Sanchez CE. Aldosterone synthesis in the brain contributes to Dahl salt-sensitive rat hypertension. Exp Physiol. 2010, 95:120-30

Gomez-Sanchez EP, Samuel J, Vergara G, Ahmad N. Effect of 3beta-hydroxysteroid dehydrogenase inhibition by trilostane on blood pressure in the Dahl salt-sensitive rat. Am J Physiol. 2005, 288:R389–93.

Goto A, Ikeda T, Tobian L, Iwai J, Johnson MA. Brain lesions in the paraventricular nuclei and catecholaminergic neurons minimize salt hypertension in Dahl salt-sensitive rats. Clin Sci (Lond). 1981, 61 Suppl 7:53s-55s.

Goto A, Ganguli M, Tobian L, Johnson MA, Iwai J. Effect of an anteroventral third ventricle lesion on NaCl hypertension in Dahl salt-sensitive rats. Am J Physiol. 1982, 243:H614-8.

Grob M, Trottier JF, Drolet G, Mouginot D. Characterization of the neurochemical content of neuronal populations of the lamina terminalis activated by acute hydromineral challenge. Neuroscience. 2003, 122:247-57.

Gross PM. Morphology and physiology of capillary systems in subregions of the subfornical organ and area postrema. Can J Physiol Pharmacol. 1991, 69:1010-25.

Guennoun R, Fiddes RJ, Gouézou M, Lombès M, Baulieu EE. A key enzyme in the biosynthesis of neurosteroids, 3 beta-hydroxysteroid dehydrogenase/delta 5-delta 4-isomerase (3 beta-HSD), is expressed in rat brain. Brain Res Mol Brain Res. 1995, 30:287-300.

Guilhaume SS, Corrêa FM. Effect of NMDA-induced lesion of the subfornical organ on the angiotensin II binding sites density and acetylcholinesterase or NADPH-diphorase activities in the lamina terminalis of the rat brain. Cell Mol Neurobiol. 2001, 21:81-90.

Gutman MB, Jones DL, Ciriello J. Contribution of nucleus medianus to the drinking and pressor responses to angiotensin II acting at subfornical organ. Brain Res. 1989, 488:49-56.

Halpain S, Wieczorek CM, Rainbow TC Localization of L-glutamate receptors in rat brain by quantitative autoradiography. J Neurosci. 1984, 4:2247-58.

Harrison-Bernard LM. The renal renin-angiotensin system. Adv Physiol Educ. 2009, 33:270-4.

Hasser EM, Bishop VS. Reflex effect of vasopressin after blockade of V1 receptors in the area postrema. Circ Res. 1990, 67:265-71.

Hendel MD, Collister JP. Contribution of the subfornical organ to angiotensin II-induced hypertension. Am J Physiol Heart Circ Physiol. 2005, 288:H680-5.

Herbert J, Forsling ML, Howes SR, Stacey PM, Shiers HM. Regional expression of c-fos antigen in the basal forebrain following intraventricular infusions of angiotensin and its modulation by drinking either water or saline. Neuroscience. 1992, 51:867-82.

Hertz L, Dringen R, Schousboe A, Robinson SR. Astrocytes: glutamate producers for neurons. J Neurosci Res. 1999, 57:417-28.

Hiyama TY, Watanabe E, Okado H, Noda M. The subfornical organ is the primary locus of sodium-level sensing by Na(x) sodium channels for the control of salt-intake behavior. J Neurosci. 2004, 24:9276-81.

Honda E, Xu S, Ono K, Ito K, Inenaga K. Spontaneously active GABAergic interneurons in the subfornical organ of rat slice preparations. Neurosci Lett. 2001, 306:45-8.

Hou X, Theriault SF, Dostanic-Larson I, Moseley AE, Lingrel JB, Wu H, Dean S, Van Huysse JW. Enhanced pressor response to increased CSF sodium concentration and to central ANG I in heterozygous alpha2 Na^+ -K^+ -ATPase knockout mice. Am J Physiol Regul Integr Comp Physiol. 2009, 296:R1427-38.

Huang BS, Ahmadi S, Ahmad M, White RA, Leenen FH. Central neuronal activation and pressor responses induced by circulating ANG II: role of the brain aldosterone-"ouabain" pathway. Am J Physiol Heart Circ Physiol. 2010, 299:H422-30.

Huang BS, Cheung WJ, Wang H, Tan J, White RA, Leenen FH. Activation of brain renin-angiotensin-aldosterone system by central sodium in Wistar rats. Am J Physiol Heart Circ Physiol. 2006, 291:H1109-17.

Huang BS, Harmsen E, Yu H, Leenen FH. Brain ouabain-like activity and the sympathoexcitatory and pressor effects of central sodium in rats. Circ Res. 1992, 71:1059-66.

Huang BS, Leenen FH. Blockade of brain "ouabain" prevents sympathoexcitatory and pressor responses to high sodium in SHR. Am J Physiol. 1996, 271:H103-8.

Huang BS, Leenen FH. Both brain angiotensin II and "ouabain" contribute to sympathoexcitation and hypertension in Dahl S rats on high salt intake. Hypertension. 1998, 32:1028-33.

Huang BS, Leenen FH. Sympathoexcitatory and pressor responses to increased brain sodium and ouabain are mediated via brain ANG II. Am J Physiol. 1996, 270:H275-80.

Huang BS, Van Vliet BN, Leenen FH. Increases in CSF [Na+] precede the increases in blood pressure in Dahl S rats and SHR on a high-salt diet. Am J Physiol Heart Circ Physiol. 2004, 287:H1160-6.

Huang BS, Veerasingham SJ, Leenen FH. Brain "ouabain," ANG II, and sympathoexcitation by chronic central sodium loading in rats. Am J Physiol. 1998, 274:H1269-76

Huang BS, Wang H, Leenen FH. Chronic central infusion of aldosterone leads to sympathetic hyperreactivity and hypertension in Dahl S but not Dahl R rats. Am J Physiol Heart Circ Physiol. 2005 , 288:H517-24.

Huang BS, Wang H, Leenen FH. Enhanced sympathoexcitatory and pressor responses to central Na+ in Dahl salt-sensitive vs. -resistant rats. Am J Physiol Heart Circ Physiol. 2001, 281:H1881-9.

Huang BS, White RA, Ahmad M, Jeng AY, Leenen FH. Central infusion of aldosterone synthase inhibitor prevents sympathetic hyperactivity and hypertension by central Na+ in Wistar rats. Am J Physiol Regul Integr Comp Physiol. 2008, 295:R166-72

Huang BS, White RA, Jeng AY, Leenen FH. Role of central nervous system aldosterone synthase and mineralocorticoid receptors in salt-induced hypertension in Dahl salt-sensitive rats. Am J Physiol Regul Integr Comp Physiol. 2009, 296:R994-R1000.

Huang BS, Zheng H, Tan J, Patel KP, Leenen FH. Regulation of hypothalamic renin-angiotensin system and oxidative stress by aldosterone. Exp Physiol. 2011, 96:1028-38.

Inagami T, Clemens DL, Celio MR, Brown A, Sandru L, Herschkowitz N, Hoffman LH, Kasselberg AG. Immunohistochemical localization of renin in mouse brain. Neurosci Lett. 1980, 18:91-8.

Ito S, Hiratsuka M, Komatsu K, Tsukamoto K, Kanmatsuse K, Sved AF. Ventrolateral medulla AT1 receptors support arterial pressure in Dahl salt-sensitive rats. Hypertension. 2003, 41:744-50.

Iwai N, Inagami T. Quantitative analysis of renin gene expression in extrarenal tissues by polymerase chain reaction method. J Hypertens. 1992, 10:717-24.

Jo H, Yang EK, Lee WJ, Park KY, Kim HJ, Park JS. Gene expression of central and peripheral renin-angiotensin system components upon dietary sodium intake in rats. Regul Pept. 1996, 67:115-21.

Jones DL. Kainic acid lesions of the median preoptic nucleus: effects on angiotensin II induced drinking and pressor responses in the conscious rat. Can J Physiol Pharmacol. 1988, 66:1082-6.

Kawamura A, Guo J, Itagaki Y, Bell C, Wang Y, Haupert GT Jr, Magil S, Gallagher RT, Berova N, Nakanishi K. On the structure of endogenous ouabain Proc. Natl. Acad. Sci. 1999, 96: 6654–6659

Kawano H, Masuko S. Region-specific projections from the subfornical organ to the paraventricular hypothalamic nucleus in the rat. Neuroscience. 2010, 169:1227-1234.

Kolaj M, Bai D, Renaud LP. GABAB receptor modulation of rapid inhibitory and excitatory neurotransmission from subfornical organ and other afferents to median preoptic nucleus neurons. J Neurophysiol. 2004, 92:111-22.

Koch RA, Barish ME. Perturbation of intracellular calcium and hydrogen ion regulation in cultured mouse hippocampal neurons by reduction of the sodium ion concentration gradient. J Neurosci. 1994, 14:2585-93.

Kumar NN, Goodchild AK, Li Q, Pilowsky PM. An aldosterone-related system in the ventrolateral medulla oblongata of spontaneously hypertensive and Wistar-Kyoto rats. Clin Exp Pharmacol Physiol. 2006, 33:71-5.

Ku YH, Jia YF, Chang YZ. Mechanisms underlying pressor response of subfornical organ to angiotensin II. Peptides. 1999, 20:171-6.

Lenkei Z, Corvol P, Llorens-Cortes C. The angiotensin receptor subtype AT1A predominates in rat forebrain areas involved in blood pressure, body fluid homeostasis and neuroendocrine control. Brain Res Mol Brain Res. 1995, 30:53-60.

Lenkei Z, Palkovits M, Corvol P, Llorens-Cortes C. Distribution of angiotensin type-1 receptor messenger RNA expression in the adult rat brain. Neuroscience. 1998, 82:827-41.

Li S, Eim C, Kirch U, Lang RE, Schoner W. Bovine adrenals and hypothalamus are a major source of proscillaridin A- and ouabain-immunoreactivities. Life Sci. 1998, 62:1023-33.

Li Z, Ferguson AV. Subfornical organ efferents to paraventricular nucleus utilize angiotensin as a neurotransmitter. Am J Physiol. 1993, 265:R302-9.

Lin W, McKinney K, Liu L, Lakhlani S, Jennes L. Distribution of vesicular glutamate transporter-2 messenger ribonucleic Acid and protein in the septum-hypothalamus of the rat. Endocrinology. 2003, 144:662-70.

Lind RW, Johnson AK. Subfornical organ-median preoptic connections and drinking and pressor responses to angiotensin II. J Neurosci. 1982, 2:1043-51.

Lind RW, Swanson LW, Bruhn TO, Ganten D. The distribution of angiotensin II-immunoreactive cells and fibers in the paraventriculo-hypophysial system of the rat. Brain Res. 1985, 338:81-9.

Lind RW, Van Hoesen GW, Johnson AK. An HRP study of the connections of the subfornical organ of the rat. J Comp Neurol. 1982, 210:265-77.

Lind RW, Van Hoesen GW, Johnson AK. An HRP study of the connections of the subfornical organ of the rat. J Comp Neurol. 1982, 210:265-77.

Lingrel J.B, and Kuntzweiler T. Na^+,K^+-ATPase. The Journal of Biological Chemistry. 1994, 269:19659-19662

Lippoldt A, Bunnemann B, Iwai N, Metzger R, Inagami T, Fuxe K and Ganten D. Cellular localization of angiotensin type 1 receptor and angiotensinogen mRNAs in the subfornical organ of the rat brain. Neuroscience Letters. 1993, 150:153-158.

Lösel RM, Feuring M, Falkenstein E, Wehling M. Nongenomic effects of aldosterone: cellular aspects and clinical implications. Steroids. 2002, 67:493-8.

Lovelace M, Watson TG, Stephenson GL. Steroid 21-hydroxylase expression in cultured rat astrocytes. Brain Res Bull. 2003, 61:609-15.

Lu B., Yang X.J., Chen K., Yang D.J., Yan J.Q. Dietary sodium deprivation evokes activation of brain regional neurons and down-regulation of angiotensin II type 1 receptor and angiotensin-convertion enzyme mRNA expression. Neuroscience 2009, 164:1303-1311

Luís C. Reis. Role of the serotoninergic system in the sodium appetite control. An Acad Bras Cienc. 2007, 79:261-83.

Ma R, Schultz HD, Wang W. Chronic central infusion of ANG II potentiates cardiac sympathetic afferent reflex in dogs. Am J Physiol. 1999, 277:H15-22.

MacKenzie SM, Clark CJ, Fraser R, Gómez-Sánchez CE, Connell JM, Davies E. Expression of 11beta-hydroxylase and aldosterone synthase genes in the rat brain. J Mol Endocrinol. 2000, 24:321-8.

Mangiapane ML, Simpson JB. Subfornical organ: forebrain site of pressor and dipsogenic action of angiotensin II. Am J Physiol. 1980, 239:R382-9.

Marvar PJ, Thabet SR, Guzik TJ, Lob HE, McCann LA, Weyand C, Gordon FJ, Harrison DG. Central and peripheral mechanisms of T-lymphocyte activation and vascular inflammation produced by angiotensin II-induced hypertension. Circ Res. 2010, 107:263-70.

Mathai ML, Evered MD, McKinley MJ. Central losartan blocks natriuretic, vasopressin, and pressor responses to central hypertonic NaCl in sheep. Am J Physiol. 1998, 275:R548-54.

Matsumura K, Simon E. Locations and properties of angiotensin II-responsive neurones in the circumventricular region of the duck brain. J Physiol. 1990, 429:281-96.

May CN, McAllen RM, McKinley MJ. Renal nerve inhibition by central NaCl and ANG II is abolished by lesions of the lamina terminalis. Am J Physiol Regul Integr Comp Physiol. 2000, 279:R1827-33.

May CN, McAllen RM. Brain angiotensinergic pathways mediate renal nerve inhibition by central hypertonic NaCl in conscious sheep. Am J Physiol. 1997, 272:R593-600.

McKenna MC, Sonnewald U, Huang X, Stevenson J, Zielke HR. Exogenous glutamate concentration regulates the metabolic fate of glutamate in astrocytes. J Neurochem. 1996, 66:386-93.

McKinley M.J, McAllen R.M, Davern P.J, Giles M.E, Penschow J.D, Sunn N, Uschakov A, Oldfield B. The Sensory Circumventricular Organs of the Mammalian Brain. 2003. Pg 56 Table 3, pg 63 Table 4

McKinley M.J, McAllen R.M, Davern P.J, Giles M.E, Penschow J.D, Sunn N, Uschakov A, Oldfield B. The Sensory Circumventricular Organs of the Mammalian Brain. 2003. Pg 56 Table 3, pg 63 Table 4

McKinley M.J, McAllen R.M, Davern P.J, Giles M.E, Penschow J.D, Sunn N, Uschakov A, Oldfield B. The Sensory Circumventricular Organs of the Mammalian Brain. 2003. Pg 9

McKinley M.J, McAllen R.M, Davern P.J, Giles M.E, Penschow J.D, Sunn N, Uschakov A, Oldfield B. The Sensory Circumventricular Organs of the Mammalian Brain. 2003. Pg 7

McKinley M.J, McAllen R.M, Davern P.J, Giles M.E, Penschow J.D, Sunn N, Uschakov A, Oldfield B. The Sensory Circumventricular Organs of the Mammalian Brain. 2003. Pg 20-21

McKinley MJ, Allen AM, Burns P, Colvill LM, Oldfield BJ. Interaction of circulating hormones with the brain: the roles of the subfornical organ and the organum vasculosum of the lamina terminalis. Clin Exp Pharmacol Physiol Suppl. 1998, 25:S61-7.

McKinley MJ, Badoer E, Oldfield BJ. Intravenous angiotensin II induces Fos-immunoreactivity in circumventricular organs of the lamina terminalis. Brain Res. 1992, 594:295-300.

McKinley MJ, Badoer E, Vivas L, Oldfield BJ. Comparison of c-fos expression in the lamina terminalis of conscious rats after intravenous or intracerebroventricular angiotensin. Brain Res Bull., 37:131-7.

McKinley MJ, Mathai ML, Pennington G, Rundgren M, Vivas L. Effect of individual or combined ablation of the nuclear groups of the lamina terminalis on water drinking in sheep. Am J Physiol. 1999, 276:R673-83.

Mellon SH, Deschepper CF. Neurosteroid biosynthesis: genes for adrenal steroidogenic enzymes are expressed in the brain. Brain Res. 1993, 629:283-92.

Moellenhoff E, Blume A, Culman J, Chatterjee B, Herdegen T, Lebrun CJ, Unger T. Effect of repetitive icv injections of ANG II on c-Fos and AT(1)-receptor expression in the rat brain. Am J Physiol Regul Integr Comp Physiol. 2001, 280:R1095-104.

Moellenhoff E, Lebrun CJ, Blume A, Culman J, Herdegen T, Unger T. Central angiotensin AT1 and muscarinic receptors in ITF expression on intracerebroventricular NaCl. Am J Physiol. 1998, 275:R234-44.

Naruse K, Takii Y, and Inagami T Immunohistochemical localization of renin in luteinizing hormone-producing cells of rat pituitary. Proc. Natl. Acad. Sci. USA. 1981, 78:7579-7583.

Naruse M, Naruse K, McKenzie JC, Schelling P, Inagami T. Regional distribution of renin and angiotensinogen in the brain of normotensive (WKY) and spontaneously hypertensive (SHR) rats. Brain Res. 1985, 333:147-50.

Nishimura M, Nanbu A, Ohtsuka K, Takahashi H, Iwai N, Kinoshita M, Yoshimura M. Sodium intake regulates renin gene expression differently in the hypothalamus and kidney of rats. J Hypertens. 1997, 15:509-16.

Nishimura M, Ohtsuka K, Nanbu A, Takahashi H, Yoshimura M. Benzamil blockade of brain Na+ channels averts Na(+)-induced hypertension in rats. Am J Physiol. 1998, 274:R635-44.

Noda M. The Subfornical Organ, a Specialized Sodium Channel, and the Sensing of Sodium Levels in the Brain. Neuroscientist. 2006, 12:80

Noda M, Shibouta Y, Inada Y, Ojima M, Wada T, Sanada T, Kubo K, Kohara Y, Naka T, Nishikawa K. Inhibition of rabbit aortic angiotensin II (AII) receptor by CV-11974, a new nonpeptide AII antagonist. Biochem Pharmacol. 1993, 20:311-8

Norenberg MD, Martinez-Hernandez A. Fine structural localization of glutamine synthetase in astrocytes of rat brain. Brain Res. 1979, 161:303-10.

Nunes FC, Braga VA. Chronic angiotensin II infusion modulates angiotensin II type I receptor expression in the subfornical organ and the rostral ventrolateral medulla in hypertensive rats. J Renin Angiotensin Aldosterone Syst. 2011, 12:440-5.

O'Callaghan EL, Bassi JK, Porrello ER, Delbridge LM, Thomas WG, Allen AM. Regulation of angiotensinogen by angiotensin II in mouse primary astrocyte cultures. J Neurochem. 2011, 119:18-26.

Okuya S, Inenaga K, Kaneko T, Yamashita H. Angiotensin II sensitive neurons in the supraoptic nucleus, subfornical organ and anteroventral third ventricle of rats in vitro. Brain Res. 1987, 402:58-67.

Osaka T, Yamashita H, Koizumi K. Inhibitory inputs to the subfornical organ from the AV3V: involvement of GABA. Brain Res Bull. 1992, 29:581-7.

Osborn JW, Hendel MD, Collister JP, Ariza-Guzman PA, Fink GD. The role of the subfornical organ in angiotensin II-salt hypertension in the rat. Exp Physiol. 2012, 97:80-8.

Osborne PG, Blair-West JR, Denton DA, Weisinger RS. Effect of varying the composition of CSF on urinary excretion in the conscious rat. Brain Res. 1989, 499:101-7.

Paxinos G, Watson C. The Rat Brain in Stereotaxic Coordinates. Orlando, FL: Academic, 1998.

Phillips MI, Shen L, Richards EM, Raizada MK. Immunohistochemical mapping of angiotensin AT1 receptors in the brain. Regul Pept. 1993, 44:95-107.

Pines G, Danbolt NC, Bjørås M, Zhang Y, Bendahan A, Eide L, Koepsell H, Storm-Mathisen J, Seeberg E, Kanner BI. Cloning and expression of a rat brain L-glutamate transporter. Nature. 1992, 360:464-7.

Ployngam T, Collister JP. An intact median preoptic nucleus is necessary for chronic angiotensin II-induced hypertension. Brain Res. 2007, 1162:69-75.

Porter JP. Chronic intracerebroventricular infusion of angiotensin II increases brain AT1 receptor expression in young rats. Brain Res Dev Brain Res. 1999, 112:293-5.

Porter JP, Anderson JM, Robison RJ, Phillips AC. Effect of central angiotensin II on body weight gain in young rats. Brain Res. 2003, 959:20-8.

Porter JP, Potratz KR. Effect of intracerebroventricular angiotensin II on body weight and food intake in adult rats. Am J Physiol Regul Integr Comp Physiol. 2004, 287:R422-8.

Potts PD, Hirooka Y, Dampney RA. Activation of brain neurons by circulating angiotensin II: direct effects and baroreceptor-mediated secondary effects. Neuroscience. 1999, 90:581-94.

Price EM, Rice DA, Lingrel JB. Site-directed mutagenesis of a conserved, extracellular aspartic acid residue affects the ouabain sensitivity of sheep Na,K-ATPase. J Biol Chem. 1989, 264:21902-6.

Pyner, S., Coote, J.H. Identification of branching paraventricular neurones of the hypothalamus that project to the rostroventrolateral medulla and spinal cord. Neuroscience. 2000, 100:549-56.

Qadri F, Edling O, Wolf A, Gohlke P, Culman J, Unger T. Release of angiotensin in the paraventricular nucleus in response to hyperosmotic stimulation in conscious rats: a microdialysis study. Brain Res. 1994, 637:45-9

Reagan LP, Flanagan-Cato LM, Yee DK, Ma LY, Sakai RR, Fluharty SJ. Immunohistochemical mapping of angiotensin type 2 (AT2) receptors in rat brain. Brain Res. 1994, 662:45-59.

Riftina F, Angulo J, Pompei P, McEwen B. Regulation of angiotensinogen gene expression in the rat forebrain by adrenal steroids and relation to salt appetite. Brain Res Mol Brain Res. 1995, 33:201-8.

Rohmeiss P, Beyer C, Hocher B, Qadri F, Gretz N, Strauch M, Unger T. Osmotically induced natriuresis and blood pressure response involves angiotensin AT1 receptors in the subfornical organ. J Hypertens. 1995, 13:1399-404. (a)

Rohmeiss P, Beyer C, Nagy E, Tschöpe C, Höhle S, Strauch M, Unger T. NaCl injections in brain induce natriuresis and blood pressure responses sensitive to ANG II AT1 receptors. Am J Physiol. 1995, 269:F282-8. (b)

Roland BL, Li KX, Funder JW. Hybridization histochemical localization of 11 beta-hydroxysteroid dehydrogenase type 2 in rat brain. Endocrinology. 1995, 136:4697-700.

Rowland NE, Li BH, Rozelle AK, Fregly MJ, Garcia M, Smith GC. Localization of changes in immediate early genes in brain in relation to hydromineral balance: intravenous angiotensin II. Brain Res Bull. 1994, 33:427-36. (a)

Rowland NE, Li BH, Rozelle AK, Smith GC. Comparison of fos-like immunoreactivity induced in rat brain by central injection of angiotensin II and carbachol. Am J Physiol. 1994, 267:R792-8. (b)

Saad WA, Camargo LA, Guarda IF, Santos TA. Subfornical organ mediates pressor effect of angiotensin: Influence of nitric oxide synthase inhibitors, AT(1) and AT(2) angiotensin antagonist's receptors. J Am Soc Hypertens. 2008, 2:326-31.

Sakai RR, McEwen BS, Fluharty SJ, Ma LY. The amygdala: site of genomic and nongenomic arousal of aldosterone-induced sodium intake. Kidney Int. 2000, 57:1337-45.

Sawchenko PE, Swanson LW. The organization of forebrain afferents to the paraventricular and supraoptic nuclei of the rat. J Comp Neurol. 1983, 218:121-44.

Schelling P, Meyer D, Loos HE, Speck G, Phillips MI, Johnson AK, Ganten D. A micromethod for the measurement of renin in brain nuclei: its application in spontaneously hypertensive rats. Neuropharmacology. 1982, 21:455-63.

Schelling, P., Meyer, D., Loos, H.-E., et al. (1982) A micromethod for the measurement of renin in brainnuclei: its application in spontaneously hypertensive rats. Neuropharmacology, 21, 455-463.

Schmid HA, Simon E. Effect of angiotensin II and atrial natriuretic factor on neurons in the subfornical organ of ducks and rats in vitro. Brain Res. 1992, 588:324-8.

Shan Z, Cuadra AE, Sumners C, Raizada MK. Characterization of a functional (pro)renin receptor in rat brain neurons. Exp Physiol. 2008, 93:701-8.

Shi P, Stocker SD, Toney GM. Organum vasculosum laminae terminalis contributes to increased sympathetic nerve activity induced by central hyperosmolality. Am J Physiol Regul Integr Comp Physiol. 2007, 293:R2279-89.

Shimizu H, Watanabe E, Hiyama TY, Nagakura A, Fujikawa A, Okado H, Yanagawa Y, Obata K, Noda M. Glial Nax channels control lactate signaling to neurons for brain [Na+] sensing. Neuron. 2007, 54:59-72.

Son YJ, Hur MK, Ryu BJ, Park SK, Damante G, D'Elia AV, Costa ME, Ojeda SR, Lee BJ. Strittmatter SM, Lo MM, Javitch JA, Snyder SH. Autoradiographic visualization of angiotensin-converting enzyme in rat brain with [3H]captopril: localization to a striatonigral pathway. Proc Natl Acad Sci U S A. 1984, 81:1599-603.

Storck T, Schulte S, Hofmann K, Stoffel W. Structure, expression, and functional analysis of a Na(+)-dependent glutamate/aspartate transporter from rat brain. Proc Natl Acad Sci U S A. 1992, 89:10955-9.

Strömstedt M, Waterman MR. Messenger RNAs encoding steroidogenic enzymes are expressed inrodent brain. Brain Res Mol Brain Res. 1995, 34:75-88.

Suckling RJ, He FJ, Markandu ND, Macgregor GA. Dietary salt influences postprandial plasma sodium concentration and systolic blood pressure. Kidney Int. 2011, 81:407-11

Sunn N, McKinley MJ, Oldfield BJ. Circulating angiotensin II activates neurones in circumventricular organs of the lamina terminalis that project to the bed nucleus of the stria terminalis. J Neuroendocrinol. 2003, 15:725-31.

Swanson LW, Lind RW. Neural projections subserving the initiation of a specific motivated behavior in the rat: new projections from the subfornical organ. Brain Res. 1986, 379:399-403.

Takahashi K, Hiraishi K, Hirose T, Kato I, Yamamoto H, Shoji I, Shibasaki A, Kaneko K, Satoh F, Totsune K. Expression of (pro)renin receptor in the human brain and pituitary, and co-localisation with arginine vasopressin and oxytocin in the hypothalamus. J Neuroendocrinol. 2010, 22:453-9.

Tanaka J. Involvement of the median preoptic nucleus in the regulation of paraventricular vasopressin neurons by the subfornical organ in the rat. Exp Brain Res. 1989, 76:47-54.

Tanaka J, Mashiko N, Kawakami A, Ushigome A, Nomura M. GABAergic systems in the nucleus tractus solitarius regulate noradrenaline release in the subfornical organ area in the rat. Auton Neurosci. 2002,100:58-65.

Ushigome A, Nomura M, Tanaka J. Modulation of noradrenaline release in the median preoptic area by GABAergic inputs from the organum vasculosum of the lamina terminalis in the rat. Neurochem Int. 2004, 44:139-44.

van den Pol AN, Trombley PQ. Glutamate neurons in hypothalamus regulate excitatory transmission. J Neurosci. 1993, 13:2829-36.

Van Huysse JW, Dostanic I, Lingrel JB, Hou X, Wu H. Hypertension from chronic central sodium chloride in mice is mediated by the ouabain-binding site on the Na,K-ATPase α_2-isoform. Am J Physiol Heart Circ Physiol. 2011, 301:H2147-53.

Van Huysse JW. Endogenous brain Na pumps, brain ouabain-like substance and the alpha2 isoform in salt-dependent hypertension. Pathophysiology. 2007, 14:213-20.

Veerasingham SJ, Leenen FH. Excitotoxic lesions of the ventral anteroventral third ventricle and pressor responses to central sodium, ouabain and angiotensin II. Brain Res. 1997, 749:157-60.

Veerasingham SJ, Leenen FH. Ouabain- and central sodium-induced hypertension depend on the ventral anteroventral third ventricle region. Am J Physiol. 1999, 276:H63-70.

Vieira AA, Nahey DB, Collister JP. Role of the organum vasculosum of the lamina terminalis for the chronic cardiovascular effects produced by endogenous and exogenous ANG II in conscious rats. Am J Physiol Regul Integr Comp Physiol. 2010, 299:R1564-71.

Waagepetersen HS, Sonnewald U, Schousboe A. Compartmentation of glutamine, glutamate, and GABA metabolism in neurons and astrocytes: functional implications. Neuroscientist. 2003, 9:398-403.

Wang H, Huang BS, Leenen FH. Brain sodium channels and ouabainlike compounds mediate central aldosterone-induced hypertension. Am J Physiol Heart Circ Physiol. 2003, 285:H2516-23.

Wang H, Leenen FH. Brain sodium channels and central sodium-induced increases in brain ouabain-like compound and blood pressure. J Hypertens. 2003, 21:1519-24.

Wang H, Leenen FH. Brain sodium channels mediate increases in brain "ouabain" and blood pressure in Dahl S rats. Hypertension. 2002, 40:96-100.

Wang HW, Amin MS, El-Shahat E, Huang BS, Tuana BS, Leenen FH. Effects of central sodium on epithelial sodium channels in rat brain. Am J Physiol Regul Integr Comp Physiol. 2010, 299:R222-33.

Wang JM, Veerasingham SJ, Tan J, Leenen FH. Effects of high salt intake on brain AT1 receptor densities in Dahl rats. Am J Physiol Heart Circ Physiol. 2003, 285:H1949-55.

Watanabe E, Hiyama TY, Shimizu H, Kodama R, Hayashi N, Miyata S, Yanagawa Y, Obata K, Noda M. Sodium-level-sensitive sodium channel $Na(_x)$ is expressed in glial laminate processes in the sensory circumventricular organs. Am J Physiol Regul Integr Comp Physiol. 2006, 290:R568-76.

Watts AG, Sanchez-Watts G, Emanuel JR, Levenson R. Cell-specific expression of mRNAs encoding Na^+,$K(^+)$-ATPase alpha- and beta-subunit isoforms within the rat central nervous system. Proc Natl Acad Sci U S A. 1991, 88:7425-9.

Xu Z, Herbert J. Effects of unilateral or bilateral lesions within the anteroventral third ventricular region on c-fos expression induced by dehydration or angiotensin II in the supraoptic and paraventricular nuclei of the hypothalamus. Brain Res. 1996, 713:36-43.

Xu Z, Herbert J. Regional suppression by lesions in the anterior third ventricle of c-fos expression induced by either angiotensin II or hypertonic saline. Neuroscience. 1995, 67:135-47.

Yamada H, Ihara N, Takahashi H, Yoshimura M, Sano Y. Distribution of the endogenous digitalis-like substance (EDLS)-containing neurons labeled by digoxin antibody in hypothalamus and three circumventricular organs of dog and macaque. Brain Res. 1992, 584:237-43. (a)

Yamada H, Naruse M, Naruse K, Demura H, Takahashi H, Yoshimura M, Ochi J. Histological study on ouabain immunoreactivities in the mammalian hypothalamus. Neurosci Lett. 1992, 141:143-6. (b)

Yamaguchi K, Morimoto A, Murakami N. Organum vasculosum laminae terminalis (OVLT) in rabbit and rat: topographic studies. J Comp Neurol. 1993, 330:352-62.

Yasuda Y, Honda K, Negoro H, Higuchi T, Goto Y & Fukuda S. The contribution of the median preoptic nucleus to renal sympathetic nerve activity increased by intracerebroventricular injection of hypertonic saline in the rat. Brain Res 2000, 867, 107–114.

Ye P, Kenyon CJ, Mackenzie SM, Nichol K, Seckl JR, Fraser R, Connell JM, Davies E. Effects of ACTH, dexamethasone, and adrenalectomy on 11beta-hydroxylase (CYP11B1) and aldosterone synthase (CYP11B2) gene expression in the rat central nervous system. J Endocrinol. 2008, 196:305-11.

Young A.B., Chu D. Distribution of GABAA and GABAB receptors in mammalian brain: Potential targets for drug development. 1990, 21:161–167

Yu L, Romero DG, Gomez-Sanchez CE, Gomez-Sanchez EP. Steroidogenic enzyme gene expression in the human brain. Mol Cell Endocrinol. 2002, 190:9-17.

Zhang ZH, Kang YM, Yu Y, Wei SG, Schmidt TJ, Johnson AK, Felder RB. 11beta-hydroxysteroid dehydrogenase type 2 activity in hypothalamic paraventricular nucleus modulates sympathetic excitation. Hypertension. 2006, 48:127-33.

Zhao X, White R, Huang BS, Van Huysse J, Leenen FH. High salt intake and the brain renin--angiotensin system in Dahl salt-sensitive rats. J Hypertens. 2001, 19:89-98.

Zhou ZH, Bubien JK. Nongenomic regulation of ENaC by aldosterone. Am J Physiol Cell Physiol. 2001 Oct, 281:C1118-30.